UCSF
UC San Francisco Electronic Theses and Dissertations

**Title**
Deciphering the Melanocortin System: Three Distinct Approaches

**Permalink**
https://escholarship.org/uc/item/4r77h2cx

**Author**
Ersoy, Baran Alp

**Publication Date**
2009

Peer reviewed|Thesis/dissertation

eScholarship.org Powered by the California Digital Library
University of California

# DECIPHERING THE MELANOCORTIN SYSTEM: THREE DISTINCT APPROACHES

by

Baran A. Ersoy

DISSERTATION

Submitted in partial satisfaction of the requirements for the degree of

DOCTOR OF PHILOSOPHY

in

Pharmaceutical Sciences and Pharmacogenomics

in the

GRADUATE DIVISION

of the

UNIVERSITY OF CALIFORNIA, SAN FRANCISCO

# Acknowledgements

My doctoral study leading to this thesis work could not have been complete without the love and support of my family, especially my wife Meghan. She gives me strength and makes me believe in myself.

*The chapter III of this thesis is coauthored with Melissa A. Calton and is a reprint of the material as it appears in Human Molecular Genetics Journal.*

*The chapter IV of this thesis is a reprint of the material as it appears in Pediatric Research Journal. The coauthor listed in this publication directed and supervised the research that forms the basis for the chapter IV of this thesis.*

# Deciphering the Melanocortin System:

# Three Distinct Approaches

*by* Baran Alp Ersoy

Human obesity is a multi-factorial trait regulated by environmental and genetic factors and is considered to be a global epidemic associated with mortality. Therefore, understanding the molecular pathways controlling the energy homeostasis is of great importance in order to develop pharmaceutical agents to treat obesity. This thesis work includes four separate research projects with the common intention of exploring the central control of energy homeostasis using three distinct research approaches. Leptin-melanocortin axis is the major central regulator of energy homeostasis where MC4R and POMC play key roles in transmitting the anorexigenic signal of the adipocyte secreted hormone leptin. In a genetic linkage study, we demonstrated that naturally occurring MC4R mutations but not the POMC or MC3R mutations are strongly associated with human obesity. Secondly, in an attempt to determine an alternative signaling pathway to leptin, the inhibition of $G_i$ protein signaling in the POMC neurons decreased the energy expenditure in a transgenic mouse model. Finally, we scrutinized the molecular mechanism underlying the physiologically relevant constitutive activity of MC4R. The data supports the evolutionary role of the N-terminal domain in the activity regulation of the G protein-coupled receptors. Overall, our findings provide essential pieces to the bigger puzzle of the melanocortin system, and contribute to the biomedical research in the pursuit of understanding the regulation of energy homeostasis in humans.

# Index


| | Page |
|---|---|
| **Thesis Introduction** | 1 |
| **Chapter I.** Pertussis toxin-sensitive $G_i$ signaling in the POMC neurons is necessary to maintain energy expenditure. | 7 |
| **Summary** | 8 |
| **Introduction** | 9 |
| **Results** | 13 |
| - Generation of mice with POMC neuron specific pertussis toxin expression. | 13 |
| - Expression of PTX in POMC neurons leads to increased body weight. | 17 |
| - Increased body weight of $ROSA26^{PTX/lacZ}/POMC^{Cre}$ mice is not due to increased food intake. | 24 |
| - $ROSA26^{PTX/lacZ}/POMC^{Cre}$ mice have decreased energy expenditure. | 26 |
| - $ROSA26^{PTX/lacZ}/POMC^{Cre}$ mice have regular compensatory feeding. | 28 |
| - $ROSA26^{PTX/lacZ}/POMC^{Cre}$ mice have regular glucose and glucocorticoid metabolism. | 30 |
| **Discussion** | 32 |
| - Inhibition of $G_i$ signaling in POMC neurons results in a similar phenotype to POMC specific deletion of AMP-activated protein kinase. | 32 |
| - Two different types of signaling pathways in the POMC neurons control food intake and energy expenditure separately. | 37 |
| - POMC neuron specific $G_i$ signaling: a possible target to by-pass leptin resistance? | 41 |
| **Experimental Procedures** | 43 |
| - Mouse Models | 43 |
| - Body Weight & Composition | 43 |
| - Food Intake | 44 |
| - Compensatory Feeding | 44 |
| - X-gal Staining | 44 |
| - mRNA Expression | 45 |
| - Plasma Leptin Level & Sensitivity | 46 |
| - Plasma Insulin Level & Glucose Tolerance Test | 47 |
| - Plasma Glucocorticoid level | 47 |
| - Energy expenditure | 47 |

**Page**

**Chapter 2.** Expanding the role of the N-terminal domain in the evolution of GPCR activity modulation. 49

**Summary** 50
**Introduction** 51
**Results** 57
- The N-terminal domain of MC4R acts as a diffusible ligand. 57
- AGRP antagonizes the diffusible MC4R2-26 N-terminal domain. 62
- The MC4R2-26 activation site does not overlap with the αMSH activation site. 64
- The peptide sequence HLWNRS is the minimum activating sequence of the N-terminal domain of MC4R. 66
- Core transmembrane residues involved in N-terminus mediated activation. 69
- Structural determinants of N-terminal domain mediated activation of the MC4R. 73
- Pharmacological modulators of MC4R activity. 76

**Discussion** 79
- Conformational complexity at the MC4R. 79
- Expanding the role of the N-terminal domain in the evolution of GPCRs . 80
- Physiological inverse-agonists as regulators of constitutively active orphan GPCRs. 82

**Experimental Procedures** 84
- MC4R ligands 84
- MC4R plasmid constructs 84
- Ligand binding assay 84
- MC4R activity, luciferase reporter assay 85
- MC4R activity, cAMP assay 86
- Peptide synthesis 86
- Molecular modeling of MC4R 87
- Statistical Analysis 87

**Chapter 3.** Association of functionally significant Melanocortin-4 but not Melanocortin-3 receptor mutations with severe adult obesity in a large North-American case control study. 88

**Summary** 89
**Introduction** 91

**Page**

**Results** 94
- Prevalence and nature of MC4R mutations in two North American cohorts of severe obese adults. 94
- Comparative functional analysis of severe adult obesity-associated MC4R mutations. 98
- Prevalence and nature of MC3R mutations in two North American cohorts of severe obese adults. 101
- Comparative functional analysis of severe adult obesity-associated MC3R mutations. 101
- In silico analysis of severe adult obesity-associated MC4R and MC3R mutations. 103

**Discussion** 106

**Experimental Procedures** 110
- Subjects - US case-control study 110
- Subjects - Canadian case-control study 110
- Sequencing 111
- In Vitro analysis of missense MC4R and MC3R mutations 111
- Assay of MC4R and MC3R activity 112
- In silico prediction of missense mutation effects 112
- SNAP Prediction 113
- Statistical Analysis 113

**Chapter 4.** Mutational Analysis of the Pro-opiomelanocortin Gene in French Obese Children Led to the Identification of a Novel Deleterious Heterozygous Mutation Located in the α-Melanocyte Stimulating Hormone Domain. 115

**Summary** 116

**Introduction** 117

**Results** 120
- Frequency of POMC mutations in obese and lean French children and identification of a patient carrying the Phe144Leu POMC mutation. 120
- Clinical and biologic phenotype of the Phe144Leu mutation carrier. 125
- Functional effect of the Phe144Leu POMC mutation. 127

**Discussion** 129

**Page**

**Experimental Procedures** 133

- Direct POMC gene sequencing 133

- Clinical and biochemical data 134
- Human MC4R (hMC4R) activation by the αMSH product of Phe144Ieu POMC 135
- Competitive binding assay 135

**Supporting Material** 136

# Figures and Tables


**Introduction** **Page**

**Figure 1.** Leptin-Melanocortin Axis. 3

**Figure 2.** Naturally occurring obesity causing MC4R mutations. 4

**Chapter I.**

**Figure 1.** Endogenous ligands that modulate POMC and AgRP neurons in the Arcuate Nucleus of the hypothalamus. 11

**Figure 2.** Depiction of transgenic constructs and the breeding 15

**Figure 3.** Hypothalamic Pertussis toxin mRNA expression. 16

**Figure 4.** Whole brain LacZ staining 18

**Figure 5.** The Weight curve 20

**Figure 6.** Body composition and length. 21

**Figure 7.** Plasma leptin level and Pharmacological leptin sensitivity 22

**Figure 8.** Hypothalamic mRNA levels of POMC, AgRP, NPY. 23

**Figure 9.** Loss of leptin sensitivity at POMC neurons. 23

**Figure 10.** Food intake and efficacy. 25

**Figure 11.** Energy expenditure 27

**Figure 12.** Food deprivation and compensatory feeding 29

**Figure 13.** Insulin levels and glucose tolerance test 30

**Figure 14.** Glucocorticoid metabolism 31

**Figure 15.** Intracellular effectors of $G_i$ protein-coupled receptor 33

**Figure 16.** Functional separation of MC4R neurons 39

**Figure 17.** Roles of leptin and $G_i$ signaling in POMC neurons 40

**Table 1.** Energy homeostasis phenotypes of POMC alteration 35

**Table 2.** Comparison of energy homeostasis: PTX vs. AMPK 36

Page

**Chapter II.**


**Figure 1.** Specific domains of GPCRs and G proteins 51

**Figure 2.** The role of the N-terminal domain in ligand binding 53

**Figure 3.** Activation mechanism of PAR1 54

**Figure 4.** The serpentine model of MC4R 58

**Figure 5.** Functional studies of MC4R Δ1-24 59

**Figure 6.** MC4R2-26 peptide is a partial agonist of MC4R Δ1-24 61

**Figure 7.** Independent modulation of MC4R2-26 activation 63

**Figure 8.** Amino acids in αMSH mediated activation of MC4R 64

**Figure 9.** Minimal activating sequence of MC4R2-26 67

**Figure 10.** Multiple alignments of the MC4R N-terminal sequences 68

**Figure 11.** Essential amino acids of MC4R2-26 for basal activation 68

**Figure 12.** The basal activity of candidate TM residues 71

**Figure 13.** Activation profile of low basal MC4R mutants 72

**Figure 14.** 3D Molecular model of MC4R - top view 75

**Figure 15.** The activation of MC4R by $ZnCl_2$ 78

**Figure 16.** Evolutionary model of the role of the N-terminal domainin GPCRs 81

**Figure 17.** Orphan receptors with high constitutive activity 83

**Table 1.** MC4R activation by βMSH, γMSH, THIQ, and MT-II 60

**Table 2.** MC4R activation by αMSH, THIQ, and MT-II 77


**Chapter III.**


**Figure 1.** Functional analysis of mutant MC4Rs 100

**Figure 2.** Functional analysis of mutant MC3Rs 102

**Figure 3.** Prevalence of rare MC4R and MC3R mutation carriers in severely obese and lean subjects 105

**Table 1.** Summary of unique or rare mutations identified in the coding regions of MC4R and MC3R 96

**Page**

**Table 2.** Summary of common variants identified in MC4R and MC3R 97

**Chapter IV.**

**Figure 1.** POMC protein and location of the variants 122

**Figure 2.** Pedigree, genotype, and clinical characteristics of the Phe144Leu POMC mutation carrier 124

**Figure 3.** Impaired activation and binding of MC4R by the αMSH product of Phe144Leu POMC 128

**Table 1.** Frequency of POMC gene variations in obese and control children 121

**Table 2.** Characteristics of POMC mutations carriers 123

**Table 3.** Endocrine characteristics of the proband with the Phe144Leu mutation 127

# Introduction

## *Obesity as a Health Threat*

The current epidemics of obesity and type 2 diabetes in the United States are of major public heath significance. According to the National Health and Nutrition Examination Survey (NHANES) the measured prevalence of obesity (measured by body mass index (BMI) > 30kg/$m^2$) in U.S adults was 30.5%, compared to 22.9% in NHANES III (1988-1994) [1]. Over the same period, an alarming increase in the prevalence of extreme obesity (BMI > 40 kg/$m^2$) was also observed, increasing from 2.9% to 4.7% of the population. By dramatically increasing mortality [2] and morbidity [3] from cardiovascular disease, obesity has emerged as a major public health issue for the 21$^{st}$ century. At least one billion people are overweight, and 300 million are obese [4]. Excess adiposity is strongly associated with hypertension, dyslipidemia, type 2 diabetes, heart failure and stroke [5]. The burden of disease is particularly high in individuals with severe obesity as they are more likely to develop more than one of these co-morbidities [6]. Obese individuals (especially those with an abdominal pattern of fat distribution) are at elevated risk of insulin resistance/type 2 diabetes, hypertension, dyslipidemia, stroke and heart failure.

The Fight against obesity has two major fronts: one is regulating the environmental factors leading to increased obesity such as unhealthy dietary

habits and lack of physical activity, and the other is a comprehensive research towards a better understanding of the molecular mechanisms that control energy homeostasis in humans. In this thesis study, we will span and extend the latter.

***The leptin-melanocortin pathway in the regulation of long-term energy homeostasis.***

Prevention of obesity in mammals is dependant on a number of systems, including the activity of an anorexigenic pathway made up of the adipocyte-secreted hormone leptin, its neuropeptide effectors pro-opiomelanocortin (POMC) and Agouti-related protein (AgRP) and the melanocortin 4 Receptor (MC4R) (Figure 1). Leptin, an adipocyte specific hormone, is secreted by the adipocyte at levels that correlate with fat mass and regulates adipose tissue mass through centrally mediated effects on satiety and energy metabolism[7]. Binding of leptin to its receptor leads to increased expression of POMC [8-10] and decreased expression of AgRP [11, 12] in two different neuron populations of the arcuate nucleus of the hypothalamus (ARC) [12-17]. The hypothalamic pro-hormone POMC is cleaved into alpha Melanocortin Stimulating Hormone ($\alpha$-MSH) by two proconvertases (PC1 & PC2) [18]. $\alpha$-MSH [19] and AgRP [20-22] are both high affinity ligands of MC4R, a G-protein coupled receptor (GPCR) expressed in the neurons of the paraventricular nucleus (PVN) in the hypothalamus (Figure 1). $\alpha$-MSH is an agonist and results in satiety [23], whereas AgRP is an antagonist/inverse agonist [20-22, 24] and is orexigenic.

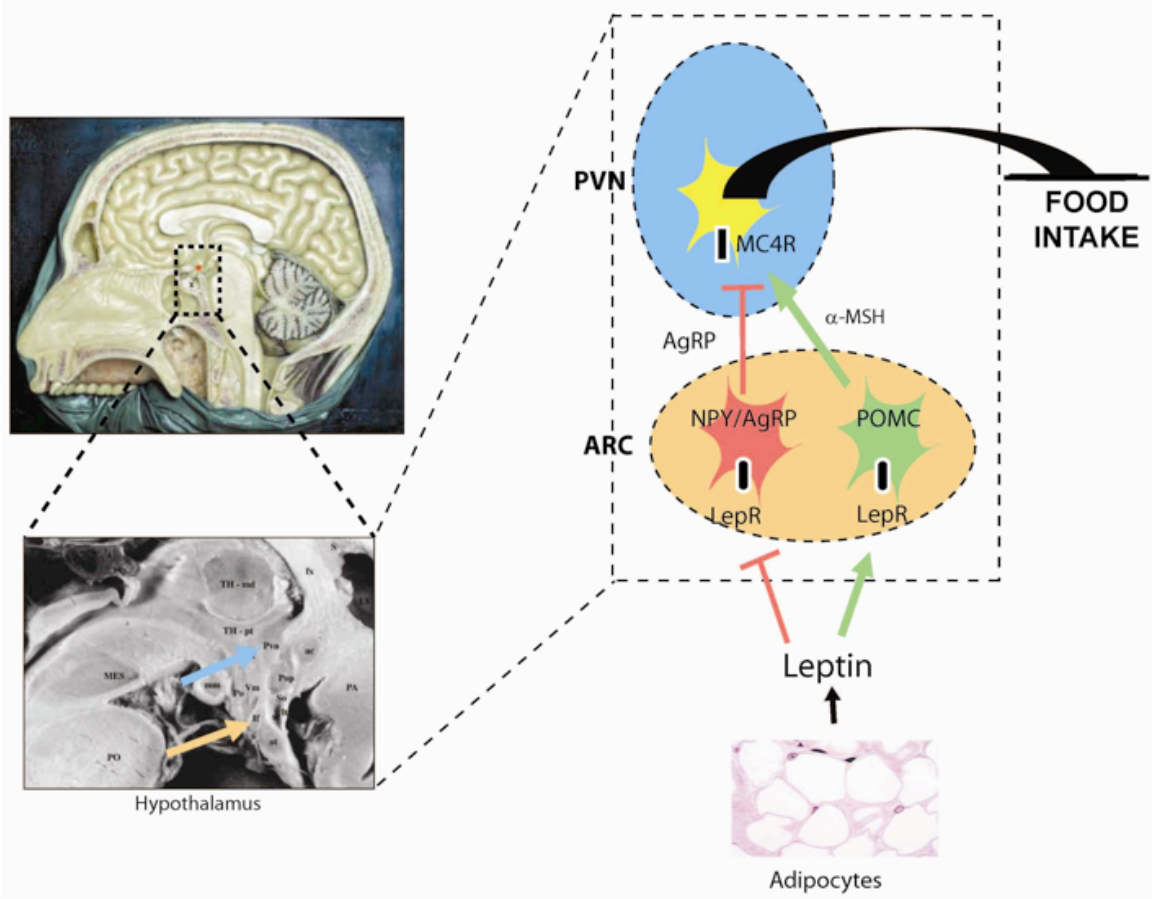


**Figure 1.** Leptin-Melanocortin Axis. Left panel shows the anatomical location of the Hypothalamus, Arcuate Nucleus (ARC), and Paraventricular Nucleus (PVN) in the human brain. Right panel depicts Leptin-Melanocortin signaling pathway.

The essential role of this axis in the regulation of long-term energy homeostasis is best demonstrated by the observation that mutation of leptin [25-27], the leptin receptor [28, 29], POMC [30-32], PC1 and MC4R [33] all cause obesity in human and mice. In particular, heterozygous mutations in MC4R are the cause of 2 to 6% of severe obesity cases in humans [34-38] (Figure 2). Finally, as MC4R is a key integrator of different signals reflecting the metabolic status, and its activation results in food intake inhibition, this receptor has become a major target for new anti-obesity drugs [39].

**Figure 2.**

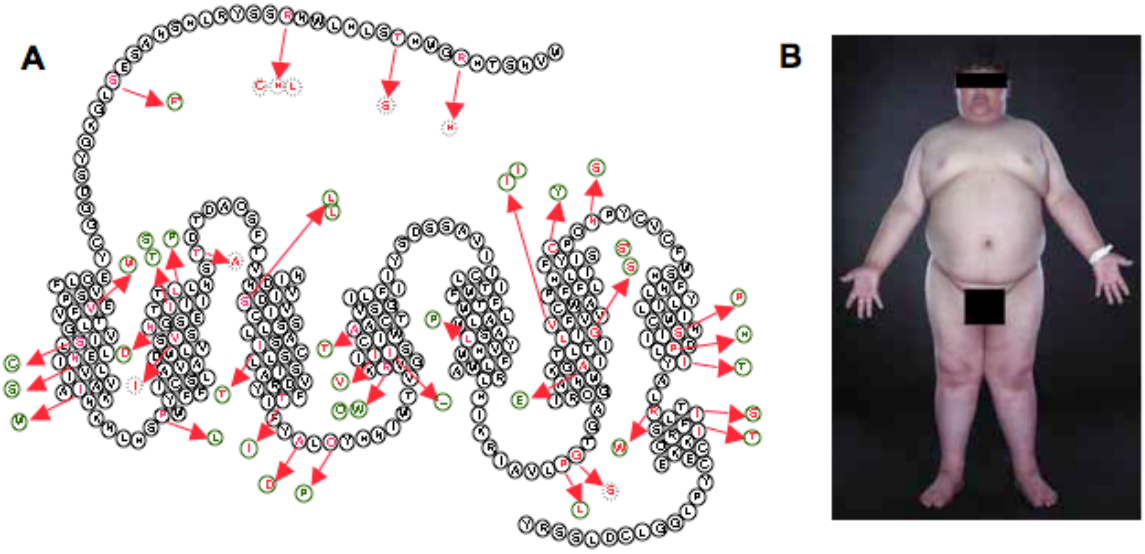


**Figure 2.** Naturally occurring obesity causing MC4R mutations. A) Serpentine model of 7TM receptor MC4R. Red arrows represent the non-synonymous point mutations. B) Representative weight phenotype of a heterozygous MC4R mutation carrier in human.

***Three distinct approaches to dissect the melanocortin system.***

The leptin-melanocortin axis is a complex system that requires the harmony of multiple components to maintain energy homeostasis. These components can be studied individually and in relation to each other to clarify the complexity of the system. In this thesis dissertation, the leptin-melanocortin axis is studied using three distinct and different approaches: transgenic mice, structural biology, and human genetics. Transgenic mouse models have become the standard in studying gene manipulations and disease states in an entire organism. In the first chapter, using a conditional transgenic mouse model we demonstrated the role of an alternative signaling pathway (other than leptin) in POMC neurons. In the second chapter, we studied the structure and function of the N-terminal mediated constitutive activity of MC4R and its implication for the other G protein-coupled receptors. Finally, genetic linkage studies help us discover and/or validate genes that are implicated in the obesity phenotype. Therefore, in the chapters 3 and 4 we studied the segregation of naturally occurring human mutations (POMC, MC3R, and MC4R) with extreme obesity (BMI>40), and their functional relevance in the melanocortin system.

***Approaches:***

*-Transgenic Mouse Model:*

**Chapter 1.** Pertussis toxin-sensitive $G_i$ signaling in the POMC neurons is necessary to maintain energy expenditure.

*-Structural Biology:*

**Chapter 2.** Expanding the role of the N-terminal domain in the evolution of GPCR activity modulation.

*-Human Genetics:*

**Chapter 3.** Association of functionally significant Melanocortin-4 but not Melanocortin-3 receptor mutations with severe adult obesity in a large North-American case control study.

**Chapter 4.** Mutational Analysis of the Pro-opiomelanocortin Gene in French Obese Children Led to the Identification of a Novel Deleterious Heterozygous Mutation Located in the α-Melanocyte Stimulating Hormone Domain.

# Chapter I

## Pertussis Toxin-sensitive $G_i$ Protein Signaling in the POMC Neurons is Necessary to Maintain Energy Expenditure.

**SUMMARY**

Several G protein-signaling pathways have been suggested to play a role in the central regulation of energy homeostasis through the agouti-related protein (AgRP) and proopiomelanocortin (POMC) expressing neurons of the Hypothalamus. However, the precise role of the POMC neuron specific $G_i$ signaling in the regulation of energy homeostasis remains unclear. To directly address this issue, we used a mouse model to inhibit $G_i$ signaling in POMC neurons by POMC neuron specific expression of the catalytic S1 subunit of pertussis toxin, a known potent inhibitor of $G_{i/o}$ signaling. Inhibition of the $G_i$ signaling in the POMC neurons resulted in a thrifty phenotype with slightly decreased/unchanged food intake, decreased energy expenditure, and increased body weight. Increased body weight was caused by decreased energy expenditure, not by increased food intake. In contrast to the previous views that defend regulation of energy expenditure and food intake by different subsets of neurons, our phenotypic analysis suggests that one specific signaling pathway within the same subset of POMC neurons, the $G_i$ signaling, can regulate energy expenditure independent from food intake. Our findings validate the importance of $G_i$ protein signaling in POMC neurons in the regulation of energy expenditure. We propose the modulation of POMC neuron specific $G_i$ protein-coupled receptors as a novel and alternative target for the pharmacological treatment of energy homeostasis disorders.

## INTRODUCTION

In the central regulation of energy homeostasis, leptin signaling is the major regulator of AgRP and POMC neuronal activity in the melanocortin system[7-24]. Leptin regulates long-term energy homeostasis by inhibiting the orexigenic AgRP neurons[11, 12] and activating the anorexigenic POMC neurons[8-10] through the same subtype of cytokine receptor, LepRb[40]. Although leptin and its target LepRb are the strongest and most studied modulators of the AgRP and POMC neurons, a number of different satiety and hunger signals have also been described to control the same subset of neurons through a different family of receptors, the G protein-coupled receptor (GPCR) family (figure 1).

GPCRs, also known as the 7TM (seven transmembrane) receptors, constitute the largest family of membrane receptors in the mammalian genome. Overall, there are nearly 400 non-odorant GPCRs that regulate different physiological mechanisms in humans[41, 42]. Therefore, modulating the activity of the tissue specific GPCRs that have specific physiological roles has been the focus of the pharmaceutical industry, making up to 40% of all available drugs in the market. At the cellular level, GPCRs couple to one of the four different subsets of G proteins to regulate intracellular signaling: $G_{\alpha s}$ and $G_{\alpha i}$ proteins regulate intracellular cAMP levels by activating or inhibiting adenylyl cyclase activity respectively[43, 44]. $G_{\alpha q}$ protein activates phospholipase C (PLC) and increases $Ca^{2+}$ mobilization[43]. Finally, $G_{\alpha 12/13}$ is involved in the Rho family

GTPase signaling[43].

When it comes to the AgRP and POMC neurons, GPCRs with neuron specific expression have been considered potential drug targets for the treatment of eating disorders[45-48]. For the AgRP neuron specific GPCRs, food intake can be regulated through $G_i$ and $G_q$ signaling. A hunger-signaling peptide, ghrelin, is secreted from the stomach and activates a $G_q$ protein-coupled receptor, Growth Hormone Segretagogue Receptor (GSHR) in the AgRP neurons to increase food intake[48, 49] (figure 1). A postprandial satiety signal, pancreatic polypeptide Y (PYY) is secreted from the pancreas and inhibits AgRP neurons through a $G_i$ protein-coupled receptor, Neuropeptide Y Receptor 2 (Y2R) to decrease food intake[46, 47, 50-52] (figure 1). Another satiety signal, Serotonin (5HT) decreases food intake by inhibiting the AgRP neurons through the $G_i$ signaling serotonin receptor subtype $5HT_{1b}$, which is specifically expressed in the AgRP neurons[53] (figure 1). For the GPCR regulated POMC neuron activity, Serotonin can also decrease food intake by activating the anorexigenic POMC neurons through the $G_q$ signaling serotonin receptor subtype $5HT_{2C}$, which is specifically expressed in the POMC neurons[45, 54-56] (figure 1).

**Figure 1.**

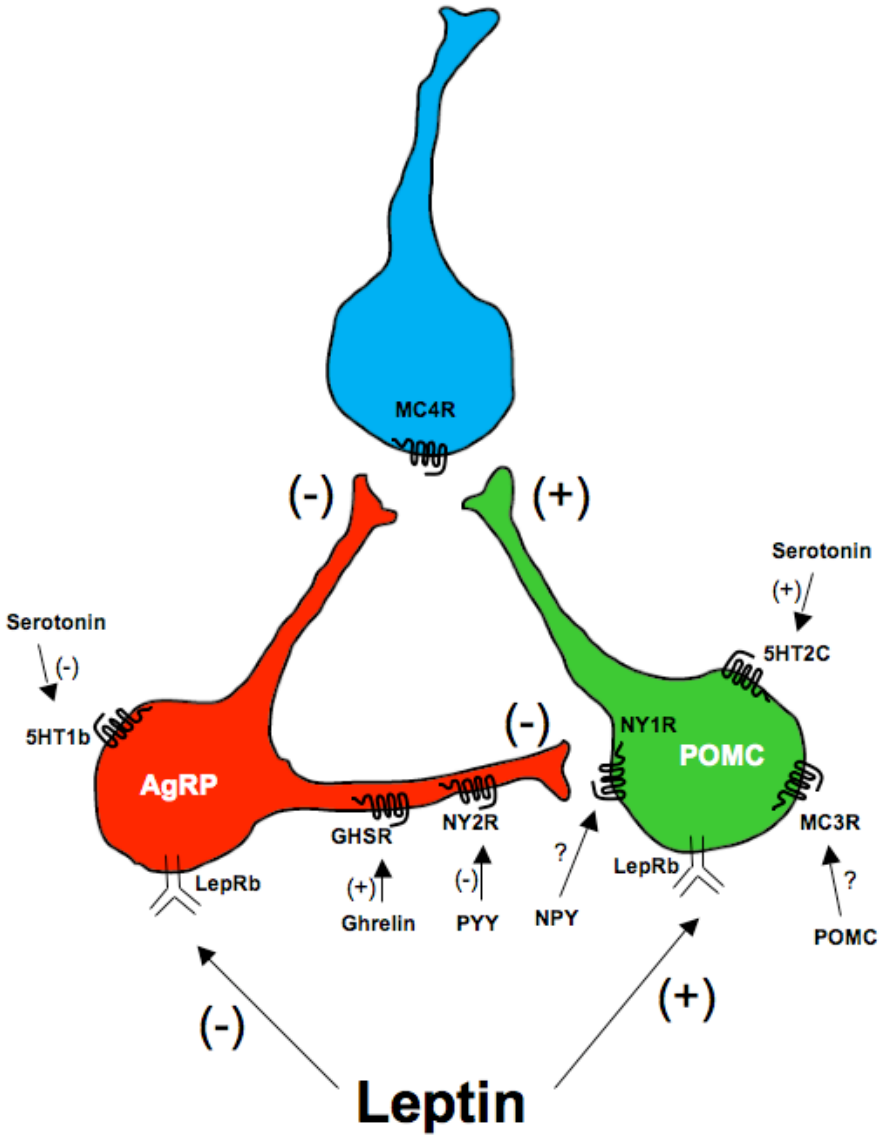


**Figure 1.** Endogenous ligands that modulate POMC and AgRP neurons in the Arcuate Nucleus of the hypothalamus. Red - AgRP/NPY neuron. Green - POMC neuron. Blue - MC4R neuron. (-) - Inhibitory effect. (+) activating effect.

Although the importance of $G_q$ protein signaling in both AgRP and POMC neurons has been well established, the knowledge on the relevance of $G_i$ signaling in regulating energy homeostasis has been limited to AgRP neurons. Therefore, in this study, we set to determine the role of $G_i$ signaling in POMC neurons in regulating energy homeostasis. We used a mouse model to inhibit $G_i$ signaling in POMC neurons by tissue specific expression of the catalytic S1 subunit of bordatella pertussis toxin[57] (PTX). PTX inhibits 4 out of 5 $G_i$ protein subtypes ($G_{\alpha}1$, $G_{\alpha}2$, $G_{\alpha}3$, $G_{\alpha}o$, not $G_{\alpha}z$) by ADP-ribosylation[57]. Inhibition of $G_i$ signaling in POMC neurons caused a thrifty energy homeostasis phenotype with slightly decreased food intake and decreased energy expenditure, leading to increased body weight. Our findings improve the understanding of the melanocortin system and widen the horizon for the drug discovery in the treatment of energy homeostasis disorders.

## RESULTS

### *Generation of mice with POMC neuron specific pertussis toxin expression.*

We used two previously described mouse models to obtain POMC neuron specific PTX expression. ROSA26$^{PTX}$ mouse model carries the catalytic S1 subunit of PTX inserted in the ROSA26 locus[58]. The insertion is designed so that PTX can only be expressed upon excision of a floxed silencer cassette by Cre recombinase[58] (ROSA26$^{PTX}$ allele, figure 2A). ROSA26$^{PTX}$ mouse has WT-like (wild type-like) phenotype in the absence of Cre Recombinase expression[58]. The system's efficacy was previously tested *in vivo* in pancreatic beta cells where contemporary presence of ROSA26$^{PTX}$ and Cre recombinase lead to inhibition of $G_{i/o}$ signaling[58]. In the second mouse model, lacZ expressing gene was inserted into the same locus instead of PTX, allowing lacZ expression as a marker in the presence of Cre recombinase[59] (ROSA26$^{lacZ}$, figure 2B). ROSA26$^{lacZ}$ mouse also carries a transgene expressing Cre recombinase under the promoter and transcriptional regulatory elements of the POMC gene[60] (POMC$^{Cre}$, figure 2C), hence allowing PTX and lacZ expression specifically in the POMC expressing neurons.

Mice homozygous for the ROSA26$^{PTX}$ allele (ROSA26$^{PTX/PTX}$) were intercrossed to mice homozygous for the ROSA26$^{lacZ}$ allele (ROSA26$^{lacZ/lacZ}$) carrying a single copy of the POMC$^{Cre}$ transgene (figure 2D). Subsequent progeny provided mice heterozygous for the ROSA26 locus (ROSA26$^{PTX/lacZ}$) with

or without the $POMC^{Cre}$ transgene. Quantitative mRNA analysis showed that the $ROSA26^{PTX/lacZ}/POMC^{Cre}$ mice had 10-fold more PTX expression in the hypothalamus compared to $ROSA26^{PTX/lacZ}$ mice (figure 3). Only the male mice in this breeding scheme were used for the phenotypic analysis (figure 2D).

**Figure 2.**

**A.**

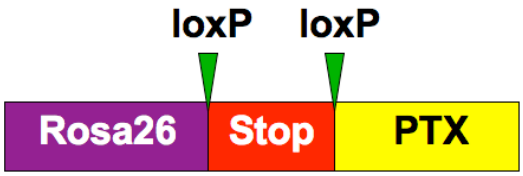


**B.**

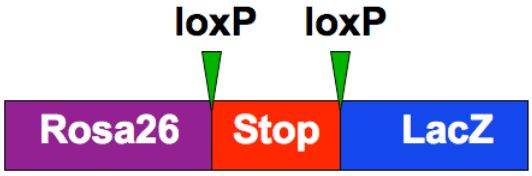


**C.**


**D.**

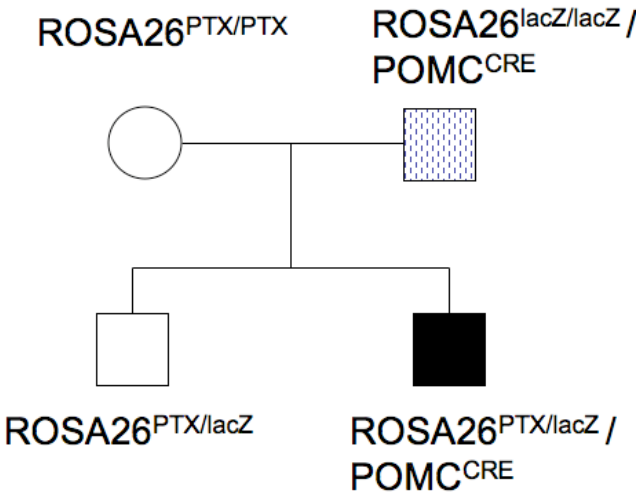


**Figure 2.** Depiction of transgenic constructs and the breeding scheme. A & B) Purple - Rosa26 promoter. loxP - Cre recombinase excision

sites. Red - Stop cassette. Yellow - Catalytic S1 subunit of bordatella pertussis toxin (PTX). Blue - Beta Galactosidase. C) Black - POMC promoter. Green - Cre Recombinase. D) Breeding scheme. Circle - Dame: ROSA26$^{PTX/PTX}$. Dash filled Square - Sire: ROSA26$^{lacZ/lacZ}$ /POMC$^{Cre}$. Square - Non-mutant male pups: ROSA26$^{PTX/lacZ}$. Black filled square - mutant male pups: ROSA26$^{PTX/lacZ}$/POMC$^{Cre}$.

**Figure 3.**

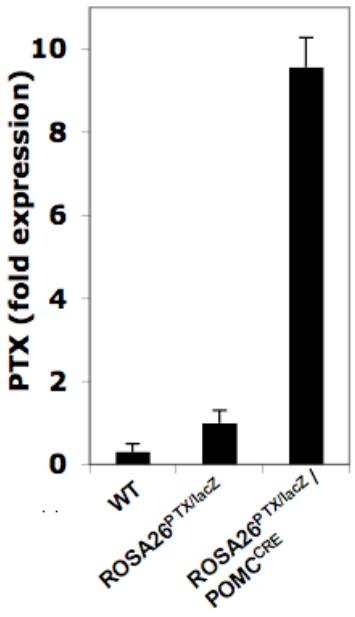


**Figure 3.** Hypothalamic Pertussis toxin mRNA expression. mRNA was purified from surgically dissected whole hypothalamus of wild type (WT) BL6, ROSA26$^{PTX/lacZ}$/POMC$^{Cre}$, and ROSA26$^{PTX/lacZ}$ mice. Total mRNA quantity was determined by spectroscopy. PTX mRNA quantity was determined by Sybr Green quantitative RT-PCR and further normalized to cyclophilin A housekeeping gene. Fold PTX mRNA expression was normalized to ROSA26$^{PTX/lacZ}$ PTX mRNA expression (1x). Error bars represent standard error for n=5.

We tested the accuracy of the POMC neuron specific expression by lacZ staining. LacZ staining of the whole brain of ROSA26$^{PTX/lacZ}$/POMC$^{Cre}$ mice was compared to ROSA26$^{WildType/lacZ}$/POMC$^{Cre}$ mice. Figure 4A and 4B show that the Cre recombinase system worked properly since the pattern of the lacZ staining was in accordance with the previously published localization of the POMC neurons in the hypothalamus[60, 61]. In addition, PTX expression in the POMC neurons did not cause neurotoxicity because the number and the size of the POMC neurons were unchanged between the ROSA26$^{PTX/lacZ}$/POMC$^{Cre}$ and ROSA26$^{WildType/lacZ}$/POMC$^{Cre}$ mice (figure 4B).

***Expression of PTX in POMC neurons leads to increased body weight.***

ROSA26$^{PTX/lacZ}$/POMC$^{Cre}$ mice were slightly but significantly overweight compared to ROSA26$^{PTX/lacZ}$ mice (figure 5A). The increased body weight was not due to an early developmental problem because ROSA26$^{PTX/lacZ}$/POMC$^{Cre}$ and ROSA26$^{PTX/lacZ}$ mice had identical body weight at the age of weaning (3 weeks old, figure 5B). 2 grams of increased body weight appeared after 5 weeks of age and persisted throughout the adulthood (figure 5A). The evaluation of the body composition by DEXA revealed that this increased body weight phenotype could be explained by the increased fat mass in ROSA26$^{PTX/lacZ}$/POMC$^{Cre}$ mice (figure 6A). The lean body mass and the length remained unchanged between the ROSA26$^{PTX/lacZ}$/POMC$^{Cre}$ and ROSA26$^{PTX/lacZ}$ mice (figure 6B and 6C).

**Figure 4.**

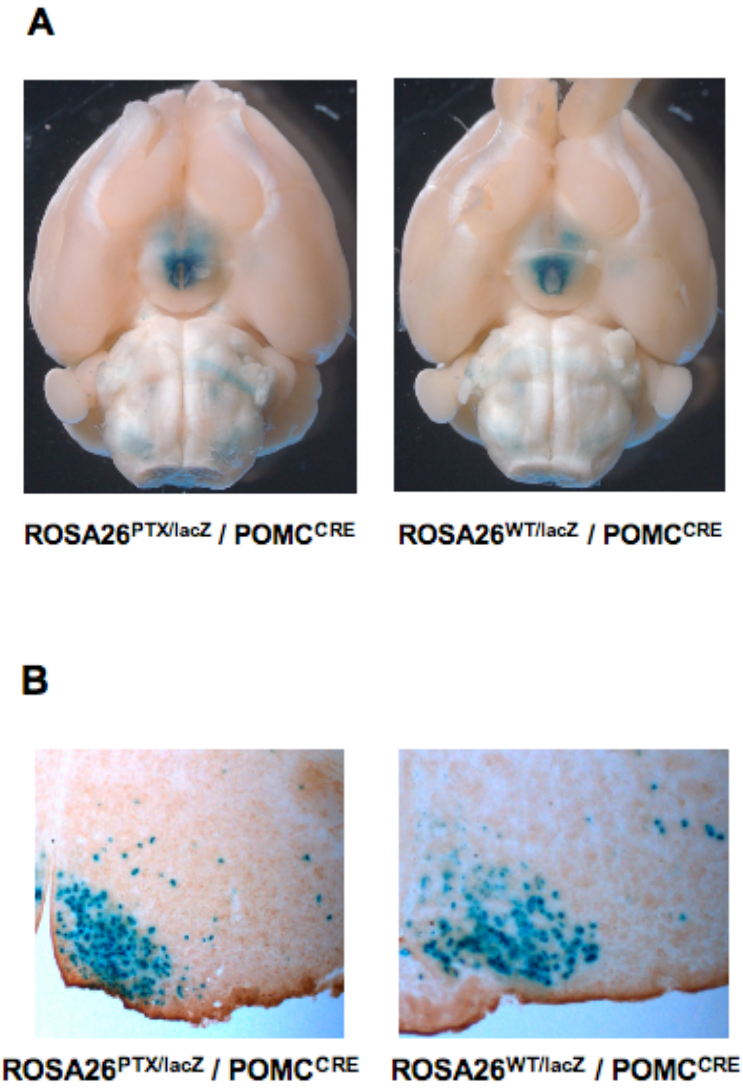


**Figure 4.** Whole brain LacZ staining. A) Localization of $POMC^{CRE}$ Cre Recombinase system to the POMC neurons. B) Neuronal anatomy of POMC expressing neurons. Whole brain and cryogenic hypothalamic brain slice lacZ stainings are representative images of n=4.

Plasma leptin level was increased in the ROSA26$^{PTX/lacZ}$/POMC$^{Cre}$ mice by nearly two folds in accordance with the increased adiposity (figure 7A). ROSA26$^{PTX/lacZ}$/POMC$^{Cre}$ mice had unaltered reduction in food intake in response to a pharmacological intraperitoneal (I.P.) dose of leptin (2.5mg/kg) compared to ROSA26$^{PTX/lacZ}$ mice (figure 7B). However, the hypothalamic mRNA expression of POMC, AgRP and NPY suggests that ROSA26$^{PTX/lacZ}$/POMC$^{Cre}$ mice had decreased leptin sensitivity at the physiological levels of leptin. In accordance with the increased plasma levels of leptin, ROSA26$^{PTX/lacZ}$/POMC$^{Cre}$ mice had decreased AgRP and NPY levels compared to ROSA26$^{PTX/lacZ}$ mice (figure 8B). Increased plasma leptin was able to induce its inhibitory effect on the AgRP/NPY neurons because this subset of neurons was not genetically altered. However, the increased plasma leptin levels in ROSA26$^{PTX/lacZ}$/POMC$^{Cre}$ mice did not lead to increased POMC mRNA compared to ROSA26$^{PTX/lacZ}$, suggesting that the inhibition of $G_i$ signaling by pertussis toxin in the POMC neurons altered the leptin sensitivity at the physiological levels (figure 8A, and figure 9).

**Figure 5.**

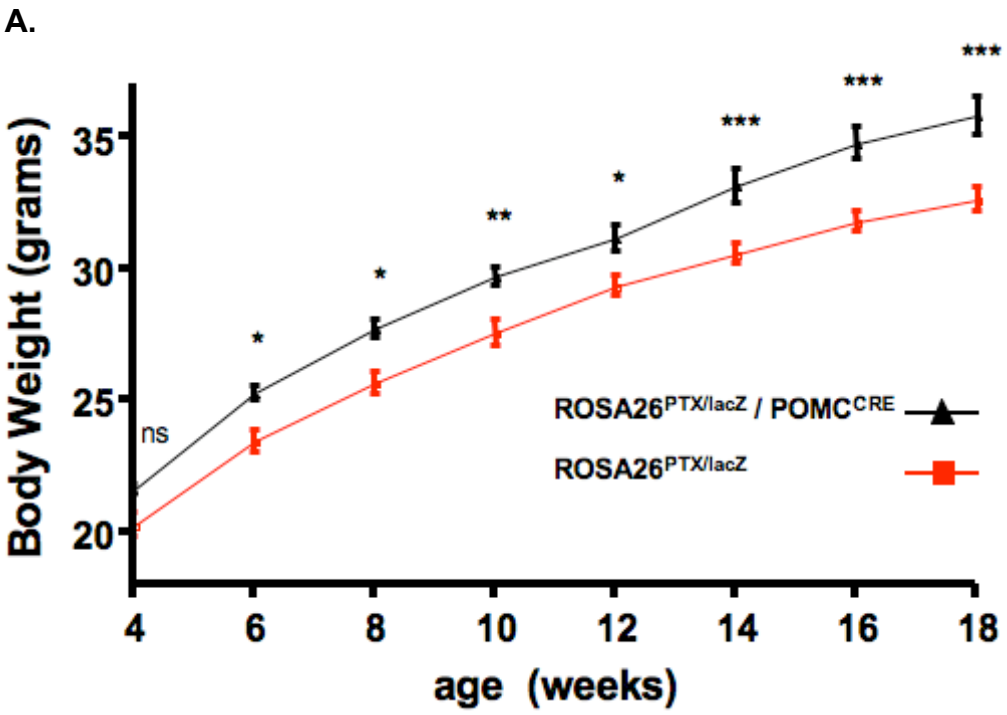


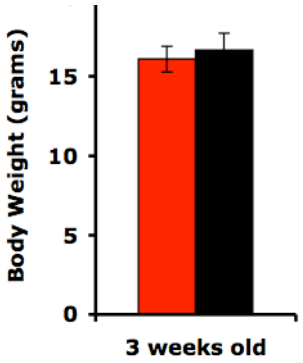


**Figure 5.** The Weight curve: ROSA26$^{PTX/lacZ}$/POMC$^{Cre}$ (black, n=10) vs. ROSA26$^{PTX/lacZ}$ (red, n=12) mice. A) Body weight curve was constructed through 18 consecutive and continuous weeks and is represented biweekly. B) Weaning body weight of ROSA26$^{PTX/lacZ}$/POMC$^{Cre}$ (black, n=8) vs. ROSA26$^{PTX/lacZ}$ (red, n=13) mice. Error bars represent the standard error. *P<0.05, **P<0.01, ***P<0.001.

**Figure 6.**

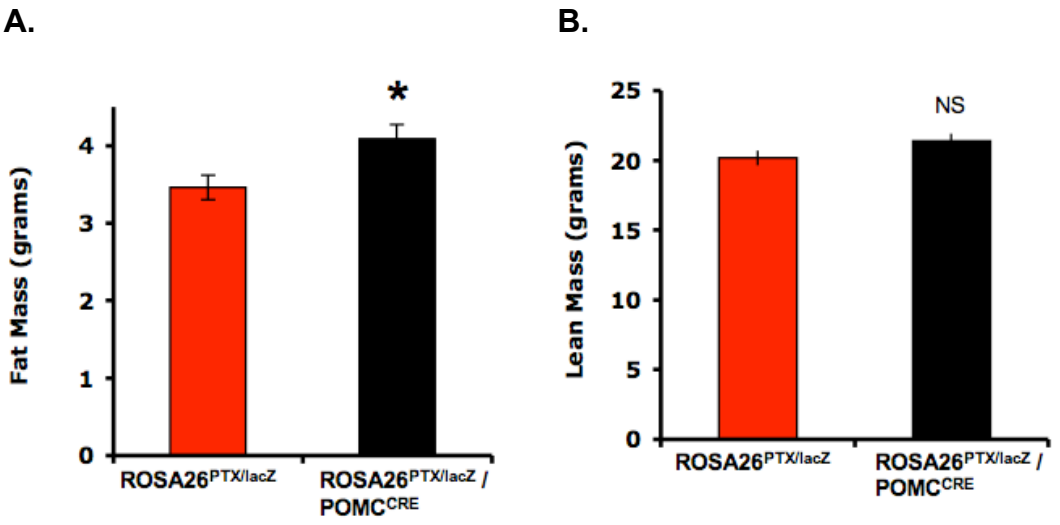


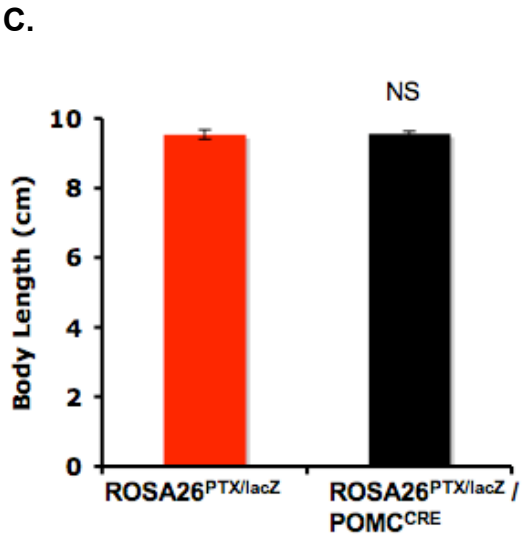


**Figure 6.** Body composition and length of ROSA26$^{PTX/lacZ}$/POMC$^{Cre}$ (black, n=7) vs. ROSA26$^{PTX/lacZ}$ (red, n=10) adult mice. Fat (A) and Lean (B) body mass as determined by DEXA. C) Nose to anus body length (n=5 for both groups). Error bars represent the standard error. *P<0.05, NS P>0.05.

**Figure 7.**

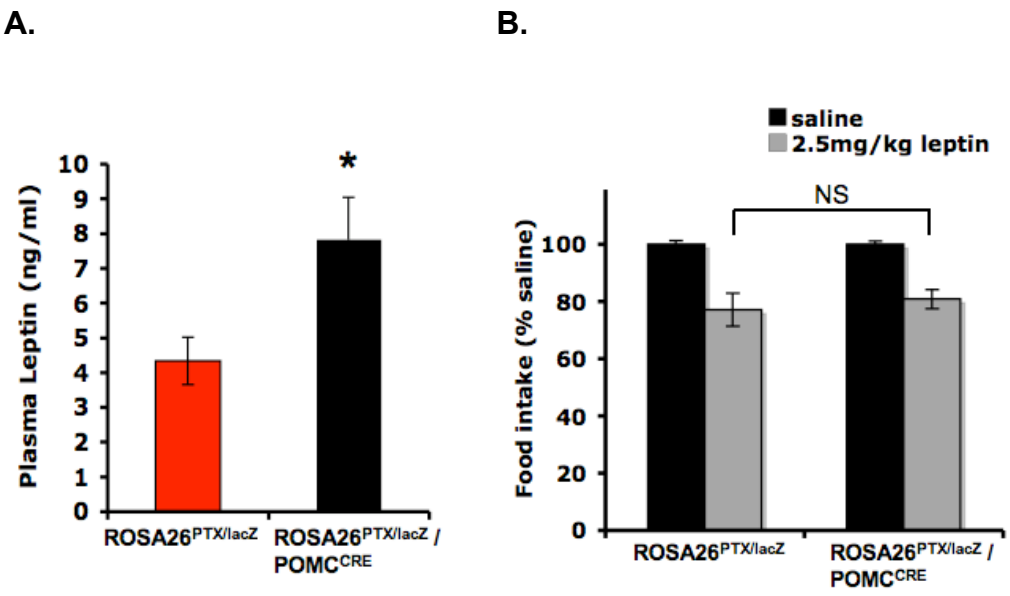


**Figure 7.** Plasma leptin level and Pharmacological leptin sensitivity of ROSA26$^{PTX/lacZ}$/POMC$^{Cre}$ vs. ROSA26$^{PTX/lacZ}$ 8 weeks old mice. A) Plasma leptin levels measured at fed state. B) Effect of 2.5mg/kg I.P. Leptin administration (grey) vs I.P. saline administration (black) on food intake. Data is normalized to daily food intake with saline administration. Error bars represent standard error for N=5. *P<0.05. NS P>0.05.

**Figure 8.**

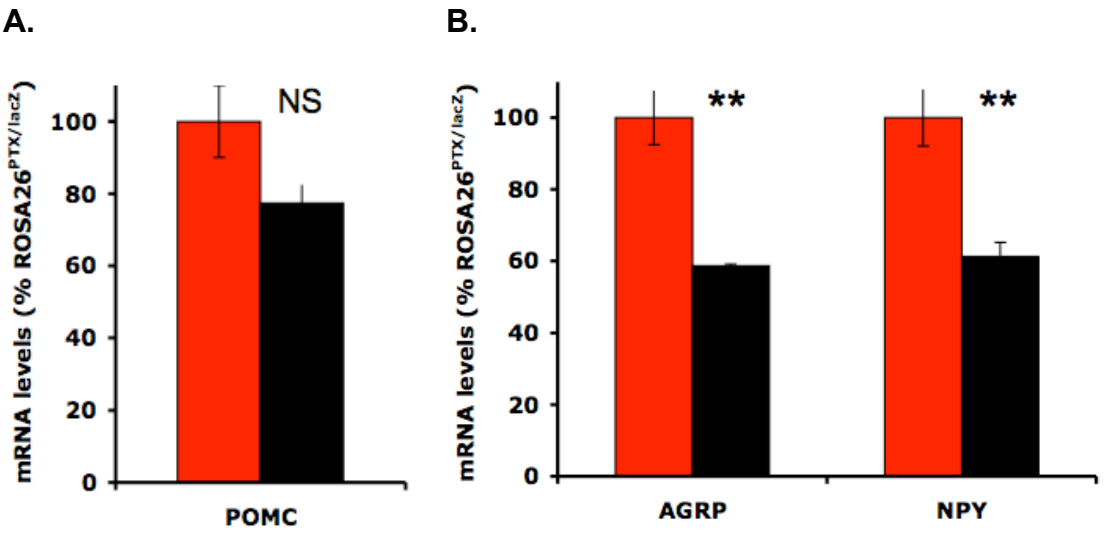


**Figure 8.** Hypothalamic mRNA levels of ROSA26$^{PTX/lacZ}$/POMC$^{Cre}$ (black) vs. ROSA26$^{PTX/lacZ}$ (red) 8 weeks old mice determined by Syber green RT-PCR. A) POMC mRNA level. B) AgRP and NPY mRNA levels. Error bars represent standard error for N=5. **P<0.01, NS P=0.07.

**Figure 9.**

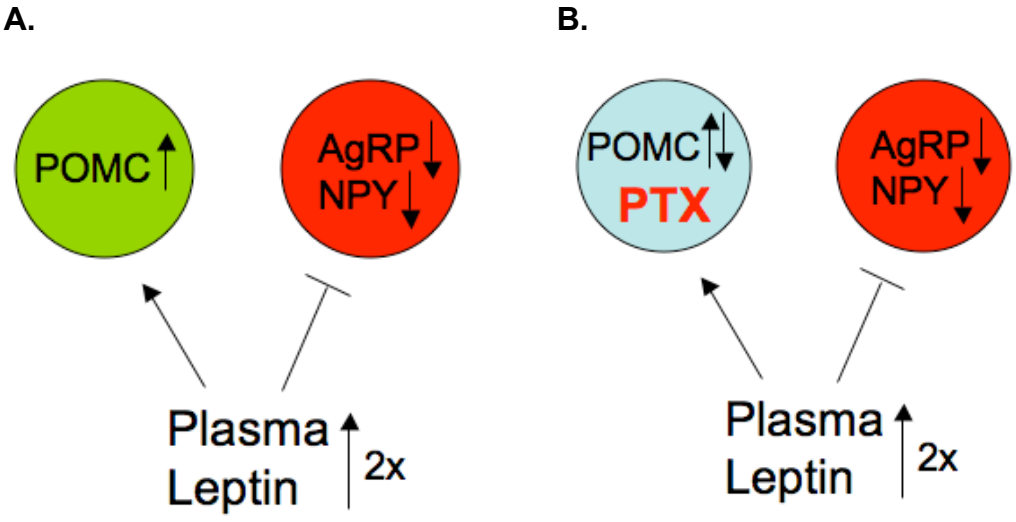


**Figure 9.** Loss of leptin sensitivity at POMC neurons in

ROSA26$^{PTX/lacZ}$/POMC$^{Cre}$ mice. A) Increased plasma leptin effects POMC and AgRP/NPY mRNA expression in wild type mice. B) Increase in POMC mRNA in response to increased plasma leptin levels is impaired due to the inhibition of $G_i$ signaling by PTX.

***Increased body weight of ROSA26$^{PTX/lacZ}$/POMC$^{Cre}$ mice is not due to increased food intake.***

To determine if the increased body weight and adiposity of ROSA26$^{PTX/lacZ}$/POMC$^{Cre}$ mice was due to increased food intake, we measured average daily food intake for 10 days. Daily grammage of food intake was identical between ROSA26$^{PTX/lacZ}$/POMC$^{Cre}$ and ROSA26$^{PTX/lacZ}$ mice (data not shown). However, ROSA26$^{PTX/lacZ}$/POMC$^{Cre}$ mice ate slightly but significantly less than ROSA26$^{PTX/lacZ}$ mice when the food intake was normalized to their respective body weights (1% decrease in food consumption per body weight, Figure 10A).

**Figure 10.**

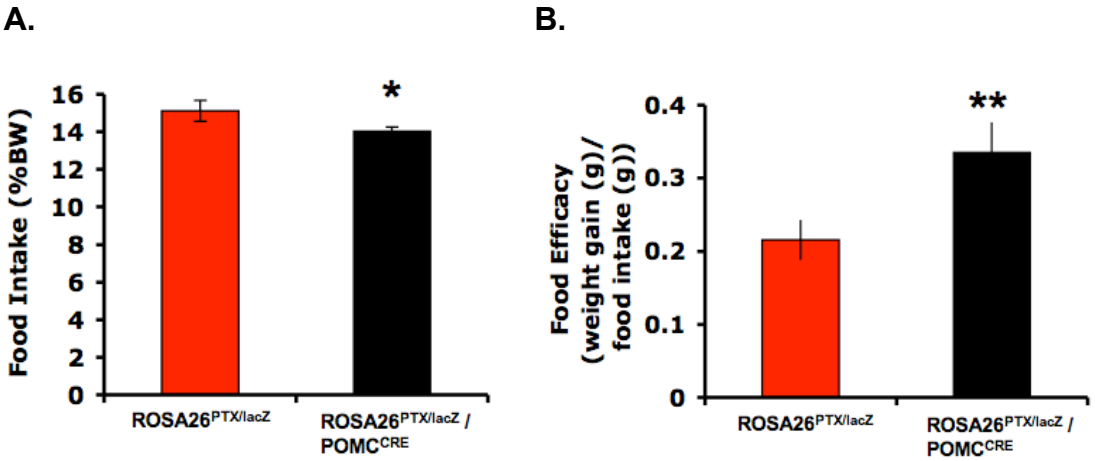


**Figure 10.** Food intake and efficacy for ROSA26$^{PTX/lacZ}$/POMC$^{Cre}$ (black) vs. ROSA26$^{PTX/lacZ}$ (red) 8 weeks old mice. A) Average daily food intake for 10 days normalized to corresponding body weights. B) Food efficacy calculated as grams of weight gained per grams of food comsumed for 10 days. Error bars represent standard error for N=9. *P<0.05, ** P<0.01.

Because ROSA26$^{PTX/lacZ}$/POMC$^{Cre}$ mice had unchanged/slightly decreased food intake despite being overweight, they had significantly increased food efficacy. ROSA26$^{PTX/lacZ}$/POMC$^{Cre}$ mice gained more weight per food consumed compared to ROSA26$^{PTX/lacZ}$ mice through the span of the 10-day measurement period (figure 10B).

***ROSA26$^{PTX/lacZ}$/POMC$^{Cre}$ mice have decreased energy expenditure.***

Oxymax study revealed that ROSA26$^{PTX/lacZ}$/POMC$^{Cre}$ mice had significantly reduced oxygen uptake compared to ROSA26$^{PTX/lacZ}$ mice independent of the light/dark cycle changes (Figure 11A). Decreased energy expenditure phenotype of ROSA26$^{PTX/lacZ}$/POMC$^{Cre}$ mice was measured at 8 weeks of age when there is a significant increase in food efficacy and body weight. This suggests that the reduced energy expenditure is the major cause of increased body weight, food efficacy and adiposity in ROSA26$^{PTX/lacZ}$/POMC$^{Cre}$ mice. Also, the respiratory exchange ratio (RER=V.$CO_2$/V.$O_2$) was decreased in ROSA26$^{PTX/lacZ}$/POMC$^{Cre}$ mice, indicating an increased usage of adipose tissue as the energy source (figure 11B). The slight increase in adiposity in the ROSA26$^{PTX/lacZ}$/POMC$^{Cre}$ mice could explain why they utilize slightly more fat as the energy source.

**Figure 11.**

**A.**

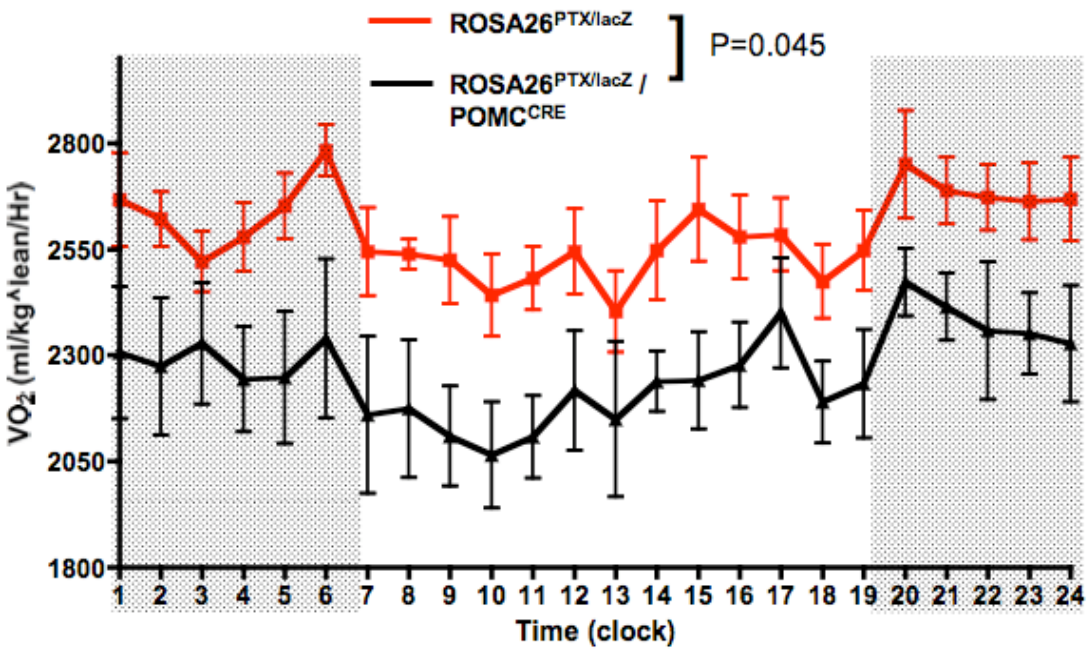


**B.**

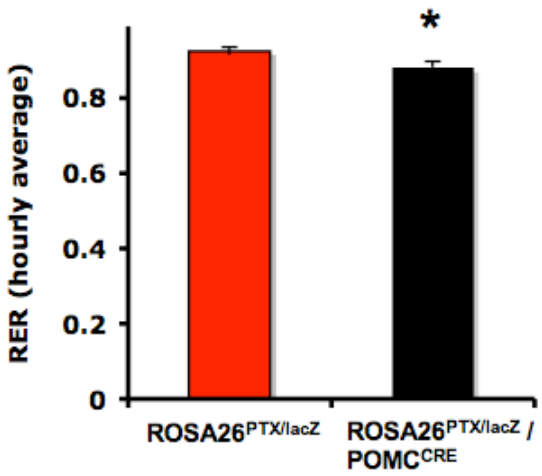


**Figure 11.** Energy expenditure of ROSA26$^{PTX/lacZ}$/POMC$^{Cre}$ (black) vs. ROSA26$^{PTX/lacZ}$ (red) 8 weeks old mice. A) Oxygen uptake ($VO_2$) measured through 24 hr period for every 10 minutes. Data is averaged to hourly oxygen

uptake and normalized to lean body mass. Dark cycle is represented with grey screens between 1-7 am and from 7 pm (19hr) until midnight (24hr). B) Respiratory exchange ratio (RER) measured through 24 hr period. Data is normalized to hourly average. Error bars represent standard error for N=5. *P<0.05.

***ROSA26$^{PTX/lacZ}$/POMC$^{Cre}$ mice have regular compensatory feeding.***

To test if the ROSA26$^{PTX/lacZ}$/POMC$^{Cre}$ mice had impaired response to adiposity signals, we tested the increased compensatory food intake following food deprivation. Albeit non-significant, ROSA26$^{PTX/lacZ}$/POMC$^{Cre}$ mice had lost slightly less weight (p=0.06) at the end of 36 hr fasting period, a trend in accordance with the reduced energy expenditure phenotype (figure 12A). ROSA26$^{PTX/lacZ}$/POMC$^{Cre}$ and ROSA26$^{PTX/lacZ}$ mice had similar 24 hr compensatory food intake after a 36 hr fasting period (figure 12B).

**Figure 12.**

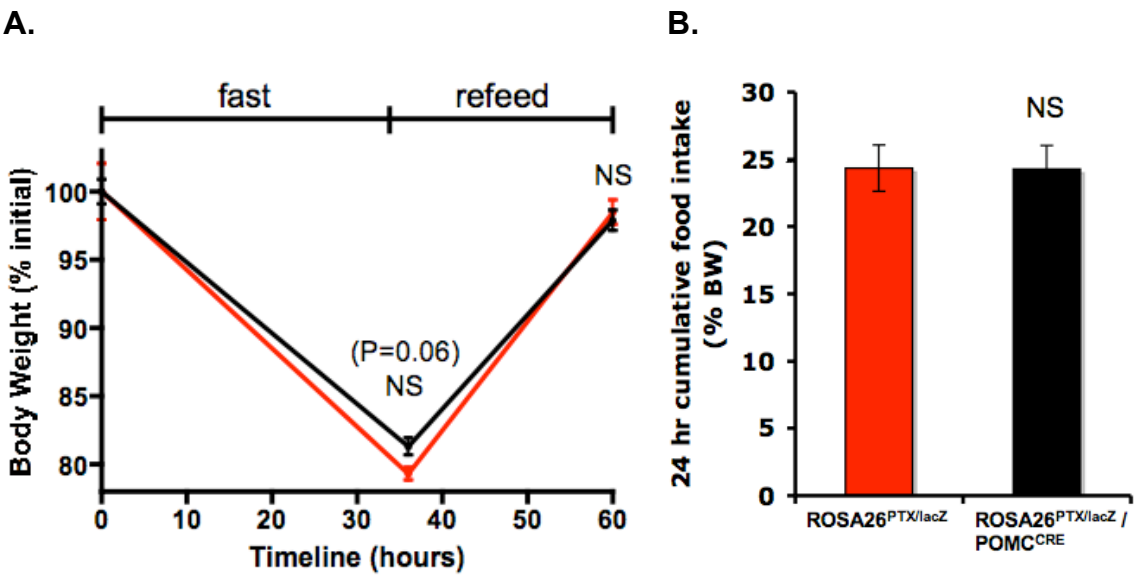


**Figure 12.** Food deprivation and compensatory feeding for ROSA26$^{PTX/lacZ}$/POMC$^{Cre}$ (black, n=9) vs. ROSA26$^{PTX/lacZ}$ (red, n=10) 8 weeks old mice. A) Change in body weight during 36 hr fasting followed up with 24 hr refeeding. B) Compensatory feeding for 24 hr following fasting. Error bars represent the standard error. NS P>0.05.

In combination with the food intake and energy expenditure data, the compensatory feeding experiment suggests that the inhibition of the $G_i$ signaling in the POMC neurons leads to an altered energy expenditure phenotype, not an altered food intake phenotype.

***ROSA26$^{PTX/lacZ}$/POMC$^{Cre}$ mice have regular glucose and glucocorticoid metabolisms.***

To test if the increased body weight led to a diabetic phenotype in ROSA26$^{PTX/lacZ}$/POMC$^{Cre}$ mice, we tested the fasting plasma insulin levels and the glucose tolerance (GTT). Glucose metabolism was unaltered in ROSA26$^{PTX/lacZ}$/POMC$^{Cre}$ mice because the fasting plasma insulin levels and glucose tolerance test (GTT) were identical to the ROSA26$^{PTX/lacZ}$ mice (figure 13A and 13B respectively).

**Figure 13.**

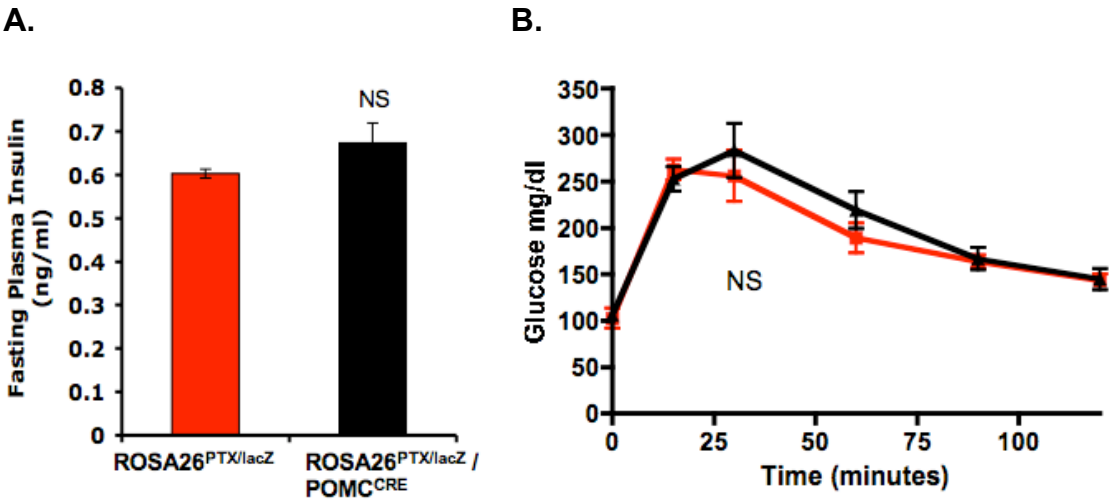


**Figure 13.** Insulin levels and glucose tolerance test for ROSA26$^{PTX/lacZ}$/POMC$^{Cre}$ (black) vs. ROSA26$^{PTX/lacZ}$ (red) 8 weeks old mice. A) Fasting plasma insulin levels. B) Glucose tolerance test (GTT). Error bars represent the standard error for N=5. NS P>0.05.

Because POMC is also expressed in the pituitary, ROSA26$^{PTX/lacZ}$/POMC$^{Cre}$ mice also expressed PTX in select pituitary cells (data not shown). Since the level of pituitary production of POMC regulates glucocorticoid metabolism, we further tested if the inhibition of $G_i$ signaling in the pituitary POMC cells induced a change in the glucocorticoid metabolism. The inhibition of $G_i$ signaling in the POMC expressing pituitary cells did not alter the pituitary POMC expression and did not lead to an increase in the plasma glucocorticoid levels compared to ROSA26$^{PTX/lacZ}$ mice (figure 14A and 14B respectively). Therefore, the decreased energy expenditure and increased body weight phenotype is independent of the pituitary POMC expression and the glucocorticoid metabolism.

**Figure 14.**

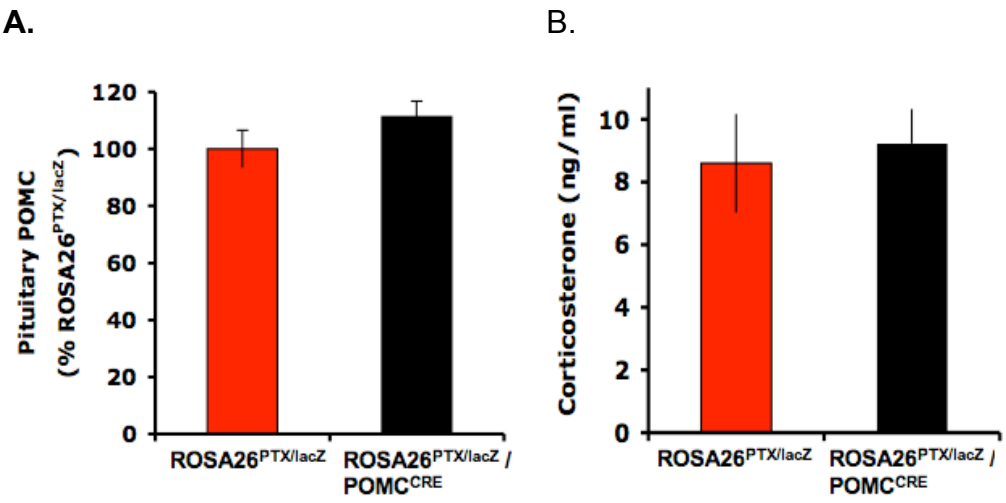


**Figure 14.** Glucose metabolism for ROSA26$^{PTX/lacZ}$/POMC$^{Cre}$ (black) vs. ROSA26$^{PTX/lacZ}$ (red) 8 weeks old mice. A) Pituitary POMC mRNA levels.

## DISCUSSION

### *Inhibition of $G_i$ signaling in POMC neurons results in a similar phenotype to POMC specific deletion of AMP-activated protein kinase.*

The major effect of $G_i$ signaling is the inhibition of adenylyl cyclase activity and a consequent decrease in the intracellular cAMP accumulation[44] (figure 15). Thus, inhibiting the $G_i$ signaling increases the cAMP dependent Protein Kinase A (PKA) activity, and its downstream protein phosphorilation and gene transcription[43] (figure 15). One such downstream target of PKA is AMP-activated protein kinase (AMPK), and its phosphorilation by PKA inactivates AMPK (figure 15). Therefore, we postulated that down regulating AMPK activity in POMC neurons would have similar consequences to inhibiting $G_i$ signaling by pertussis toxin. Among 14 different publications on 14 different POMC neuronal modifications, POMC neuron specific deletion of AMPK$\alpha$2 ($POMC^{AMPK\alpha2(-/-)}$) reduces AMPK signaling and results in similar energy homeostasis phenotype to $ROSA26^{PTX/lacZ}/POMC^{Cre}$ mice with increased body weight, unchanged food intake, and decreased energy expenditure[61-74] (Table 1 and 2).

Further determination of decreased hypothalamic AMPK activity in $ROSA26^{PTX/lacZ}/POMC^{Cre}$ mice compared to $ROSA26^{PTX/lacZ}$ mice would solidify this hypothesis. However, the difference in hypothalamic AMPK activity between $POMC^{AMPK\alpha2(-/-)}$ and wild type (WT) mice was shown to be minimal[67] (90%

reduced AMPK activity compared to WT). Therefore, determining a reduction vs. deletion of AMPK signaling in POMC neurons could present a greater challenge.

**Figure 15.**

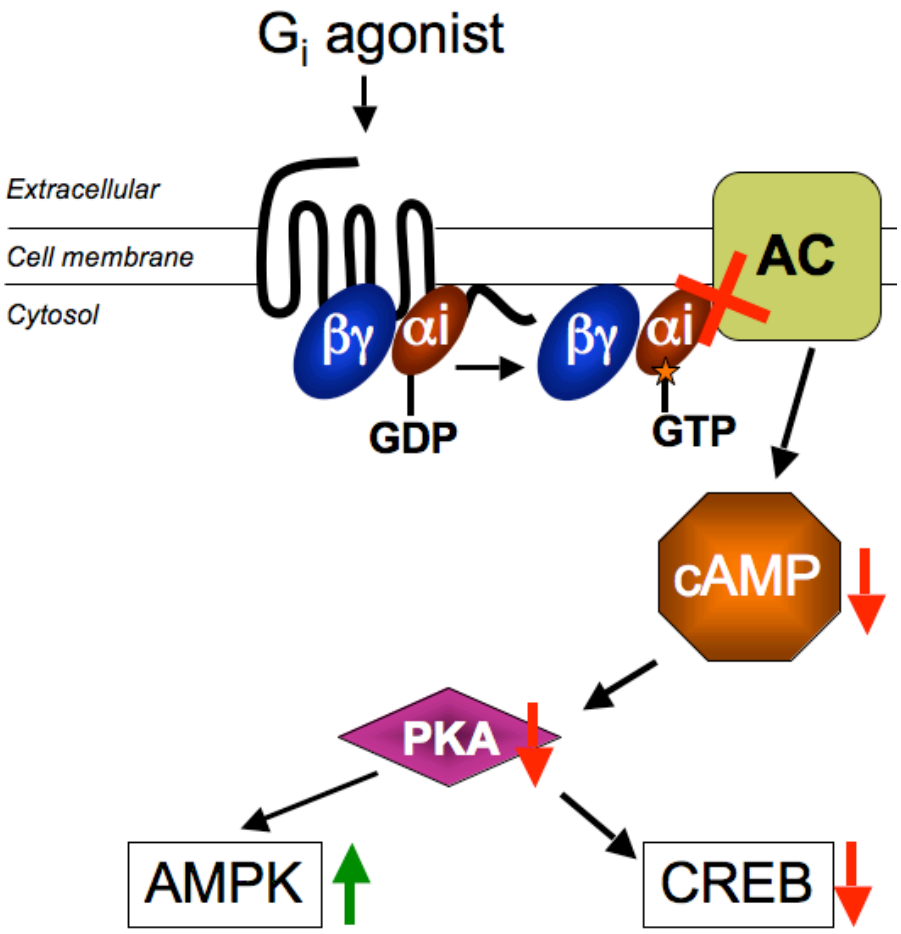


**Figure 15.** Intracellular effectors of $G_i$ protein-coupled receptor activation. Phosphorilated $G_i$ protein complex inhibits adenylyl cyclase activity and its production of cAMP. Reduction in the intracellular cAMP concentration leads to a decrease in the active conformation of cAMP dependent

Protein Kinase A (PKA). Less active PKA results in decreased CREB (cAMP responsive element-binding protein) signaling and more active AMPK (AMP-activated protein kinase) signaling because PKA activates and inhibits these signaling pathways respectively.

**Table 1.**

| | Weight | Food Intake | Lean Mass | Fat Mass | $VO_2$ |
|---|---|---|---|---|---|
| Tfam Neuronal Ablation | + | + | + | + | - |
| DTR Neuronal Ablation | + | + | ND | ND | ND |
| POMC (-/-) | + | + | ND | ND | ND |
| STAT3(-/-) | in female only + | in female only + | No Change | in female only + | ND |
| gp130(-/-) | No Change | No Change | No Change | No Change | ND |
| PTEN (-/-) | + | + | ND | + | No Change |
| Socs3 (-/-) | No Change/ HFD - | No Change | ND | No Change | + |
| Irs2 (-/-) | No Change | No Change | ND | ND | ND |
| AMPK$\alpha$2(-/-) | + | No Change | ND | + | - |
| PDK1 (-/-) | Only 6-8 weeks + | Only at week 6 + | ND | ND | ND |
| InsR (-/-) | No Change | No Change | ND | ND | ND |
| LepR (-/-) (1) | + | No Change | No Change | + | No Change |
| LepR (-/-) (2) | + | ND | No Change | + | Males + / Females - |
| PTP1B (-/-) | No Change/ HFD - | No Change | No Change | - | No Change |

**Table 1.** Energy homeostasis phenotypes of various POMC genetic alteration studies. Abbreviations: (+) increase. (-) decrease. ND - Not determined. HFD - High Fat Diet. $VO_2$ - Oxygen consumption. Tfam - mitochondrial transcription

factor A. DTR - Dyphteria Toxin. Stat3 - Signal Transducer and Activator of Transcription 3. gp130 - Glycoprotein 130. PTEN - phosphatase and tensin homolog. Socs3 - Suppressor of cytokine signaling 3. Irs2 - Insulin receptor substrate 2. AMPK$\alpha$2 - 5' AMP-activated protein kinase alpha 2 subunit. PDK1 - Pyruvate dehydrogenase kinase, isozyme 1. InsR - Insulin receptor. LepR - Leptin receptor. PTP1B - Protein tyrosine phosphatase 1B.

**Table 2.**

| | **ROSA26$^{PTX/lacZ}$/ POMC$^{Cre}$** | **POMC$^{AMPK\alpha2(-/-)}$** |
|---|---|---|
| Weight | + | + |
| Food intake | No Change/ Slight Decrease | No change |
| Fat mass | + | + |
| $VO_2$ | - | - |
| Pharmacological Leptin Sensitivity | No Change | No Change |
| Glucose | No Change | No Change |
| POMC, AgRP/NPY expression | Altered | No Change |

**Table 2.** Comparison of energy homeostasis phenotypes: ROSA26$^{PTX/lacZ}$/POMC$^{Cre}$ vs. POMC$^{AMPK\alpha2(-/-)}$.

***Two different types of signaling pathways in the POMC neurons control food intake and energy expenditure separately.***

Increased food intake and decreased energy expenditure come hand in hand in severely obese patients, hence rising the probability that decreased energy expenditure is an inevitable secondary consequence of increased food intake and body weight. However, such an assumption would lead to the conclusion that there is no primary metabolic regulation of energy expenditure; it is a mere consequence of increased weight gain. To the contrary, various investigations provide strong evidence for the metabolic regulation of energy expenditure and food intake independent of each other.

Leptin's pharmacological effect of decreased food intake has been well established and is also repeated in this study (figure 7B). Also, when administered to food-restricted lean mice, leptin increases energy expenditure independent of food intake and body weight[75]. Therefore, leptin must be a direct metabolic regulator of energy expenditure since increased energy expenditure is not an instantaneous secondary effect of decreased food intake and decreased body weight.

Recently, another study demonstrated the divergence of food intake and energy expenditure regulation further downstream of leptin signaling. Balthasar

et al. hypothesized that different subset of MC4R expressing neurons can modulate food intake and energy expenditure independent from each other[76]. MC4R knock out mice have increased food intake and reduced energy expenditure because they cannot relay the leptin's anorexigenic signal[13, 17, 33, 77, 78]. Therefore, all MC4R expressing neurons in the hypothalamus were thought to regulate food intake and energy expenditure in unison[76] (Figure 16, previous view). Nonetheless, In the MC4R knockout mouse, the rescue of MC4R activity specifically to Sim1 (Single-minded gene 1) expressing neurons (limited to the Paraventricular Nucleus (PVH) and Amygdala) rescued only the increased food intake phenotype; energy expenditure remained low. Therefore, the authors proposed that different subsets of MC4R expressing neurons must regulate food intake and energy expenditure independent from each other[76] (figure 16, new view).

**Figure 16.**

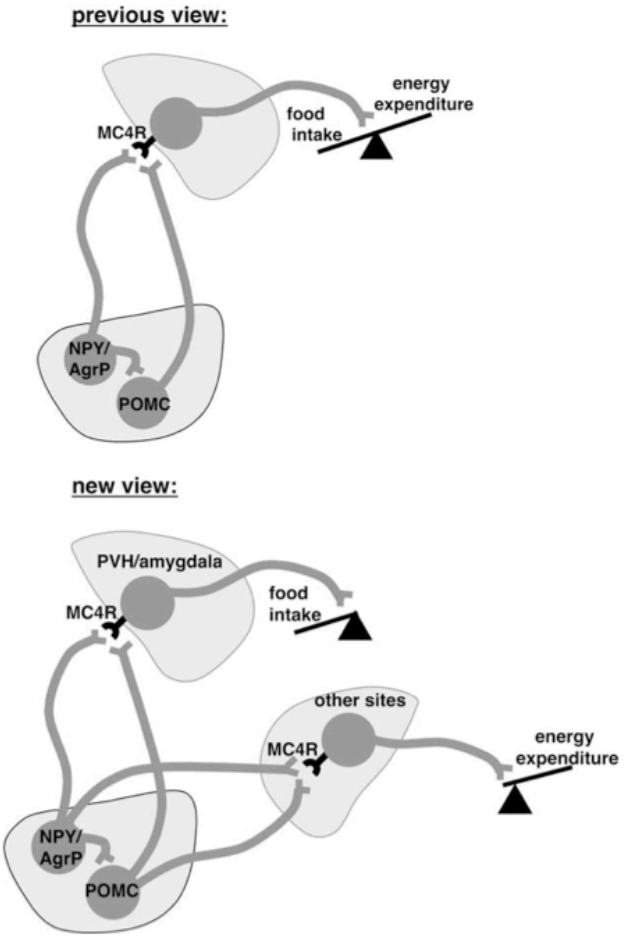


*Balthasar N. et al. Cell 2005*

**Figure 16.** Functional separation of MC4R neurons as published by Balthasar et al. Two different subset of MC4R expression neurons regulate food intake and energy expenditure separately and independent from each other.

On the other hand, our results suggest that food intake and energy expenditure do not necessarily require different subset of neurons. Altering only one specific signaling pathway in POMC neurons, the $G_i$ signaling pathway specifically changed energy expenditure independent of food intake. This is

reminiscent of the POMC$^{AMPK\alpha2(-/-)}$ mouse model where the increased body weight is correlated to decreased energy expenditure, not the food intake[67]. In the POMC neurons where the major regulator of food intake is leptin signaling, the $G_i$ signaling specifically regulates energy expenditure (Figure 17). Our results provide further evidence that decreased energy expenditure in obesity is not necessarily a secondary effect of increased body weight. Alteration of energy expenditure alone in the absence of increased food intake is a sufficient cause to increase the body weight.

**Figure 17.**

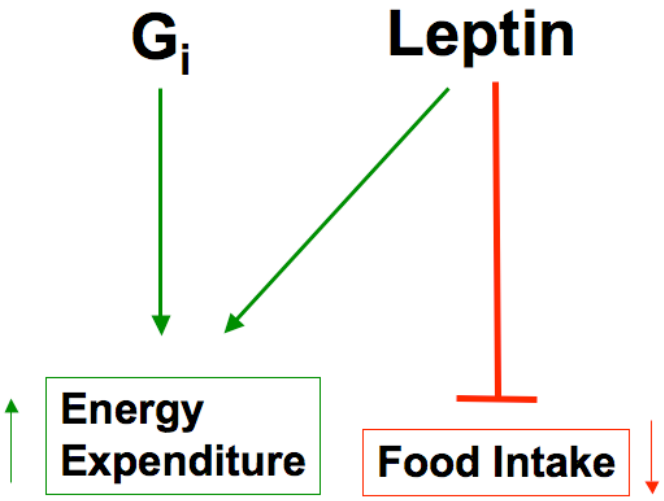


**Figure 17.** Cross-talk and roles of leptin and $G_i$ signaling in POMC neurons.

***POMC neuron specific $G_i$ signaling: a possible target to by-pass leptin resistance?***

Leptin resistance develops quickly with obesity[79]. Obese patients do not respond to pharmacologically administered leptin; therefore, they cannot benefit from its anorexigenic effect. In fact, plasma leptin levels of obese patients are already elevated due to increased adiposity. Many pharmaceutical and academic laboratories study the cause of leptin resistance in order to use leptin as a pharmaceutical agent to treat obesity, or to increase the sensitivity of obese patients to their own physiologically elevated leptin levels.

In the POMC and AgPR neurons, leptin signals through LepRb receptor that transmits its intracellular signal through Jak2 and Stat3 proteins[79]. Down regulation of leptin signaling by negative feedback and leptin resistance occur early in the signaling pathway. Therefore, an alternative pathway that by-passes leptin signaling in POMC neurons could prove to be beneficial for the patients with leptin resistance. One such mechanism has been utilized to activate POMC neurons independent of the leptin signaling. Activation of a $G_q$ protein-coupled receptor ($5HT_{2C}$) specifically expressed on the POMC neurons by Dexfenfluramine has the similar anorexigenic effect of leptin, and it promotes weight loss in obese patients with leptin resistance[45].

Our study also suggests that modulating the $G_i$ signaling pathway in POMC neurons could regulate energy homeostasis. Since the inhibition of $G_i$

signaling pathway in POMC neurons leads to weight gain due to decreased energy expenditure, an antagonist for a POMC neuron specific $G_i$ protein-coupled receptor has a potential to be developed into a drug for the treatment of cachexia. It is also plausible that; in a reversible manner, activation of a POMC neuron specific $G_i$ protein-coupled receptor could trigger increased energy expenditure. Such a therapeutic could be beneficial for obese patients with leptin resistance. In order to validate these possible treatment opportunities, further research in determining POMC specific $G_i$ protein-coupled receptors, and pharmacological testing of their specific ligands will be essential.

## MATERIALS AND METHODS

All procedures were performed with the approval of the University of California San Francisco (UCSF) Institutional Animal Care and Use Committee (IACUC). Mice were housed at 21°C with normal 12 hr. light-12 hr. dark cycle and free access to water and food. All mice were 129/Sv and C57BL/6J background with over 99% homology to C57BL/6J gene expression (7-13 times backcrossed to C57BL/6J background). Only the male mice were utilized in the experiments.

***Mouse Models*** - $ROSA26^{PTX}$ [58], $ROSA26^{lacZ}$ [59], and $POMC^{CRE}$ [60] mice have been previously described. $ROSA26^{PTX}$ mouse was obtained from S.R. Coughlin (UCSF, San Francisco CA). $ROSA26^{lacZ}$, and $POMC^{CRE}$ mice were provided by A.W Xu (UCSF, San Francisco CA).

***Body Weight & Composition*** - Mice body weight was measured every week from the age of weaning until 18 weeks old. Body composition as fat and lean body mass was measured for 8 to 12 weeks old adult mice by Dual Energy X-Ray Absorptiometry (DEXA) instrument, Lunar PIXImus2 (Lunar Corp, Madison, WI). The length of the mice was measured under anesthesia at 8 weeks of age from the tail root (anus) to the snout in centimeters.

***Food Intake*** - mice were single-caged for food intake study after weaning at 3 weeks. After a week of acclimation food intake was measure every day for a period of 10 days. Body weight was measured at the beginning and the end of 10 days food intake measurement period. Daily food intake was averaged for 10 days and normalized to average body weight throughout the 10 day period. Food efficacy was calculated by dividing food intake per day (grams) by weight gain per day (grams).

***Compensatory Feeding*** - 7 weeks old mice were single-caged and acclimated for a week prior to the experiment. Food was removed at $7.00^{AM}$ on day 1 and replaced 36 hrs after at $7.00^{PM}$ on day 2. 24 hr compensatory food intake was measured at $7.00^{PM}$ on day 3. Body weight was measured at the beginning ($7.00^{AM}$ on day 1), at the end of fasting ($7.00^{PM}$ on day 2), and at the end of 24 hr compensatory feeding period ($7.00^{PM}$ on day 3). Body weight and food intake were normalized to initial body weight.

***X-gal Staining*** - 8 weeks old mice were first anesthetized with an I.P. injection of avertin (20 mg/ml, 0.2ml by ten grams of body weight) and perfused with cold PBS (15ml) followed by freshly prepared 4% paraformaldehyde and 0.2% glutaraldehyde in PBS (1ml/gram weight of mice) into the left ventricle of the heart with a butterfly needle 27 X3/8 with an 8 inch tubing (Abbott Laboratories North Chicago, IL). Surgically removed whole brain and pituitary samples were post-fixed in 4% paraformaldehyde for 2 hrs following the perfusion, then washed

(3x 10mins) with 0.1% Triton X-100 in PBS at room temperature. Xgal staining was performed overnight at 37C in PBS containing 5 mM potassium ferricyanide, 5 mM potassium ferrocyanide, 1 mM $MgCl_2$, and 1 mg/ml X-gal. For cryosectioning, brain and pituitary samples were incubated at 4C in 30% sucrose for 24 hrs. Brain and pituitary were embedded in M-1 embedding matrix (Thermo Electron Co., Pittsburgh, PA) and frozen on dry ice for at least 1 hour. With a cryostat (LEICA CM 1800 Cryostat) section of 10 to 30 um were cut and mounted on Superfrost/Plus microscope slides (Fisherbrand, Pittsburgh, PA) and kept at -80C. Imaging the X-gal staining in the arcuate nucleus was performed using Zeiss Axio Imager Optical Microscope before (whole brain) and after the cryosectioning (slice).

***mRNA Expression*** - Fed 8 weeks old mice were sacrificed. The hypothalamus and pituitary tissue we dissected and immediately preserved in RNA later solution (Qiagen, Valencia CA). mRNA was extracted from the tissue using Rneasy mini kit (Qiagen, Valencia CA) and was processed according to the manufacturer protocol. After mRNA purification, remaining DNA was eliminated by Dnase Turbo (Ambion, Applied Biosystem Inc., Foster City, CA), and total mRNA yield was measured by spectrophotometry. Oligo dT primers and reverse transcriptase (Superscript II, Invitrogen, Carlsbad CA) were used in RT-PCR to convert 1.5μg mRNA into cDNA. Final cDNA was quantified by real time PCR assay using primer sets designed to amplify gene expression of interest (PTX, POMC, AgRP, NPY). We used a 2X SYBRgreen master mix (Applied Biosystem

Inc., Foster City, CA) and 0.1μM of primer per reaction. Real time PCR was performed on a light cycler, 7900HT (Applied Biosystem Inc. Foster City, CA) and each reaction was normalized with two internal housekeeping genes (beta-actin, cyclophilin A) for control. PTX, POMC, AgRP, NPY, beta-actin, and cyclophilin A primer sets are available upon request.

***Plasma Leptin Level & Sensitivity***

*Plasma leptin* - 8 weeks old fed mice were sacrificed and plasma was collected from blood in serum separator tubes (BD microtainer, Franklin Lakes, NJ). Plasma leptin level was determined by Leptin ELISA according to the manufacturer's manual (Leptin EIA kit, Alpco Inc. Windham NH). 5μl of serum per sample was run in duplicate for each mouse.

*Pharmacological leptin sensitivity* - leptin was obtained from the National Hormone and Peptide program (NHPP) and was suspended in phosphate buffer saline (PBS), pH 7.4, for I.P. administration. 7 weeks old mice were single-caged and acclimated for one week prior to the experiment. All mice were given PBS by I.P. injection at 8.00 $^{AM}$ and 5.00 $^{PM}$. 24 hr food intake was measured and standardized for 3 consecutive days. On the forth day, mice were given leptin (2.5mg leptin per kg body weight) by I.P. injection at 8.00 $^{AM}$ and 5.00 $^{PM}$. 24 hr food intake upon leptin administration was measured and normalized to food intake upon PBS administration.

***Plasma Insulin Level & Glucose Tolerance Test*** - For serum Insulin measurement and glucose tolerance test 8 weeks old mice were fasted overnight prior to testing. The blood was collected by the tail vain the next morning. Plasma was separated by centifugation, and the plasma insulin level was determined by Insulin ELISA (ultra sensitive insulin EIA, Alpco Inc. Windham NH) using 5μl serum sample size. For the glucose tolerance test mice were injected with 2 grams/kg body weight of 20% D-glucose by I.P. administration. At 15, 30, 60 and 120 minutes blood glucose was sampled from the tail and measured with a glucometer (Ascensia Elite XL, Bayer Co. Tarrytown NY).

***Plasma Glucocorticoid level*** - 8 weeks old fed mice were sacrificed by quick euthanasy technique, and plasma was collected from blood in serum separator tubes (BD microtainer, Franklin Lakes, NJ). Plasma corticosterone level was determined by Corticosterone ELISA (Corticosterone EIA, Cayman Inc. Ann Arbor, MI) using 50μl of serum sample.

***Energy expenditure*** - Metabolic rate was determined by measuring $VO_2$ and $VCO_2$ levels by Oxymax system (Columbus Instruments, OH) located in a limited access room, minimizing factors that could affect the behavior and the activity of the mice. 7 weeks old mice were single-caged and acclimated for a week. On the day of the experiment, mice were placed in bedded Oxymax chambers (4" X 5" X 8") and were provided with water and food supply. Mice were acclimated to Oxymax chambers for 2 hr, and the $VO_2$ and $VCO_2$ measurements were

collected every 10 minutes for the following 24 hr. Data was averaged to hourly metabolic rate and normalized to the lean body mass (determined by DEXA).

# Chapter II

## Expanding the Role of the N-terminal Domain in the Evolution of GPCR Activity Modulation

*...The Molecular mechanism of the N-terminal domain mediated constitutive activity of Melanocortin-4 Receptor.*

**SUMMARY**

A large number of G protein-coupled receptors rely on their N-terminal domains for ligand recognition and activation. However, most of the information on the activation of these receptors has been provided through the study of those identified and studied on the bases of their ability to be activated by specific diffusible physiological or pharmacological ligands interacting directly with their core transmembrane regions. This raises the question of the functional and evolutionary link between N-terminal mediated and direct GPCR activation. Here we address this issue by dissecting the molecular interactions underlying both modes of activation in a single receptor, the Melanocortin-4 Receptor. We find that activation of this receptor by its N-terminal domain specifically requires amino-acids outlining the conserved rotamer toggle-switch domain while the high-affinity physiological agonist of this receptor requires a separate sets of residues for activation. The additional observation that the activation by the N-terminal domain can be independently modulated by the physiological inverse-agonist of MC4R leads us to suggest that a number of constitutively active orphan GPCR could have physiological inverse agonists as sole regulators.

## INTRODUCTION

Seven trans-membrane G protein-coupled receptors (GPCRs) are the largest and most diverse superfamily of membrane-bound receptors and the target of half of all pharmaceutical drugs. These molecules have an extracellular N-terminal domain and a simple architectural core of seven trans-membrane helices (TM1 to TM7) connected by extracellular and cytoplasmic loops (figure 1).

**Figure 1.**

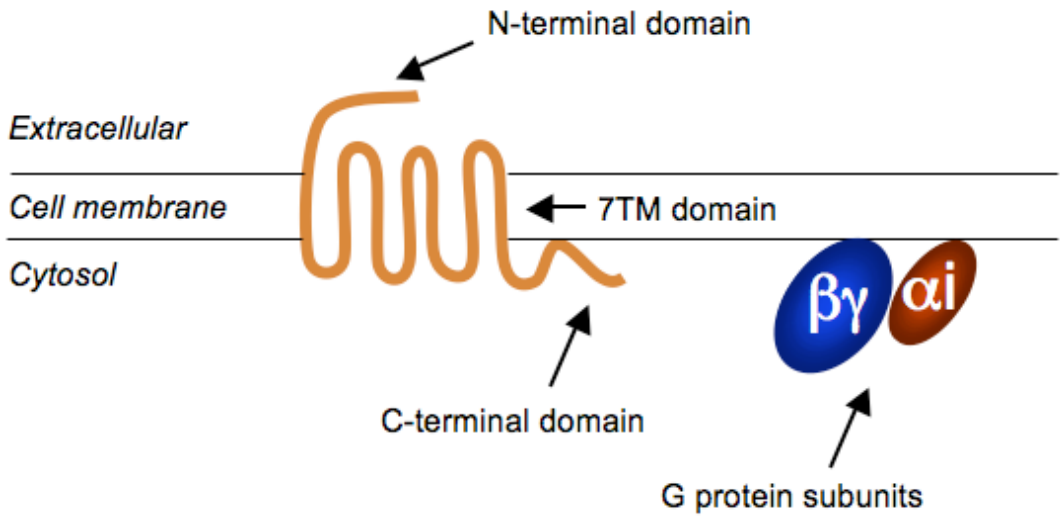


**Figure 1.** Specific domains of G protein-coupled receptors and G proteins. Two straight lines represent the phospholipid bilayer of the cell membrane. Serpentine (snake-like) model of GPCR is depicted in orange, 7TM (seven transmembrane) helical domain spans through the cell membrane.

The GPCR superfamily is subdivided into different sub-groups on the basis of phylogenetic criteria as well as conserved residues within the helices and the size and characteristics of their N-terminal domain which plays an essential role in the activation of most classes of GPCRs. Class B Secretin receptors have a conserved N-terminal Cysteine network that stabilizes their structure, and altering the N-terminal domain impairs ligand interactions (figure 2). Class B adhesion receptors have a diverse variety of N-terminal domain motifs, which determine the ligand specificity of the receptors (figure 2). Class C glutamate receptors have a conserved N-terminal Venus flytrap that regulates ligand binding and receptor activity (figure 2). Frizzled/Smoothened receptors possess N-terminal Wnt binding domains for ligand recognition and activation[80-82] (figure 2). For classA/Rhodopsin receptors, the largest family of GPCRs, the role of the N-terminal domain in the activation of the receptors has been significantly less addressed with the exceptions of protease-activated receptors (PARs), in which activation of the receptor is dependent on proteolytic cleavage and unmasking of an N-terminal domain that acts as a tethered ligand[83] figure (figure 3A) , and glycoprotein receptors (figure x).

**Figure 2.**

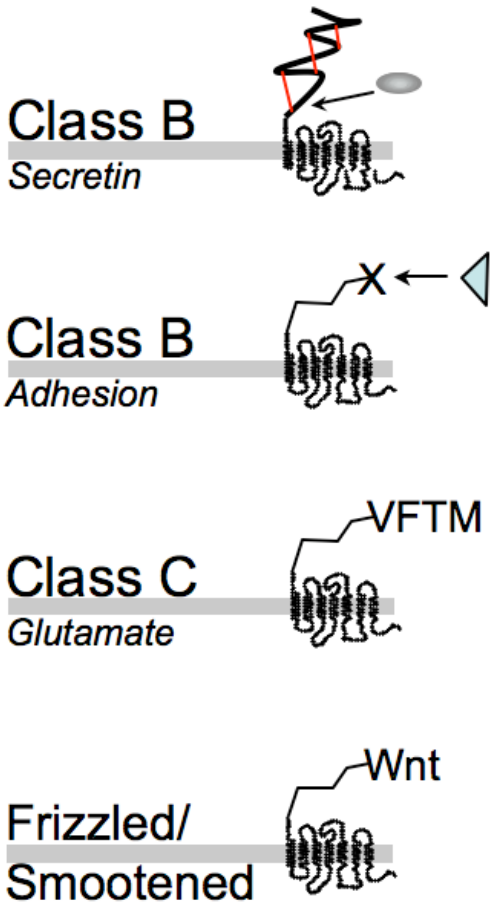


**Figure 2.** The role of the N-terminal domain in ligand binding and recognition in GPCRs. Class B Secretin-like receptors - red lines depict the conserved Cyteine network. Class B Adhesion receptors - "X" represents possible diverse N-terminal motifs. Class C Glutamate receptors - VFTM (Venus Flytrap Motif). Frizzled/Smoothened receptors - Wnt motif.

**Figure 3.**

**A.**

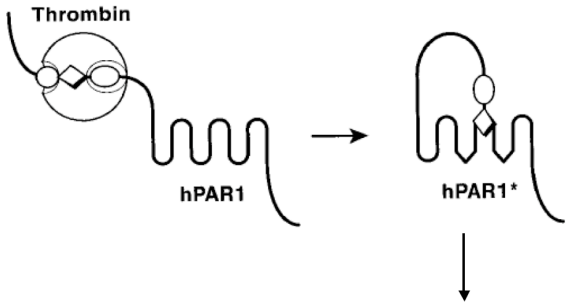


**B.**

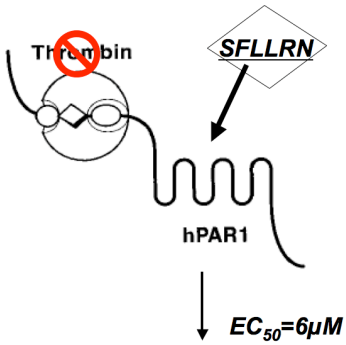


*Coughlin SR, PNAS 1999*

**Figure 3.** Activation mechanism of PAR1. A) Proteolytic cleavage of the N-terminal domain by thrombin unmasks an activating neo-N-terminal sequence, which interacts and activates the receptor through the 7TM domain. B) In the absence of Thrombin, exogenous addition of a peptide that mimics the neo-N-terminal domain can activate the receptor with low affinity.

Despite this recognized role of the N-terminal domain in GPCR activation, a very limited number of studies have attempted to understand the functional molecular interactions between this domain and the core of the receptor. This is due to the historic emphasis on Rhodopsin, a class A GPCR in which the ligand is covalently linked to the core of the receptor and the first GPCR for which a crystal structure was available, and to the focus on GPCRs identified and studied on the bases of their ability to be activated by specific high-affinity diffusible pharmacological ligands interacting directly with the core transmembrane regions of the receptor.

Here we define and compare the relative molecular interactions underlying activation by the N-terminal domain and by a physiological high-affinity agonist at a single receptor, the Melanocortin-4 Receptor (MC4R). MC4R is one of five melanocortin receptors (MCRs), a subfamily of the a group of class A $G_s$-coupled GPCRs. MC4R is expressed in the central nervous system and is essential for the maintenance of long-term energy balance in humans. Heterozygous mutations in MC4R are the most common genetic cause of severe human obesity and over 80 naturally occurring pathogenic mutations in this receptor have been described[34, 35, 37, 38, 84]. A number of studies have mapped the interaction of the endogenous physiological agonist of MC4R, $\alpha$–MSH, to acidic amino-acids in TM2 and TM3 of the receptor. In addition to this high-affinity ligand, the N-terminal domain of MC4R also activates the receptor, which therefore displays a constitutive activity shown to be of *in vivo* functional

relevance[85, 86]. Remarkably, MC4R, and two other members of the melanocortin receptor sub-family, are also unique among GPCRs in physiologically responding to endogenous antagonists[87-90]. Indeed, Agouti Related protein (AGRP), released by an independent population of neurons is both an antagonist, as it inhibits $\alpha$–MSH activation of MC4R, and an inverse-agonist as it inhibits its constitutive activity.

Using a peptid mimic of the MC4R N-terminal domain as a pharmacological agent, we find that inverse agonism by the endogenous ligand AGRP at this receptor can be attributed to specific antagonism of the N-terminal domain. By comparing the activation of the receptor by its N-terminal domain and by $\alpha$-MSH through systematic alanine-scanning mutagenesis, we find that activation by these agonists occurs through distinct molecular mechanisms. Interestingly, the N-terminal domain activates the receptor through a set of amino acids that are crucial for a conserved mode of activation among class A GPCRs, suggesting that inverse agonism may be the original mechanism for modulation of the activity of this receptor.

## RESULTS

### *The N-terminal domain of MC4R acts as a diffusible ligand.*

We had previously demonstrated that the N-terminal domain of MC4R is a tethered ligand and is essential for the maintenance of its constitutive activity[86]. Specifically, a receptor lacking the first 24 N-terminal amino acids (MC4R Δ1-24, figure 4) responds normally to a panel of agonists and to AGRP antagonism of α-MSH (figure 5 and Table 1) but has a low constitutive activity that can be rescued by co-expression of the MC4R N-terminal domain chimerically linked to the trans-membrane domain of CD-8[86]. The activation of MC4R by its N-terminal domain resembles that of PAR1, in which unmasking of the active site requires proteolytic cleavage by thrombin[83, 91] (figure 3A). In the case of PAR1, it had been shown that, in the absence of thrombin, exogenous addition of a synthetic peptide mimicking the unmasked active N-terminal domain can also lead to the activation of the receptor[83] (figure 3B). To determine whether this could also be the case for MC4R, we tested whether a peptide mimicking amino acids 2 through 26 of the N-terminal domain would act as a partial agonist for MC4R Δ1-24. Indeed, at 100mM, MC4R2-26, but not MC4R20-39, increased the activity of MC4R Δ1-24 to the level of the constitutive activity of WT MC4R (Figure 6A). The low potency of the N-terminal domain activation ($EC_{50}$=72mM) (Figure 6B) is compatible with the high local concentration in the tethered form and is similar to that observed in the case of PAR1[91] (figure 3B).

**Figure 4.**

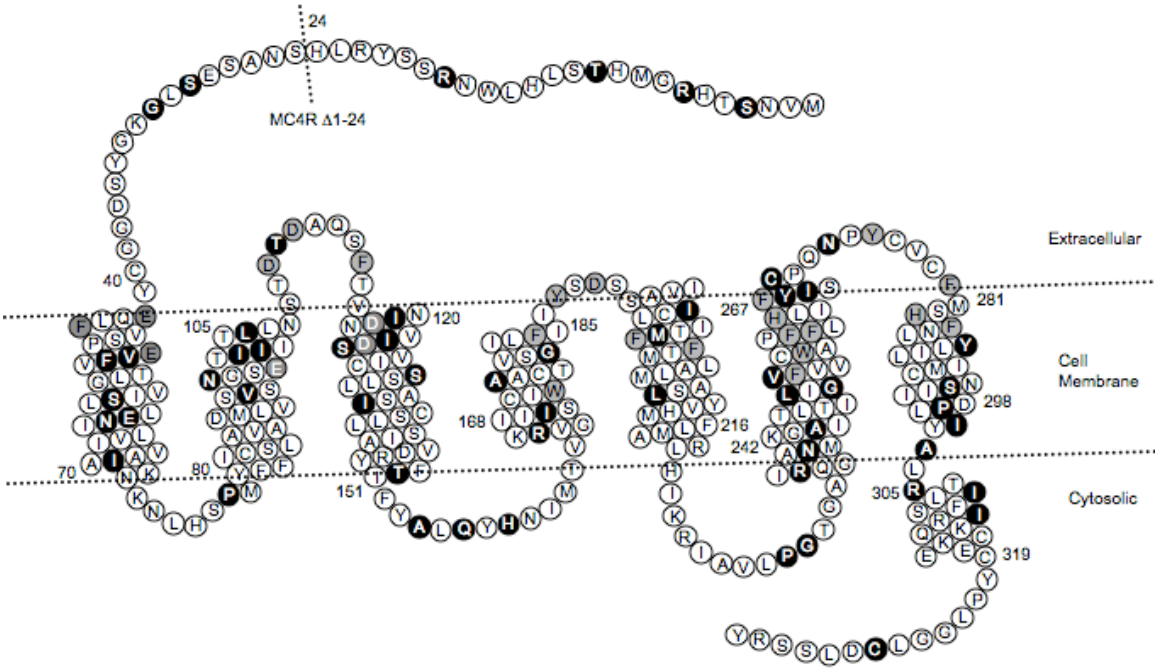


**Figure 4.** The serpentine of MC4R outlining the studied amino acids. MC4R Δ1-24, ATG translational start site (dashed line). Naturally occurring obesity causing mutations (white on black). Mutations that cause premature termination of translation or frame shift are not shown. Residues implicated exclusively in the αMSH activation of MC4R (white on grey). Alanine mutagenesis targeted polar and aromatic amino acids (black on grey).

**Figure 5.**

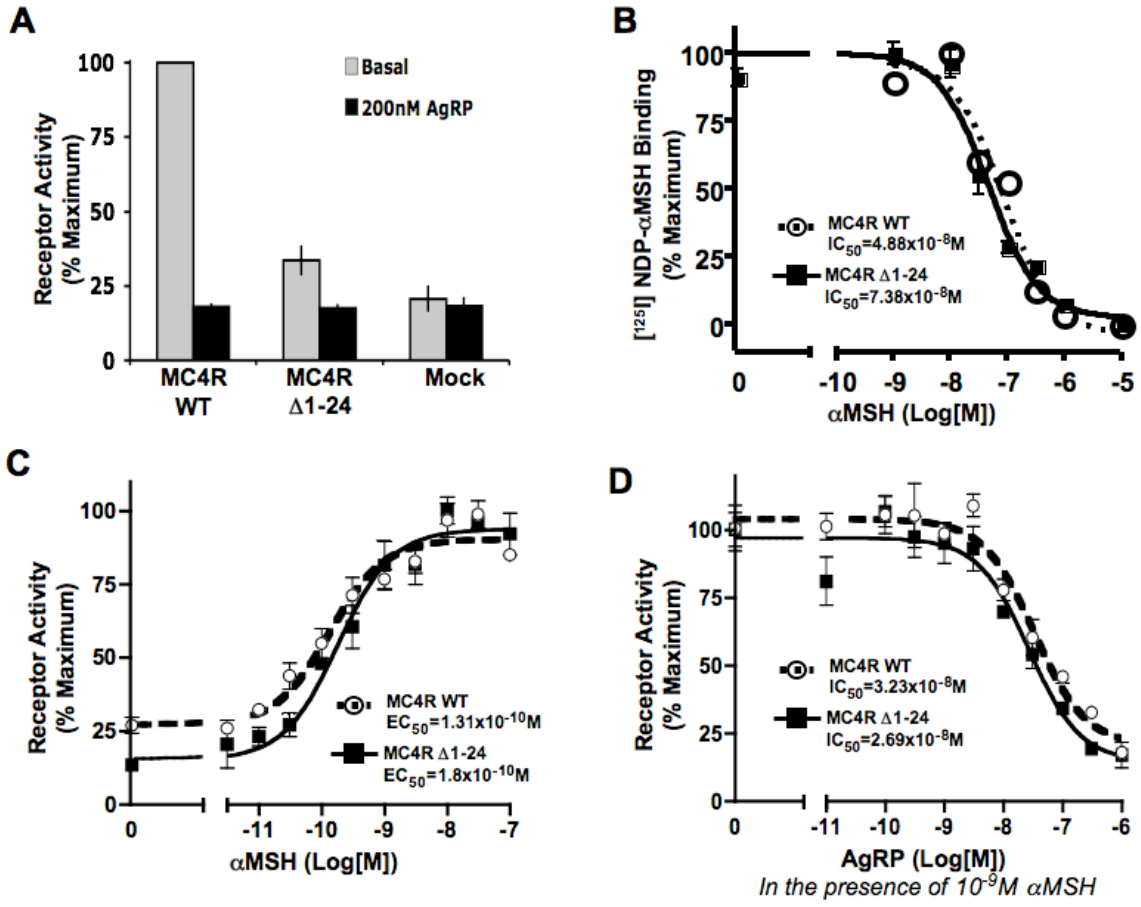


**Figure 5.** Functional studies of MC4R Δ1-24. A) Δ1-24 and WT MC4R basal activity. Black bars represent inverse agonism by AgRP. B) αMSH binding of Δ1-24 and WT MC4R. C) Δ1-24 and WT MC4R activation by αMSH. D) AgRP antagonism of αMSH activation for Δ1-24 and WT MC4R. Error bars represent standard error for the triplicate.

**Table 1.**

| WT MC4R | $EC_{50}$ (nM) | $EC_{50}$ $CI_{95}$ | $E_{max}$ (% WT maximum) | $E_{max}$ $CI_{95}$ |
|---|---|---|---|---|
| **βMSH** | 0.6027 | 0.27 to 1.35 | 84.51 | 79.41 to 89.60 |
| **γMSH** | 268.5 | 145.40 to 495.90 | 94.68 | 86.26 to 103.1 |
| **MTII** | 0.04381 | 0.01652 to 0.1162 | 77.41 | 72.14 to 82.67 |
| **THIQ** | 0.07545 | 0.0379 to 0.1503 | 94.17 | 89.16 to 99.18 |

| MC4R Δ1-24 | $EC_{50}$ (nM) | $EC_{50}$ $CI_{95}$ | $E_{max}$ (% WT maximum) | $E_{max}$ $CI_{95}$ |
|---|---|---|---|---|
| **βMSH** | 1.675 | 0.52 to 5.38 | 84.67 | 73.03 to 96.32 |
| **γMSH** | 194.8 | 110.10 to 344.90 | 94.2 | 84.57 to 103.8 |
| **MTII** | 0.02308 | 0.007 to 0.0758 | 74.66 | 67.05 to 82.28 |
| **THIQ** | 0.1887 | 0.1055 to 0.3376 | 90.79 | 84.33 to 97.25 |

**Table 1.** MC4R activation by βMSH, γMSH, THIQ, and MT-II. One-way ANOVA test shows non-significant difference between Δ1-24 and WT MC4R activation. Sigmoidal dose response curves, $EC_{50}$, $E_{max}$ values and their 95% confidence intervals were calculated using Prism 4. N = 5 for all experiments.

**Figure 6.**

**A.**

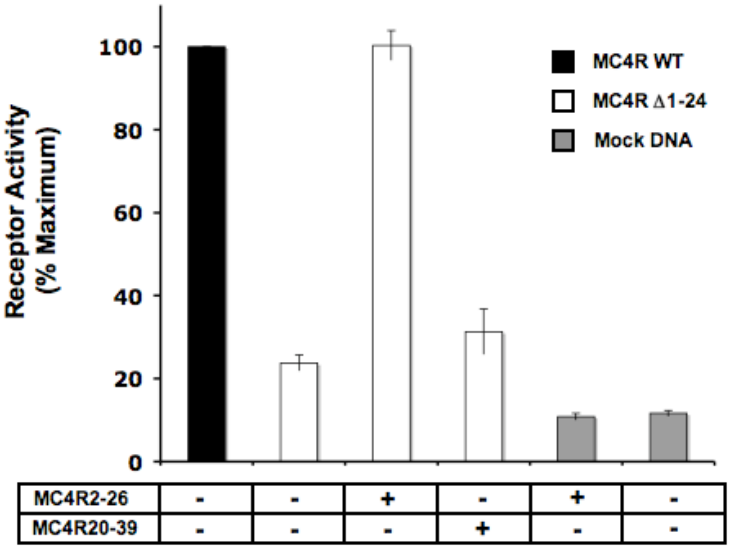


**B.**

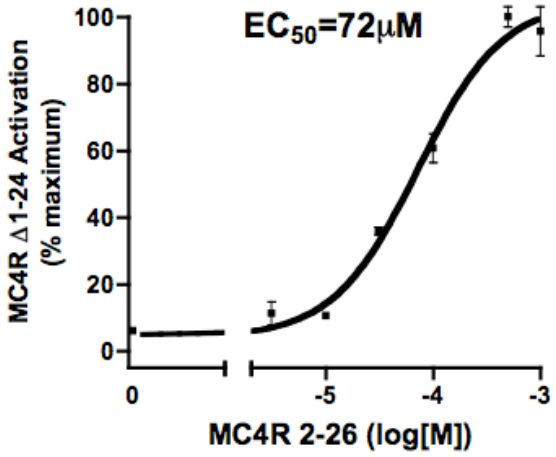


**Figure 6.** MC4R2-26 peptide is a partial agonist of MC4R Δ1-24. A) The full 2-39 amino acid sequence of MC4R N-terminal domain has been synthesized as two peptides: 2nd through 26th amino acids (MC4R2-26) and 20th through 39th amino acids (mock peptide). Stimulation of MC4R Δ1-24 with 2-26 vs. 20-39 N-terminal peptides.

The assay control for background activation was done using pcDNA3.1 that encodes LacZ. B) MC4R2-26 dose response. MC4R Δ1-24 transfected cells were stimulated with increasing concentrations of MC4R2-26. Receptor activation is calculated as percentage of maximal activity recorded in the presence of MC4R2-26 (0.5mM).

***AGRP antagonizes the diffusible MC4R2-26 N-terminal domain.***

AGRP is both an antagonist of α-MSH and an inverse-agonist at the MC4R[89, 90]. Its antagonist activity is independent of the N-terminal domain (Supplemental Figure 5D). Availability of an active diffusible N-terminal domain allowed us to test whether the inverse-agonist activity of AGRP could be exclusively assigned to antagonism of the N-terminal domain (Figure 7A). AgRP antagonized the activation of MC4R Δ1-24 by MC4R2-26 with an identical $EC_{50}$ as that for the inverse agonism of AgRP on the WT receptor (Figure 7B). In addition, MC4R2-26 displaced radio-labeled AgRP with similar affinities for WT and Δ1-24 MC4R (Figure 7C). Together, these data indicate that the inverse agonist activity of AGRP at the MC4R can be attributed to its antagonism of the N-terminal domain of that receptor.

**Figure 7.**

**A.**

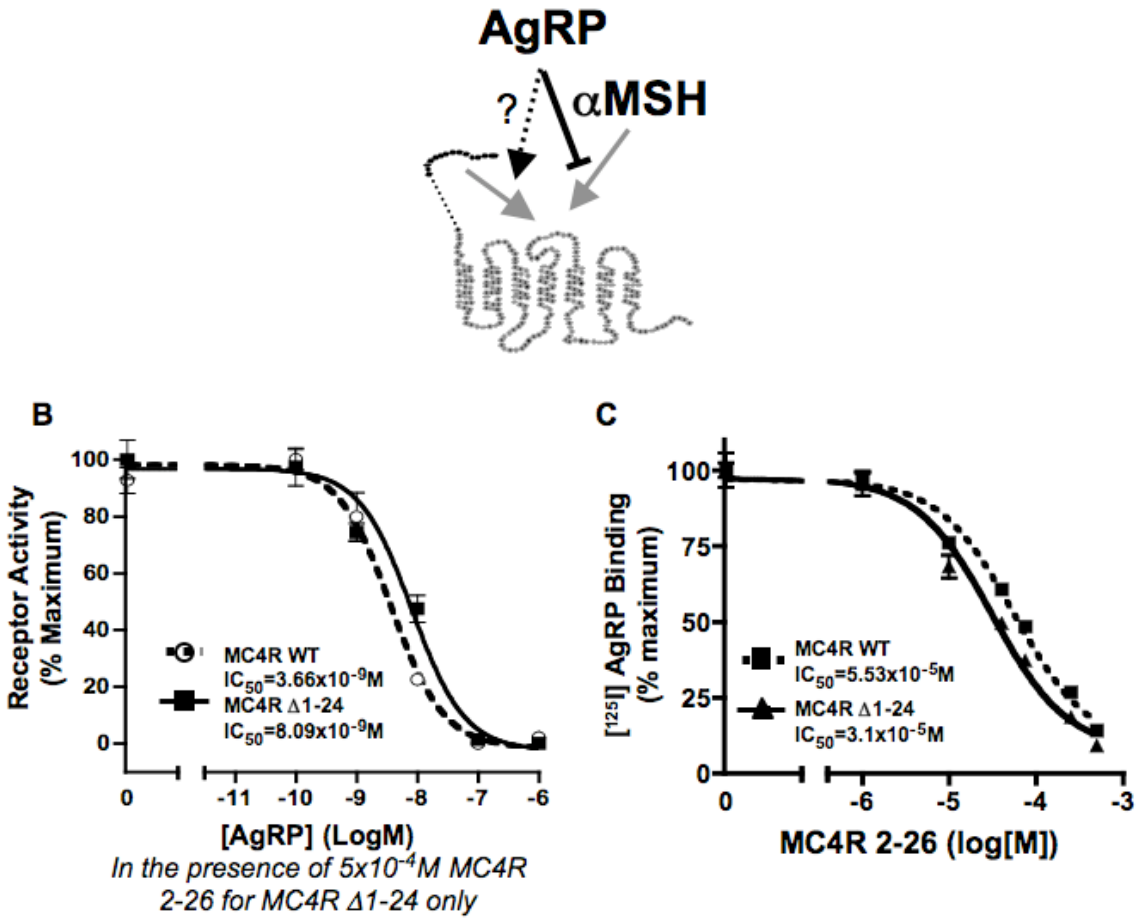


**Figure 7.** Independent modulation of MC4R2-26 activation. A) The model of Independent regulation of N-terminal domain by the AgRP. B) AgRP antagonism of MC4R2-26 activation of MC4R Δ1-24 compared to AgRP inverse agonism of WT MC4R. C) MC4R2-26 binding to Δ1-24 and WT MC4R. $^{125}$I AgRP is used as the competitive radio-labeled ligand. Error bars represent standard error for the triplicate.

***The MC4R2-26 activation site does not overlap with the αMSH activation site.***

Three acidic residues in the second and third transmembrane domains of melanocortin receptors ($E_{100}$ , $D_{122}$ , and $D_{126}$ in MC4R, Figure 1 - white on grey) are essential for their activation by melanocortins. Alanine substitution of these residues impairs αMSH binding and activation but does not decrease the constitutive activity of the receptor[86] (figure 8A). To determine if the activation site of MC4R by its N-terminal domain overlaps with α-MSH, we tested whether these mutations also affected activation by the N-terminal domain. When introduced into MC4RΔ1-24, E100A, D122A and D126A impaired activation of the receptor by αMSH but not by MC4R2-26 (Figure 8B) demonstrating that these three residues are not implicated in activation by the N-terminal domain.

**Figure 8.**

**A.**

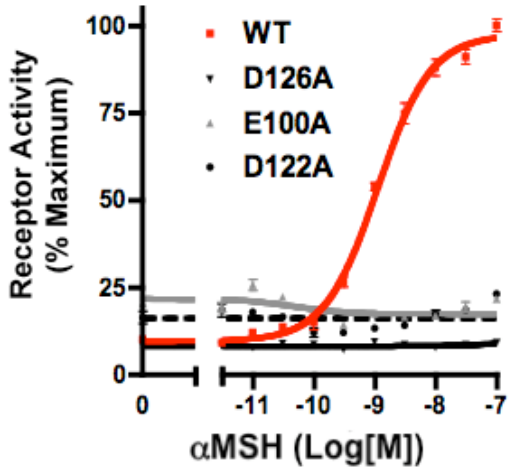


*(Figure 8 continued on the next page)*

**Figure 8.**

**B.**

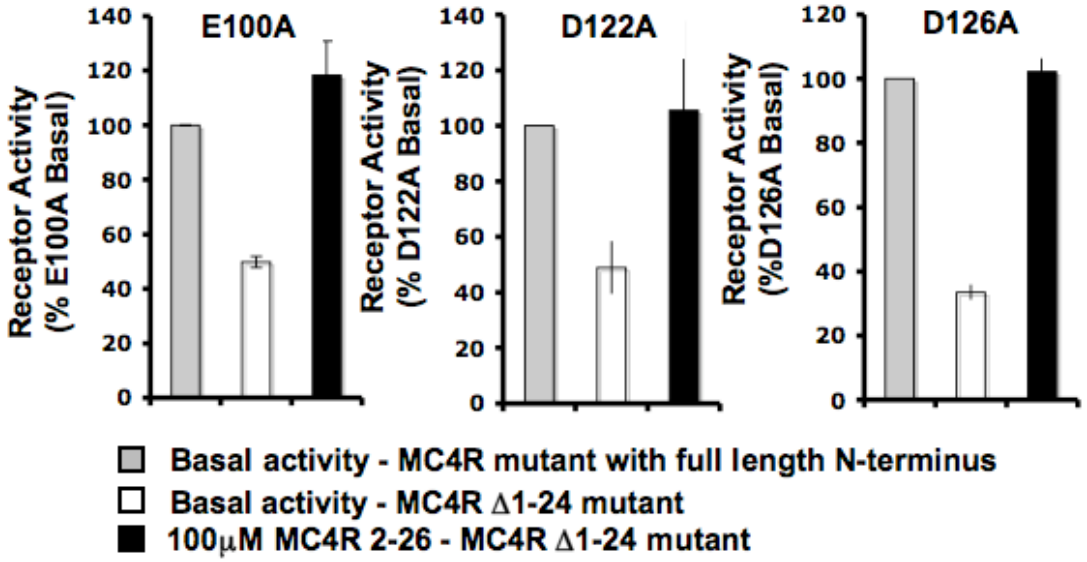


**Figure 8.** Acidic amino acids that are essential for αMSH mediated activation of MC4R. A) αMSH activation of E100A (grey), D122A (dashed), and D126A (black) MC4Rs vs. WT receptor (red). B)The basal activity of full length E100A, D122A, and D126A MC4Rs (black). The basal activity of truncated Δ1-24 MC4R E100A, Δ1-24 MC4R D122A, and Δ1-24 MC4R D126A (white). MC4R2-26 stimulation of truncated Δ1-24 MC4R E100A, Δ1-24 MC4R D122A, Δ1-24 MC4R D126A (grey). Error bars represent standard error for the triplicate.

***The peptide sequence HLWNRS is the minimum activating sequence of the N-terminal domain of MC4R.***

To further outline the molecular basis of the N-terminal activation of MC4R, we first delineated the minimal activating region of the N-terminal domain. We tested overlapping peptides spanning the MC4R N-terminus for their activity at MC4R Δ1-24. Setting hexapeptides as the shortest sequence length, all possible combinations produced 9 smaller overlapping peptides in addition to the original MC4R2-26 peptide (Figure 9). While MC4R2-26 showed the greatest activity, some of its segments failed to activate MC4R Δ1-24 (Figure 9). All activating peptides shared the common sequence $His_{14}$-$Leu_{15}$-$Trp_{16}$-$Asn_{17}$-$Arg_{18}$-$Ser_{19}$ (MC4R14-19). Notably, this minimal activating sequence encompasses the most conserved portion of the N-terminal region throughout several species (figure 10), encompasses Arg18, a previously described genetic "hotspot" for obesity-causing mutations in the MC4R[86, 92, 93] and can be targeted by a specific antibody with relevant physiological consequences[93], as antibodies against the overlapping rat MC4R11-25 act as inverse agonists *in vitro* and lead to increased food intake and body weight in rats.

We further determined the relative role of specific amino-acids within this minimal activating sequence. Substitutions of His14, Arg18 and W16 significantly decreased the activity of MC4R14-19 suggesting that N-terminal

domain activation may be due to interaction with accessible aromatic or charged residues in the transmembrane core of the receptor (Figure 11).

**Figure 9.**

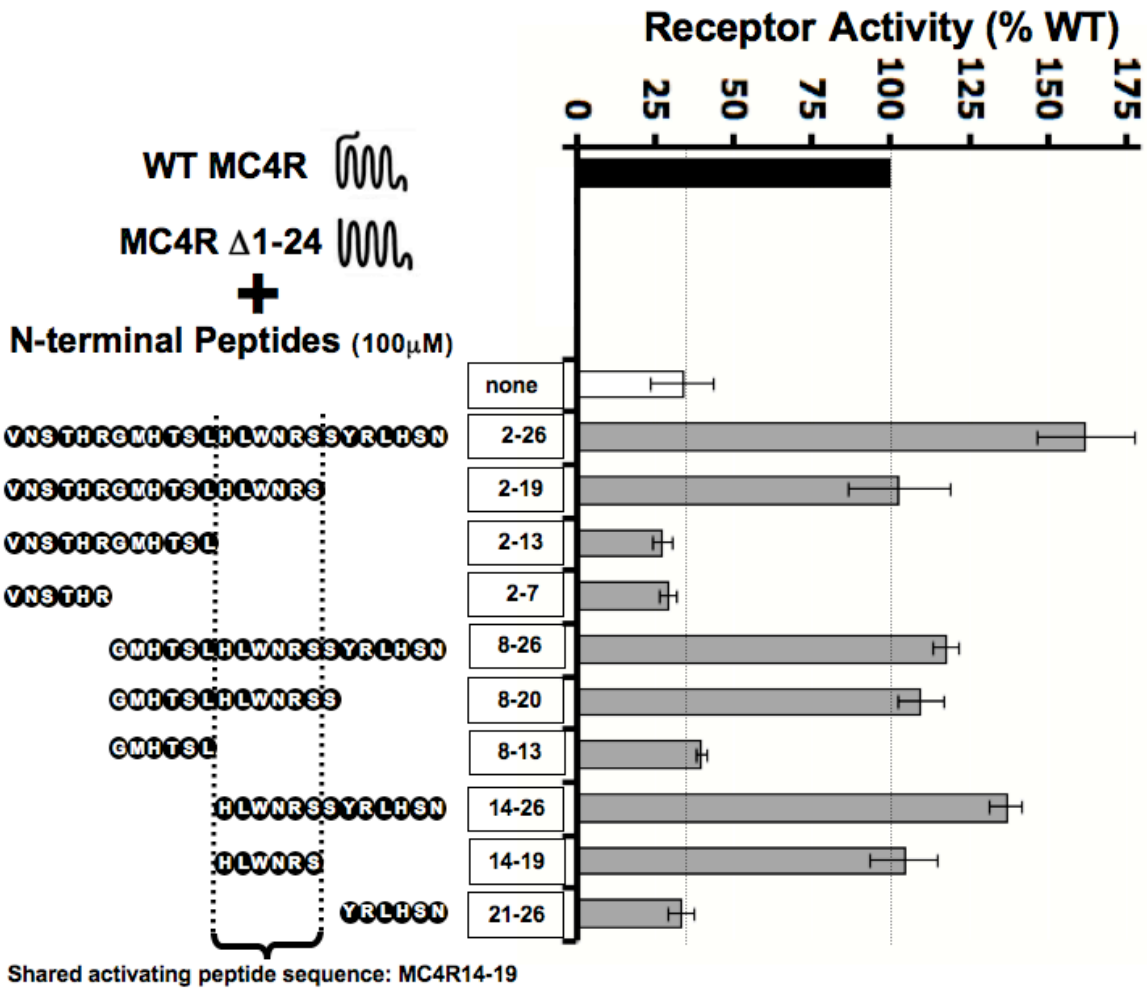


**Figure 9.** Determination of the minimal activating sequence of MC4R2-26 for basal activation. Small overlapping segments of MC4R2-26 peptide are displayed on the left panel of the figure. The bar graph represents the WT basal activity (black), MC4R Δ1-24 basal activity (white), and the stimulation of MC4R Δ1-24 by the corresponding peptide on the left (grey). Error bars represent standard error for the triplicate.

**Figure 10.**

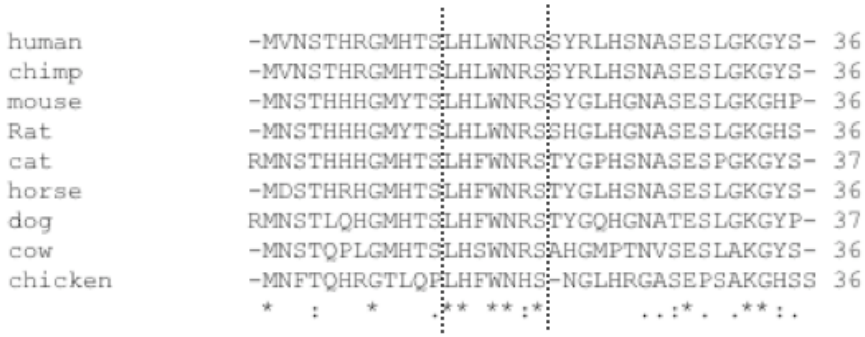


**Figure 10.** Multiple alignments of the MC4R N-terminal sequences of multiple species. 100% conserved residues are marked by star (*). 13th through 19th amino acids are bracketed between vertical dashed lines.

**Figure 11.**

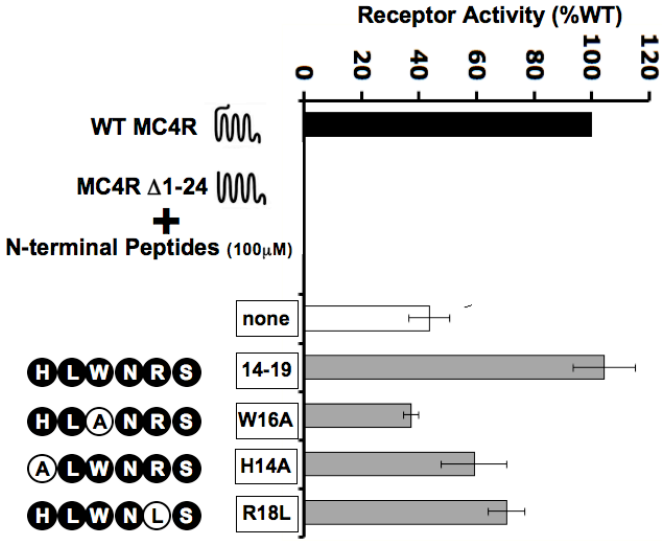


**Figure 11.** Determination of the essential amino acids of MC4R2-26 for basal activation. Single amino acid substitutions of the minimal

activating peptide are displayed on the left panel of the figure. The mutated residues are indicated with black font on white background whereas the original sequence is indicated with white font on black background. The bar graph represents the WT basal activity (black), MC4R Δ1-24 basal activity (white), and the stimulation of MC4R Δ1-24 by the corresponding peptide on the left (grey). Error bars represent standard error for the triplicate.

***Core transmembrane residues involved in N-terminus mediated activation.***

We reasoned that mutations in amino acids solely implicated in the N-terminal mediated activity of MC4R would impair the constitutive activity of the receptor but not the activation of the receptor by αMSH. We first surveyed naturally-occurring obesity-causing mutations studied in our laboratory for such a biochemical phenotype (Figure 4, white on black)[92, 94-101]. Out of 71 mutations examined, 8 had decreased basal activity and a conserved response to αMSH. Five of these mutations were in the N-terminal domain of the receptor (R7H, R18H, R18C, R18L, T11A)[86, 92], and three were in the intracellular domains of the receptor (V95I, A154D, G231S)[92, 95], but none was located in the solvent-accessible region of the receptor.

Because of the positively charged nature of the N-terminal domain, we systematically screened all the remaining negatively charged solvent-accessible

residues for such a biochemical phenotype by Alanine scanning mutagenesis (Figure 4, among black on grey). Substitution of these acidic amino acids did not alter the basal or αMSH activation of the receptor (Figure 12A).

Because mutational analysis of the N-terminal domain suggested a possible role for an aromatic residue mediating its activity, we also tested all remaining accessible aromatic and basic residues in a similar manner (Figure 4, among black on grey). Of 17 residues tested, mutagenesis of 9 (W174A, Y187A, F201A, F202A, W258A, F261A, F262A, H264A, and F284A) led to significantly reduced basal activity compared to the WT receptor (Figure 12B and 12C). Of these mutants, W174A, Y187A, F202A, F261A, H264A, F284A had a significantly altered response to α-MSH (figure 13A and 13B) but three mutant receptors (F201A, W258A, F262A) displayed a normal response to the agonist α-MSH making them identical to MC4R Δ1-24 for their functional profile, and thus candidates for activation by the N-terminal domain (Figure 13C and table 2). We next tested whether any of the 3 residues exclusively altering the constitutive activity of the receptor were implicated in its activation by the N-terminal domain. When introduced into MC4R Δ1-24, mutations of the residues F201, W258, and F262 to alanine impaired activation of the receptors by exogenously added N-terminal peptide, confirming their specific involvement in the partial agonism of the N-terminal domain of the receptor (Figure 13D).

**Figure 12.**

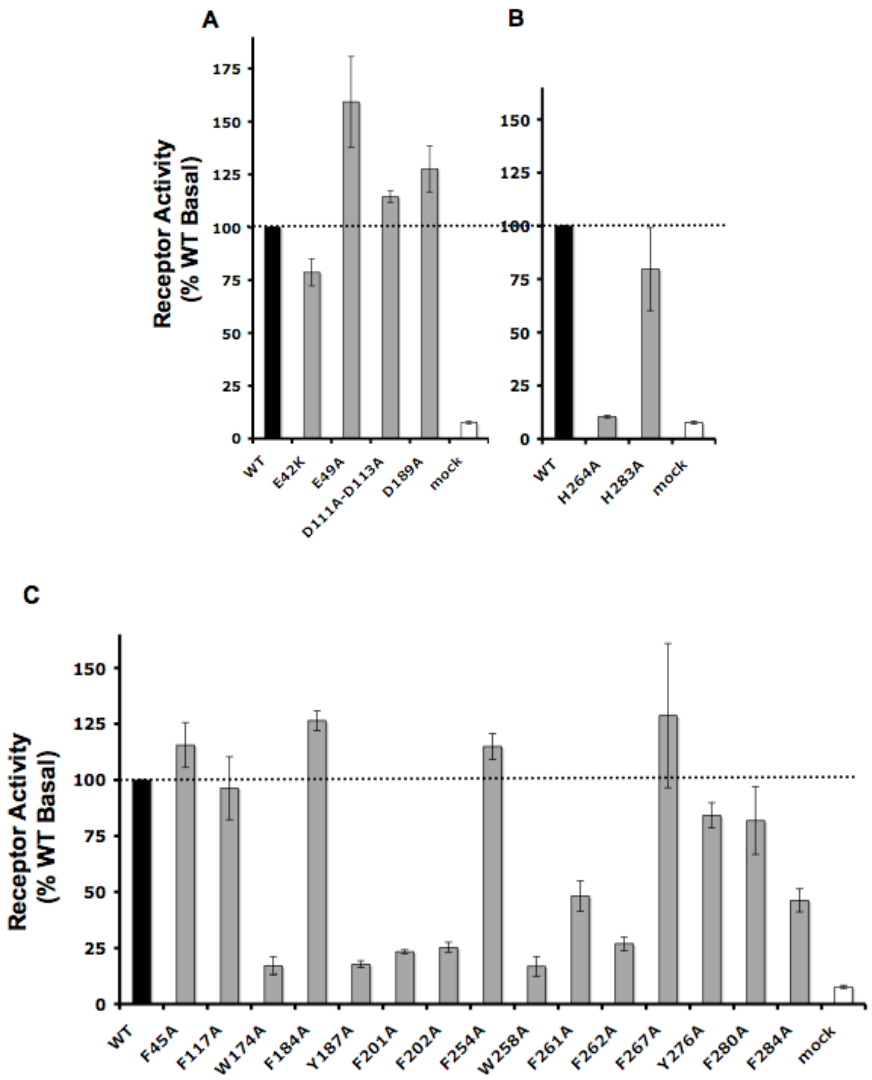


**Figure 12.** The basal activity of the previously unstudied acidic, basic and aromatic residues accessible from the extracellular domain. A) Acidic residues. B) Basic residues C) Aromatic residues. Dashed line and the black bars represent the WT basal activity. MC4R mutations' basal activity (grey bars). Mock DNA (white bars). Error bars represent standard error for the triplicate.

**Figure 13.**

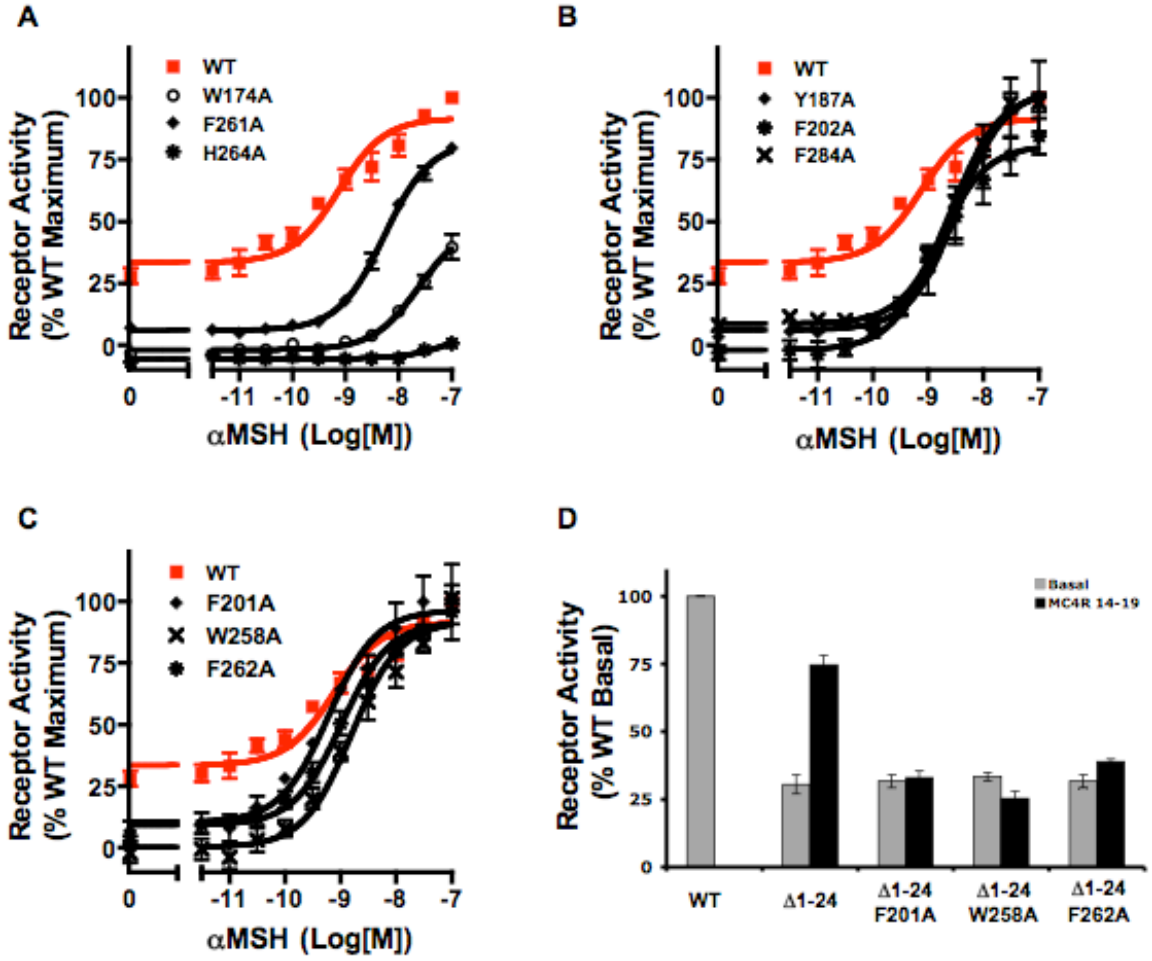


**Figure 13.** Activation profile of low basal MC4R mutants. A) and B) W174A, F261A, H264A, Y187A, F202A, F284A mutations αMSH dose response. C) F201A, W258A, F262A mutations αMSH dose response. D) The activation of MC4R Δ1-24 mutants by MC4R14-19 peptide. Error bars represent standard error for the triplicate. WT MC4R αMSH dose response curve marked in red.

***Structural determinants of N-terminal domain mediated activation of the MC4R.***

As distinct sets of residues in the TM domain appear to be involved in interactions with the N-terminus and with exogenous ligands, we sought to establish the relative location of these molecular actors. In the absence of a structure for the MC4R, such a structural framework can be obtained from a homology-based model, since the crystal structures of related receptors are available. We built a homology model of the TM domain of the MC4R based on the recently obtained crystal structure of the β2-Adrenergic receptor (β2AR)[102, 103]. Helix ends were estimated from the structure of the β2AR and no structural modifications were performed on the backbone.

As shown on Figure 14, most amino acids involved specifically in activation by the hormone, including the well characterized negatively charged residues E100, D122 and D126[104], are clustered at the extracellular portion of TM2 and TM3. In sharp contrast, residues involved solely in the activation by the N-terminus are located at the interface between TMV and TMVI, forming a spatially distinct cluster from residues involved in a-MSH activation. Interestingly, this cluster correspond to $W286^{6.48}$ and $F290^{6.52}$ in the β2AR, in which it comprises the "rotamer toggle switch", a conserved molecular switch that has been proposed to be involved in activation of the amine and opsin receptor families[105].

It should also be noted that while the cytoplasmic end of the TMV of the MC4R shares common motifs with that of the β2AR, the upper half (towards the extra-cellular region) is significantly divergent, and does not include the normally conserved P5.50. This suggests that the helical bulge observed in the β2AR and in rhodopsin is likely to be absent in the melanocortin receptors which would thus bring F202 towards the center of the bundle and F201 towards TMVI, explaining the similar functional profiles of the MC4R mutants F201A and F202A.

***Figure 14.***

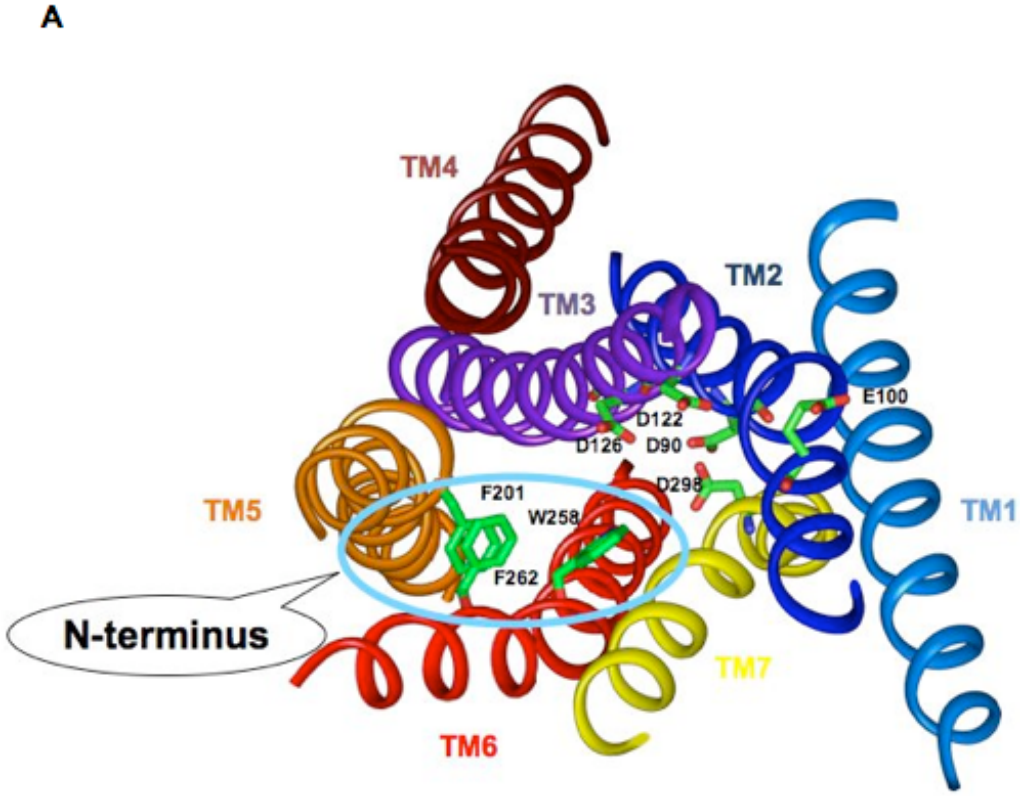


(Figure 14 continued on the next page)

*Figure 14.*

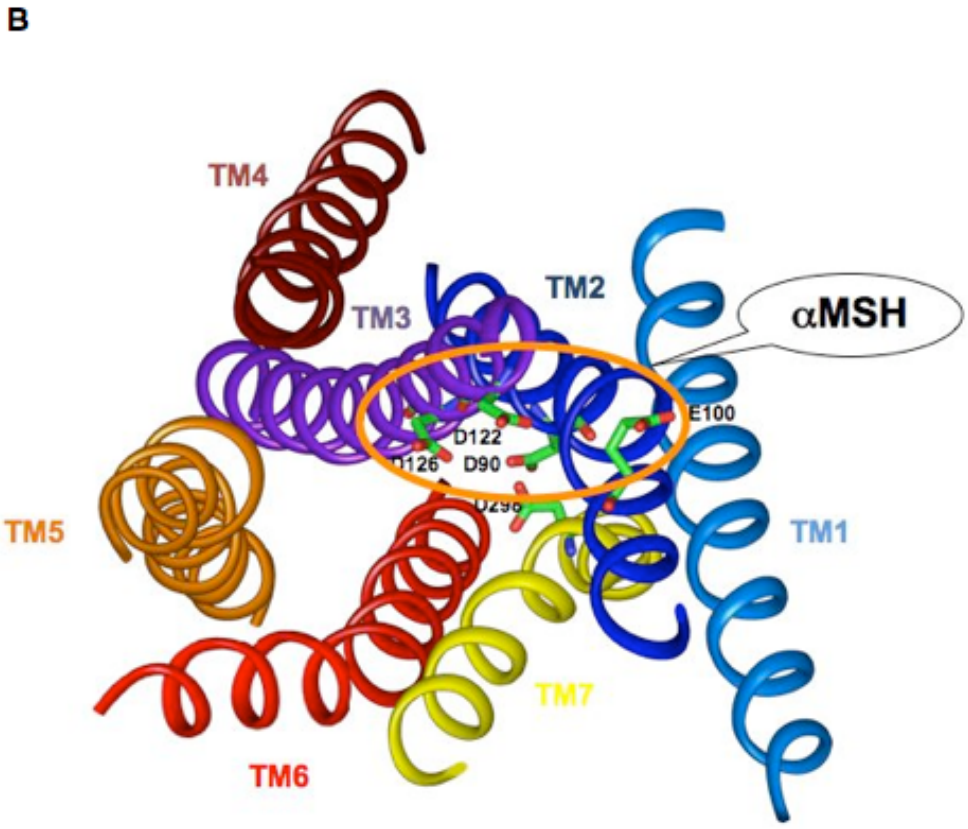


**Figure 14.** 3D Molecular model viewed from the top extracellular surface of MC4R. Ligand specific activation sites are displayed. A) F201, W258, and F262 as activation site downstream of N-terminal domain, circled in blue. B) E100, D122, and D126 as the α-MSH specific activation site, circled in orange. MC4R 3D TM alignment is done by taking $\beta_2$AR crystal structure as a model.

***Pharmacological modulators of MC4R activity.***

Due to its potential for the treatment of obesity, the discovery of pharmacological MC4R agonists has been extensive. To determine if the increased potency of two pharmacological MC4R super agonists MT-II (melanotan II) and THIQ (tetrahydroiso-quinolone) rises from the utilization of both the αMSH and the N-terminal domain activation sites, we tested the activation of F201A, W258A, and F262A mutations by these agents (table 2). Our results indicate that MT-II did not use the N-terminal activation site because its potency and efficacy were not reduced when the N-terminal activation site was mutated. On the other hand, both F262 and W258 were necessary for full activation by the pharmacological super agonist THIQ. THIQ also requires acidic amino acids that are essential for αMSH activation [106]. Therefore, the use of both the αMSH and N-terminal domain activation sites could provide an explanation for the much higher potency and efficacy of THIQ when compared to αMSH.

At pharmacological doses, Zinc cation can activate MC4R with an $EC_{50}$ of 13mM[107]. Zinc also boosts αMSH efficacy but not the potency when combined together[107], suggesting that the effect is additive but not synergistic. We determined that Zinc activation was independent of αMSH activation site by finding that E100A, D122A, D126A did not alter Zinc activation (data not shown). Instead, our results indicate that Zinc activation of MC4R requires both the N-

terminal domain and its activation site because Zinc failed to activate MC4R Δ1-24 and the mutations of the N-terminal domain activation site (F201A, W258A, F262A). Zinc acts as a mediator between the N-terminal domain and its activation site because MC4R Δ1-24 Zinc activation was rescued in the presence of 100μM MC4R2-26.

**Table 2.**

| αMSH | $EC_{50}$ (nM) | $EC_{50}$ $CI_{95}$ | $E_{max}$ (% WT maximum) | $E_{max}$ $CI_{95}$ |
|---|---|---|---|---|
| **WT** | 0.7453 | 0.44 to 1.28 | 91.69 | 86.46 to 96.92 |
| **F201A** | 0.601 | 0.34 to 1.07 | 96.43 | 88.22 to 104.6 |
| **W258A** | 1.562 | 1.02 to 2.40 | 91.87 | 84.42 to 99.32 |
| **F262A** | 1.039 | 0.76 to 1.43 | 91.67 | 86.94 to 96.41 |
| **MTII** | | | | |
| **WT** | 0.04381 | 0.0165 to 0.1162 | 77.41 | 72.14 to 82.67 |
| **F201A** | 0.07338 | 0.0317 to 0.1699 | 81.32 | 74.34 to 88.31 |
| **W258A** | 0.07224 | 0.0266 to 0.1964 | 78.85 | 69.89 to 87.81 |
| **F262A** | 0.03766 | 0.0089 to 0.1594 | 78.42 | 67.75 to 89.10 |
| **THIQ** | | | | |
| **WT** | 0.07545 | 0.0379 to 0.1503 | 94.17 | 89.16 to 99.18 |
| **F201A** | 0.2164 | 0.1083 to 0.4322 | 101.00 | 92.12 to 109.8 |
| **W258A** | 0.5696** | 0.3654 to 0.8881 | 92.14 | 85.55 to 98.73 |
| **F262A** | 0.3966** | 0.2108 to 0.7459 | 96.55 | 88.67 to 104.4 |

**Table 2.** MC4R activation by αMSH, THIQ, and MT-II. P values for the significance of difference between WT and mutant MC4R activations was tested

by One-way ANOVA. $P < 0.05$ (*), $P < 0.01$ (**). Sigmoidal dose response curves, $EC_{50}$, $E_{max}$ values and their 95% confidence intervals were calculated using Prism 4. $N \geq 3$ for all experiments.

**Figure 15.**

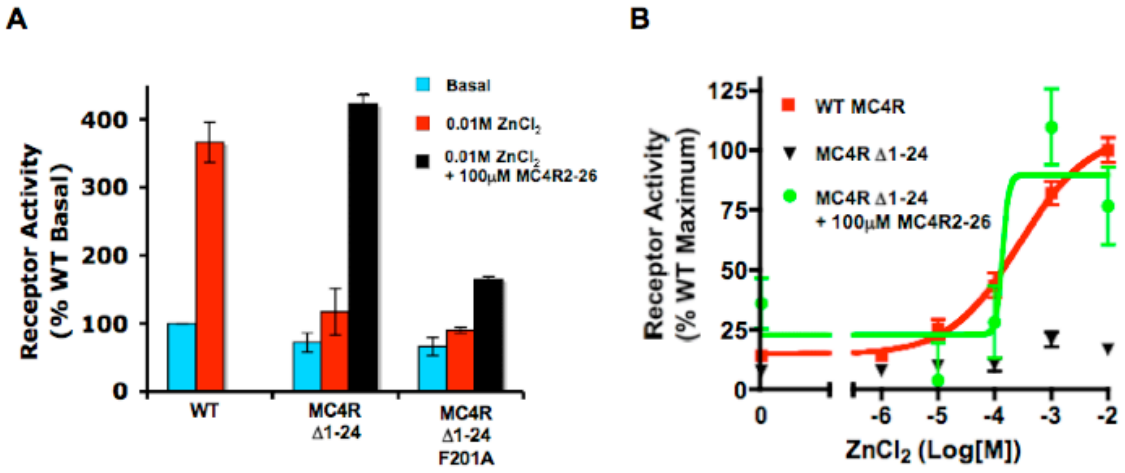


**Figure 15.** The activation of MC4R, MC4R Δ1-24, MC4R Δ1-24 F-201A by $ZnCl_2$. A) Single dose activation by 0.0M $ZnCl_2$ alone or in combination with 100μM MC4R2-26. B) Dose response curve: Red - WT MC4R with $ZnCl_2$, Black - MC4R Δ1-24 with $ZnCl_2$, Green - MC4R Δ1-24 with $ZnCl_2$ in the presence of 100μM MC4R2-26. cAMP accumulation upon receptor activation was measured by cAMP enzyme immunoassay.

## DISCUSSION

### *Conformational complexity at the MC4R.*

In this study, we have identified a scaffold of aromatic residues in the MC4R that mediates N-terminal induced self-activation targeted by the physiological inverse agonist AGRP. This region is not necessary for the agonist effect of the diffusible endogenous ligand α-MSH suggesting that both modes of activation trigger different conformational pathway during activation of MC4R. This conformational complexity is similar and can be superimposed onto that observed for the extensively studied β2AR in which a number of structurally different agonists disrupt distinct combinations of stabilizing intramolecular interactions[105]. For example, in the β2AR, the aromatic catechol ring of the catecholamines interacts directly with the aromatic residues of the rotamer toggle switch while it is not required for activation by the partial agonist salbutamol. Indeed, our observation of an essential role for W16 in the minimal activating N-terminal MC4R hexapeptide also suggests the possibility that its aromatic ring similarly directly interacts with the rotamer toggle switch, an interaction that could be facilitated by the absence of a second extra-cellular loop (ECL2), which is a specific characteristic of melanocortin receptors[108].

***Expanding the role of the N-terminal domain in the evolution of GPCRs .***

Historically, Class A GPCRs have been identified and studied on the bases of their ability to be activated by specific high-affinity diffusible pharmacological ligands interacting directly with the core transmembrane regions of the receptor. However major exceptions include glycoprotein receptors (FSHR, TSHR, LHR), in which the proximal portion of a large N-terminal domain suppresses the receptor's activity in the absence of a ligand, and ligand binding to this region relieves this inhibition[109], as well as protease-activated receptors (PARs) for which activation of the receptor is dependent on proteolytic cleavage and unmasking of an N-terminal domain that acts as a tethered ligand[83]. Our findings at the MC4R provides an evolutionary link between these different modes of activation and suggests a more central role for the N-terminal domain in the evolution of activity modulation at class A GPCRs (Figure 16). Indeed, we propose that most modes of activation found at GPCRs can derive from the ancestral interaction of the N-terminal domain with the core of the receptor adapting towards different degrees of activation or modulation by ligands. For a subset of class A receptors such as PARs and glycoprotein receptors, this N-terminal mediated regulation was modified by endogenous factors like proteases and ligands (Figure 16). MC4R represents an intermediate situation in which the N-terminal mediated activation is negatively modulated by an endogenous ligand and an endogenous agonist independently regulates the receptor positively, with AGRP also blocking this interaction. At the end of the spectrum, class A GPCRs

may have lost the sensitivity to their N-terminal domain due to the preferential adaptation to their endogenous ligands, whether it is diffusible as in the β2AR or covalently bound as in Rhodopsin.

**Figure 16.**

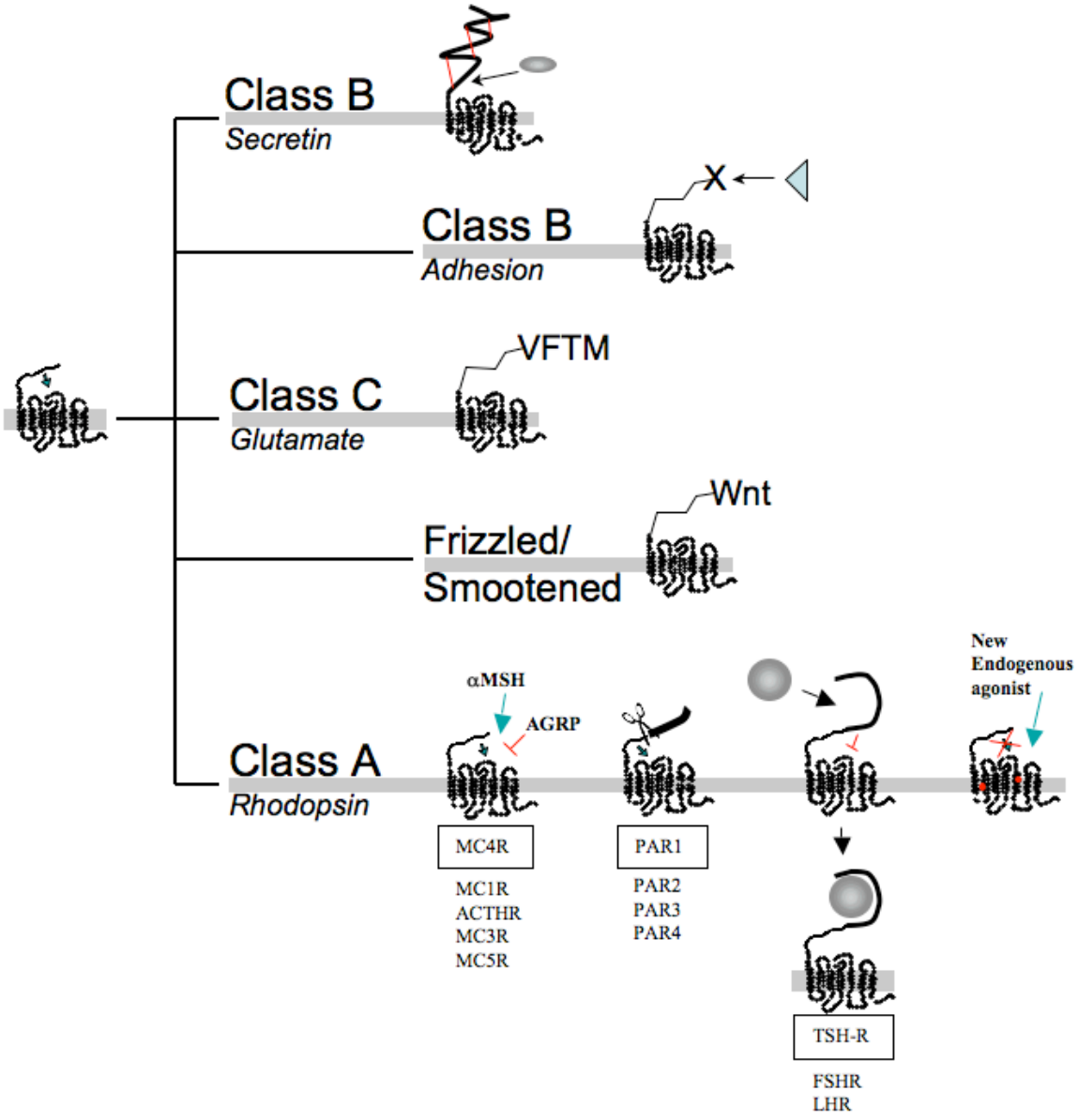


**Figure 16.** Evolutionary model of the role of the N-terminal domain

in GPCRs. Class A GPCR activation and N-terminal modifications are shown on the right panel. N-terminal domains of GPCRs are not structural representations; they depict their functional role. Secretin receptor family - red lines represent the cystein network. Adhesion receptor family - "X" represents multiple diverse N-terminal motifs. Glutamate receptor - Venus Flytrap motif (VFTM). Frizzled/Smoothened receptor family - Wnt motif.

***Physiological inverse-agonists as regulators of constitutively active orphan GPCRs.***

Another consequence of the framework proposed above and specifically of our observation that the N-terminal/AGRP interaction can independently modulate the activity at the MC4R is the suggestion that physiological negative regulation by inverse agonist might be the unique mode of regulation at GPCRs. Indeed, despite extensive efforts in the search for physiological agonists, a large number of GPCRs remain orphan or have proposed physiological ligands with pharmacological characteristics that are not compatible with a physiological role. The high constitutive activity of a number of these orphan receptors could indicate that inverse agonism is the only physiological modulation at these receptors and would explain the failure of deorphanizing studies using high throughput assays limited to detecting agonism (figure 17). Whether the interaction of an activating N-terminal domain and a physiological inverse agonist

will be the basis for activity modulation at these GPCRs remains to be tested but GPR61 is a recent example of a GPCR with a high constitutive activity, which is also mediated by the agonistic effect of its own N-terminal domain[110].

**Figure 17.**

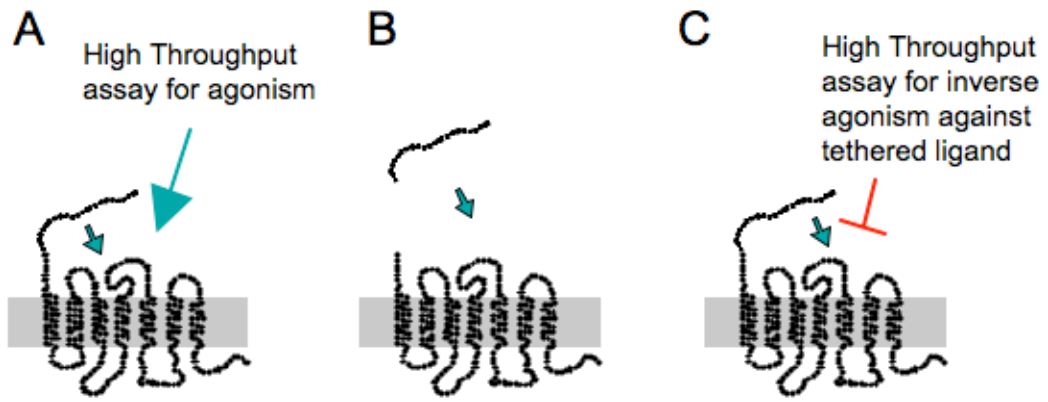


**Figure 17.** Orphan receptors with N-terminus mediated high constitutive activity. A) The current method of deorphanizing GPCRs. B) Proposed method to test N-terminal mediated activation. C) How constitutively active orphan receptors should be studied.

## Experimental Procedures

***MC4R ligands*** - Melanotan-II was obtained from Genscript (Piscataway, NJ). 1,2,3,4-tetrahydroisoquinoline (THIQ) was provided by Merck Research Labs (Rahway, NJ). Melanocyte stimulating hormone and AgRP were purchased from Phoenix Pharmaceuticals (Belmont, CA).

***MC4R plasmid constructs*** - Wild-type (WT) and E42K human MC4R genes were cloned from genomic DNA into the vector pcDNA 3.1 as previously described[96]. MC4R Δ1-24 was made as described, and the prolactin signal peptide and a Flag epitope tag (DYKDDDD) were added to both WT and MC4R Δ1-24 for identical membrane localization[86].

***Ligand binding assay*** - HEK 293 cells were stably transfected with either MC4R Δ1-24 or WT MC4R using Effectene transfection kit (Qiagen, Valencia, CA) previously. Competitive binding was measured as a function of the displacement of a radio labeled MC4R super agonist, [$^{125}$I]-NDP-αMSH or antagonist/inverse agonist, [$^{125}$I]-AgRP (PerkinElmer Life and Analytical Sciences, Billerica, MA) in the presence of increasing concentrations of a competitive ligand. Stably transfected cells were incubated for two hours in binding buffer with radioligand and with αMSH or N-terminal domain peptide as competitive ligands. At the end of the binding assay, cells were lysed and binding - as a function of loss of radioactivity - has been measured using a gamma counter (Packard Instruments,

Meriden, CT). The gamma counter readings were normalized for non-specific binding and plotted as a percentage of the maximum radioligand binding. Best-fit estimates of the $IC_{50}$ and their 95% confidence intervals were obtained by non-linear regression fitting of the sigmoidal dose response curves using Prism 4.

***MC4R activity*** - *luciferase reporter assay:* MC4R activaty was measured as previously described[35, 96, 99]. Briefly, HEK293 cells were transfected with WT or mutant MC4R plasmid, cre-luciferase plasmid, and renilla luciferase using Effectene transfection kit (Qiagen, Valencia, CA). Transfected cells were incubated for 6 hours in stimulation medium (aMEM medium with 0.1 mg/ml bovine serum albumin (BSA) and 0.25 mM isobutylmethylxanthine (Sigma, St Louis, MO) for basal stimulation). Choice of stimulation factor was added to the basal medium at the desired concentration. Luciferase activity, representing the cAMP production through MC4R activation, was assessed using the Steady-Glo Luciferase Assay System (Promega, Madison, WI) and a microplate luminescence counter (Packard Instrument, Downers Grove, IL). Renilla activity, representing solely the transfection efficiency, was assessed for each individual transfection using dual luciferase assay kit (Promega, Madison, WI) on a luminometer (Analytical Luminescence Laboratory instrument, San Diego, CA). Luciferase activity upon MC4R activation was normalized over the transfection efficiency by dividing the cre-luciferase activity by the renilla luciferase activity. The results were finally normalized as a percentage of the maximum stimulation observed. Best-fit estimates of the $EC_{50}$s, $IC_{50}$s and their 95% confidence

intervals were obtained by non-linear regression fitting of the sigmoidal dose response curves using Prism 4.

***MC4R activity, cAMP assay*** - HEK293 cells were transfected with WT or mutant MC4R and renilla plasmids. Transfection efficiency has been measured through renilla luciferase activity. Non-acetylated cAMP level has been measured by enzyme immunoassay (cAMP EIA) according to the manufacturer's manual (Amercham Biosciences). Raw data for the triplicate has been normalized to the percentage of WT MC4R activity.

***Peptide synthesis*** - Fmoc-Asn(Trt)-OH, Fmoc-Arg(Pbf)-OH, Fmoc-Gly-OH, Fmoc-His(Trt)-OH, Fmoc-Leu-OH, Fmoc-Met-OH, Fmoc-Ser(tBu)-OH, Fmoc-Thr(tBu)-OH, Fmoc-Trp(Boc)-OH, Fmoc-Tyr(tBu)-OH, Fmoc-Val-OH and Rink Amide MBHA resin (0.66 meq/g) were purchased from Novabiochem (San Diego, CA). All peptides were assembled as amides on an Applied Biosystems (Foster City, CA) model 433a automated peptide synthesizer (0.1-0.25 mmol scale) using modified cycles with HBTU/DIEA mediated coupling, DMF as solvent (Fisher or EM Science), and a deprotecting solution of 1:1:98 1,8-Diazabicyclo[5.4.0]undec-7-ene:Hexamethyleneimine:DMF. 0.5 M Acetic Anhydride in DMF was added for 5 minutes to cap some peptides. Peptides containing Met were cleaved with 95:2.5:2.5 TFA:TIS:Thioanisole for 1.5 hrs. and the filtrate precipitated with refrigerated diethyl ether, precipitate spun down with centrifugation, decanted, and the crude peptide suspended in a 1:1 H2O:ACN

0.1% TFA solution, for peptides not containing Met anisole was substituted for thioanisole. The proper molecular mass was confirmed by a Waters (Milford, MA) ZMD ESI-MS. Analytical HPLC on either a c4, c18, or diphenyl vydac 4.6 x 150 mm 5 µm column was performed before and after prep (c4 vydac 22 x 250 mm 10 µm) or semiprep (c18 alltech 10 x 250 mm 5 µm) purification to assess peptide purity (≥80%) using H2O (0.1% w/v TFA)/ACN (0.1% w/v TFA) gradients. All peptides were lyophilized following HPLC purification.

***Molecular modeling of MC4R*** - A homology model of the seven transmembrane helices of the MCR4r was constructed based in the crystal structure of the b2-adrenergic receptor (PDB id P32245). The sequence alignment was based on the most conserved residues found in all class A GPCRs[111]. Side chains were placed using SCWRL 3.0. Local geometries were optimized with 1026 steps of steepest descent energy minimization using the Gromas package.

***Statistical Analysis*** - For the competitive ligand binding assay, best-fit estimates of the $IC_{50}$ and its 95% confidence intervals were obtained by non-linear regression fitting of the one site competition curves using Prism 4. For MC4R activity dose response curves, best-fit estimates of the $EC_{50}$, $IC_{50}$ and their 95% confidence intervals were obtained by non-linear regression fitting of the sigmoidal dose response (variable slope) curves using Prism 4.

# Chapter III

## Association of functionally significant Melanocortin-4 but not Melanocortin-3 receptor mutations with severe adult obesity in a large North-American case control study*.

**In association with Melissa A. Calton*

## SUMMARY

Functionally significant heterozygous mutations in the Melanocortin-4 receptor (*MC4R*) have been implicated in 2.5% of early-onset obesity cases in European cohorts. The role of mutations in this gene in severely obese adults, particularly in smaller North American patient cohorts, has been less convincing. More recently, it has been proposed that mutations in a phylogenetically and physiologically related receptor, the Melanocortin-3 receptor (*MC3R*), could also be a cause of severe human obesity. The objectives of this study were to determine if mutations impairing the function of MC4R or MC3R were associated with severe obesity in North American adults. We studied MC4R and MC3R mutations detected in a total of 1821 adults (889 severely obese and 932 lean controls) from two cohorts. We systematically and comparatively evaluated the functional consequences of all mutations found in both *MC4R* and *MC3R*. The total prevalence of rare *MC4R* variants in severely obese North American adults was 2.25% ($CI_{95\%}$ of 1.44-3.47) compared to 0.64% ($CI_{95\%}$ of 0.26-1.43) in lean controls ($p<0.005$). After classification of functional consequence, the prevalence of MC4R mutations with functional alterations was significantly greater as compared to controls ($p<0.005$). In contrast, the prevalence of rare *MC3R* variants was not significantly increased in severely obese adults (0.67% ($CI_{95\%}$ of 0.27-1.50) vs. 0.32% ($CI_{95\%}$ of 0.06-0.99)) ($p=0.332$). Our results confirm that mutations in *MC4R* are a significant cause of severe obesity, extending this

finding to North American adults. However, our data suggest that *MC3R* mutations are not associated with severe obesity in this population.

## INTRODUCTION

Obesity results from the interaction between a genetic predisposition and deleterious environmental factors[112]. Both common variants with small effects[113, 114] and rare variants with larger individual effects have been shown to contribute to the genetic predisposition to obesity[115]. In particular, rare heterozygous mutations in the coding sequence of the melanocortin-4 receptor (*MC4R*) gene account for a significant number of severe obesity cases[116-121]. MC4R belongs to the family of seven trans-membrane G-protein-coupled receptors (GPCR) and is expressed at low levels in hypothalamic nuclei involved in the regulation of food intake and in particular neurons of the para-ventricular nucleus (PVN)[122]. MC4R regulates food intake by integrating a satiety signal provided by its agonist α-MSH and an orexigenic signal provided by its antagonist Agouti-related protein (AGRP)[33, 123]. Both of these ligands are expressed in distinct neuronal populations of the arcuate nucleus of the hypothalamus and are coordinately regulated by the adipocyte-secreted hormone, leptin, to control food intake and maintain long-term energy homeostasis[124]. Mice lacking both alleles of *mc4r* (*mc4r* -/- mice) develop a maturity onset hyperphagic obesity syndrome by 10 weeks of age[13]. Mice heterozygous for an *mc4r* deletion (*mc4r* +/- mice) show an average weight that is intermediate between that of wild-type and *mc4r -/-* mice[13].

Numerous studies, mostly in European populations have documented a prevalence of 2.67% [$CI_{95}$: 2.1-3.6] of nonsense, frameshift and missense *MC4R*

mutations in early-onset obesity[92]. More recently, such mutations have also been implicated in the development of severe adult obesity in these same populations. For example *MC4R* mutations were found in 2.35% ($CI_{95}$ 0.9-3.8) of severely obese French adults[92]. Fewer studies, in relatively small number of patients, have explored the prevalence of *MC4R* mutations in severely obese North American patients[120, 125, 126]. Results have been inconsistent leading to the suggestion that environmental differences could selectively impact the relative effects of *MC4R* mutations in these populations.

Another melanocortin receptor, the melanocortin 3 receptor (MC3R), is closely related to MC4R and is expressed in the arcuate nucleus of the hypothalamus[122, 127]. MC3R has also been implicated in long-term energy homeostasis in rodents[128, 129]. Homozygous null *mc3r-/-* mice have an increased fat mass through increased feed efficiency[128, 129].

Evidence for a causative role for MC3R in human obesity is scarce. Few heterozygous *MC3R* mutations have been detected in early-onset obese patients[130, 131]. Large-scale studies, systematically comparing the prevalence of rare *MC3R* mutations in cases and controls to formally determine if, similarly to *MC4R*, such mutations are associated with severe obesity have not yet been performed.

In this study, we used two cohorts of North American adult subjects to compare the prevalence and the function of MC4R and MC3R mutations found in

patients with severe obesity and in non-obese controls. Our results confirm that *MC4R* mutations are a significant cause of severe obesity and extend this finding to North American adults. In contrast, our data does not support a similar role for *MC3R* mutations in the predisposition to this condition.

## RESULTS

### *Prevalence and nature of MC4R mutations in two North American cohorts of severe obese adults.*

We analyzed the prevalence and nature of *MC4R* coding region mutations detected in 1821 adults (889 severely obese and 932 controls) from our previously reported cohorts[100, 132]. A total of 26 subjects carried rare variants in the *MC4R* coding region (Table 1): 20 in the severely obese group (2 subjects both carried Leu211Del and Pro299His mutations) and 6 among the controls. In the severely obese adults, 17 missense mutation carriers, 2 nonsense mutation carriers, and 3 frameshift mutation carriers were identified (for a total of 20 different carriers). Six control subjects carried six different missense mutations. The total prevalence of rare *MC4R* variants in severely obese North American adults was 2.25% ($CI_{95\%}$ of 1.44-3.47) compared to a prevalence of 0.64% ($CI_{95\%}$ of 0.26-1.43) in lean controls (p=0.005) [OR=4.3].

In addition, a total of 41 subjects carried the common variant Val103Ile and 12 subjects carried the common variant Leu251Ile (Table 2). The frequency of these two variants was similar to that described in other studies (2.43-5.31% for Val103Ile and 0.96-3.23% for Leu251Ile)[92, 120, 125, 133, 134]. The prevalence of these polymorphisms was not statistically different between case and controls in our studies (p=0.775, 0.774 respectively), most likely due to limited power to

detect an association, and thus failed to replicate the small, but significant association with decreased body weight seen in a larger study for the Val103Ile variant[135].

**Table 1.**

| Gene | Mutation | | No. Severely Obese Carriers (n=889) | No. Control Carriers (n=932) | In Silico Prediction | | In Vitro Functional Study | |
|---|---|---|---|---|---|---|---|---|
| | DNA | Protein | | | PolyPhen | SNAP | Class-ification | Assayed Difference compared to WT |
| **MC4R** | | | | | | | | |
| **Cohort I** | c.11C>T | Ser4Phe[†‡] | 1 | 0 | + | +(0; 58%) | - | |
| | c.105C>A | Tyr35stop[†] | 1 | 0 | nonsense | nonsense | + | nonsense |
| | c.606C>A | Phe202Leu[‡] | 1 | 0 | - | - (0; 53%) | - | |
| | c.634_635delT | Leu211Del | 1 | 0 | frameshift | frameshift | + | frameshift |
| | c.691G>A | Gly231Ser | 1 | 0 | - | - (4; 85%) | - | |
| ***Severely obese*** | c.706C>T | Arg236Cys[‡] | 2 | 0 | ++ | + (3; 78%) | - | |
| | c.806T>A | Ile269Asn[‡] | 2 | 0 | + | + (4; 82%) | + | EC50 |
| | c.812G>T | Cys271Phe[‡] | 1 | 0 | - | + (5; 87%) | + | ⇓Emax |
| | c.895C>T | Pro299Ser[‡] | 1 | 0 | + | + (4; 82%) | + | ⇓Emax |
| | c.919C>T | Gln307stop[†] | 1 | 0 | nonsense | nonsense | + | nonsense |
| | c.335C>T | Thr112Met | 0 | 1 | - | + (3; 78%) | - | |
| ***Lean*** | c.473A>G | His158Arg[‡] | 0 | 1 | ++ | + (6; 93%) | - | |
| | c.523G>A | Ala175Thr | 0 | 1 | - | - (3; 78%) | - | |
| | c.719A>G | Asn240Ser[‡] | 0 | 1 | - | - (3; 78%) | - | |
| **Cohort II** | c.89C>T | Ser30Phe[‡] | 1 | 0 | + | +(4; 82%) | - | |
| | c.95G>A | Gly32Glu | 1 | 0 | - | - (1; 82%) | - | |
| | c.182A>G | Glu61Lys | 1 | 0 | + | + (5; 87%) | + | ⇓Emax |
| | c.380C>T | Ser127Leu | 1 | 0 | + | - (0; 53%) | + | No Emax |
| | c.634_635delT | Leu211Del | 2 | 0 | frameshift | frameshift | + | frameshift |
| ***Severely obese*** | c.896C>A | Pro299His | 2 | 0 | + | + (6; 93%) | + | ⇓Emax |
| | c.907G>A | Ala303Thr | 1 | 0 | - | + (2; 70%) | + | EC50 |
| | c.976T>C | Cys326Arg | 1 | 0 | ++ | + (4; 82%) | - | |
| | c.583A>G | Ile195Val[‡] | 0 | 1 | - | - (0; 53%) | - | |
| ***Lean*** | c.914G>A | Arg305Gln[‡] | 0 | 1 | ++ | + (4; 82%) | + | ⇓Emax |
| | **TOTAL** | | **20*** | **6** | | | | |

*(Table 1 continued on the next page)*

**Table 1. (continued)**

| Gene | Mutation | | No. Severely Obese Carriers (n=889) | No. Control Carriers (n=932) | In Silico Prediction | | In Vitro Functional Study | |
|---|---|---|---|---|---|---|---|---|
| | DNA | Protein | | | PolyPhen | SNAP | Class-ification | Assayed Difference compared to WT |
| **MC3R** | | | | | | | | |
| **Cohort I** | c.260T>C | Ile87Thr†‡ | 1 | 0 | + | + (0; 58%) | - | |
| | c.779C>T | Ala260Val†‡ | 1 | 0 | - | - (3; 78%) | - | |
| | c.824T>C | Met275Thr†‡ | 1 | 0 | ++ | + (4; 82%) | - | |
| ***Severely obese*** | c.397_726delins228 | c.397_726delins228†‡ | 1 | 0 | Del/ins | Del/ins | + | Del/ins |
| | c.205A>T | Ser69Cys†‡ | 0 | 1 | - | - (1; 69%) | - | |
| ***Lean*** | c.245T>C | Phe82Ser†‡ | 0 | 1 | + | + (4; 82%) | + | ⇓Emax |
| **Cohort II** | | | | | | | | |
| | c.839C>G | Thr280Ser†‡ | 1 | 0 | ++ | + (2; 70%) | + | ⇓Emax |
| ***Severely Obese*** | c.889C>G | Leu297Val†‡ | 1 | 0 | - | + (3; 78%) | - | |
| ***Lean*** | c.245T>C | Phe82Ser†‡ | 0 | 1 | + | + (4; 82%) | + | ⇓Emax |
| | **TOTAL** | | **6** | **3** | | | | |

*Note: Two patients from Cohort II carry both Leu211del and Pro299His mutations.

**Table 1.** Summary of unique or rare mutations identified in the coding regions of *MC4R* and *MC3R*. For PolyPhen predictions: benign is denoted as -; possibly damaging is +, and probably damaging is ++. For SNAP predictions: neutral is denoted as -, and non-neutral as +, both followed by (reliability index; % expected accuracy). For *in vitro* classification: no functional alteration denoted as -, and functional alteration as +, followed by reason for functional alteration classification. Mutations are classified has having an *in vitro* functional alteration when: response did not reach a maximum, $EC_{50}$ was significantly different ($p<0.05$) compared to that of the WT by ANOVA followed by Dunnett's post-test, and/or had an $E_{max}$ of less than 50% wild type receptor maximum activity.

†: mutations never previously described, ‡: mutations for which α-MSH dose response had never been described, ⇓: decreased.

**Table 2.**

| Gene | Variant | No. Severely Obese Carriers (n=889) | No. Lean Control Carriers (n=932) | P value |
|---|---|---|---|---|
| **MC4R** | Val103Ile | 19 | 22 | 0.755 |
| | Leu251Ile | 6 | 6 | 0.774 |
| **MC3R** | Arg257Ser | 1 | 7 | 0.070 |
| | Thr6Lys/Val81Ile Haplotype | | | |
| | Wild type | 391 | 414 | 0.950 |
| | Heterozygous for 6K/81I | 93 | 113 | |
| | Homozygous for 6K/81I | 13 | 11 | |

**Table 2.** Summary of common variants identified in *MC4R* and *MC3R*. The number of severely obese adult carriers (out of n=889) and lean control carriers (out of n=932) for each variant for both *MC4R* and *MC3R* are listed.

***Comparative functional analysis of severe adult obesity-associated MC4R mutations.***

Nonsense and frameshift mutations in GPCRs generally lead to loss of function of the protein, and we considered them, *a priori*, to be functionally severe. However, most of the detected rare *MC4R* mutations are missense mutations, which may or may not significantly affect the function of the receptor. We therefore determined whether documenting the functional consequences of all mutations would strengthen the observed association between rare *MC4R* mutations and severe obesity. We systematically evaluated the agonist activation of each of the missense MC4R mutants found in obese and lean subjects to that of the wild-type receptor in an *in vitro* assay. We chose this assay as it will more sensitively detect most functional alterations in MC4R including impairment in membrane expression and/or ligand binding[119]. We considered a missense mutation to have functional alteration when: 1) a mutation had α-MSH dose response that did not reach a maximum, 2) a mutation had an $EC_{50}$ that was significantly different ($p<0.05$) compared to that of the wild type receptor, and/or 3) a mutation had an $E_{max}$ of less than 50% wild type receptor maximum activity. Including the 2 nonsense and 2 deletion mutations, 10 mutations, found only in obese subjects (in a total of 12 obese carriers), modified the agonist activation of the receptor in our *in vitro* assay while only 1 mutation found in control subjects (Arg305Gln) had such an *in vitro* phenotype (Table 1, Figure 1). After classification of functional consequences, the prevalence of functionally altered

*MC4R* mutations was significantly greater than compared to controls (p=0.001) [OR=12.7] (Figure 3).

**Figure 1.**

**A.**

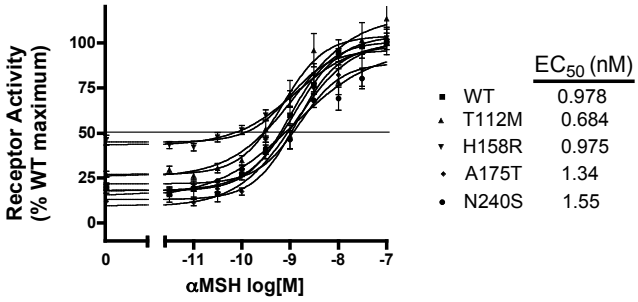


**B.**

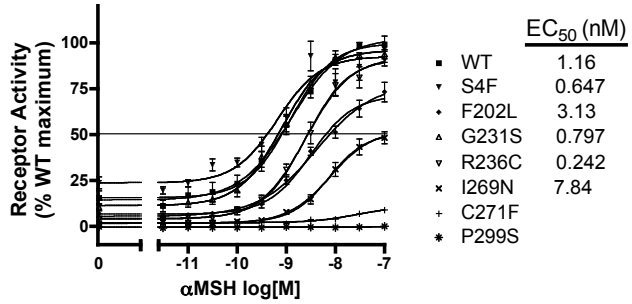


**C.**

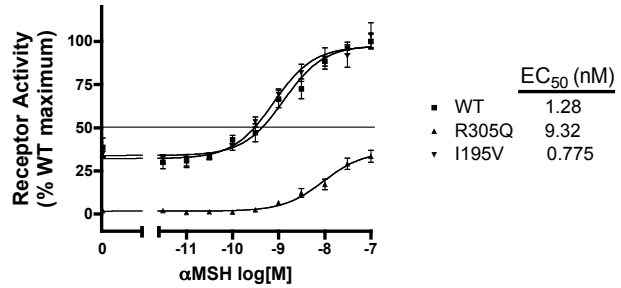


*(Figure 1 continued on the next page)*

**Figure 1. (continued)**

**D.**

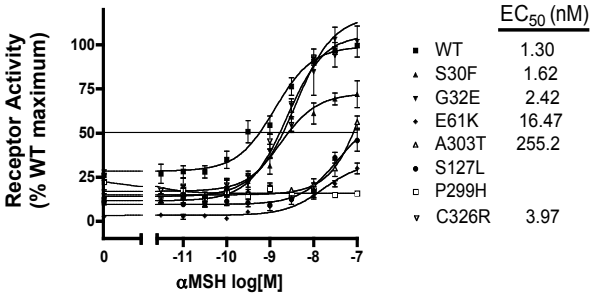


**Figure 1.** Functional analysis of mutant MC4Rs. $\alpha$-MSH dose response curves of mutants identified in A) lean controls of Cohort I (n=554), B) severely obese cases of Cohort I (n=510), C) lean controls of Cohort II (n=378), and D) severely obese cases of Cohort II (n=379). Data points represent mean ±SEM of at least three experiments performed in triplicate. Mean ($CI_{95}$) of the EC50 (nM) is indicated for each variant, when the variant response reached a maximum. For comparison purposes, the activities range from basal activity (0%) to the maximal activity (100%) of each receptor.

***Prevalence and nature of MC3R mutations in two North American cohorts of severe obese adults.***

To determine whether, as is the case for *MC4R*, rare *MC3R* mutations are associated with obesity, we examined the coding sequence of this gene in the same 889 cases and 932 controls.

The haplotype of 2 previously described common variants Thr6Lys and Val81Ile[136] were identified in 13 obese and 11 controls (not significant, p=0.950; Table 2). In addition, one mutation, Arg257Ser, was found in both control and severely obese subjects and was not considered further in the analysis (Table 2). Six severely obese and three controls carried rare heterozygous mutations in *MC3R* (Table 1). The prevalence of rare *MC3R* variants in the severely obese patients was 0.67% ($CI_{95\%}$ of 0.27-1.50) compared to 0.32% ($CI_{95\%}$ of 0.06-0.99) in controls (not significant, p=0.332).

***Comparative functional analysis of severe adult obesity-associated MC3R mutations.***

As with MC4R, we systematically and comparatively evaluated the agonist activation of each of the mutant *MC3R* found in obese and lean subjects. Two *MC3R* mutations identified in two obese adults and one *MC3R* mutation identified in two control subjects was functionally altered *in vitro* (Table 1; Figure 2).

Arg257Ser, found in both case and control subjects was also classified as a mutation with functional consequence. The prevalence of variants with functional alterations was the same in cases and controls (p= 0.625; Figure 3).

**Figure 2.**

**A.**

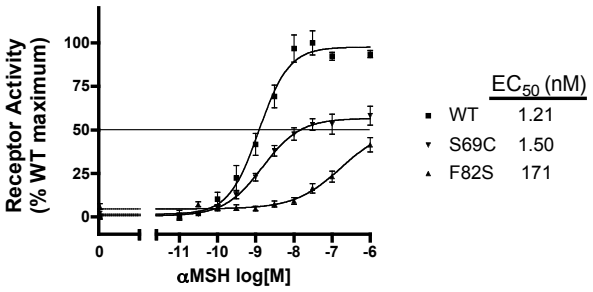


**B.**

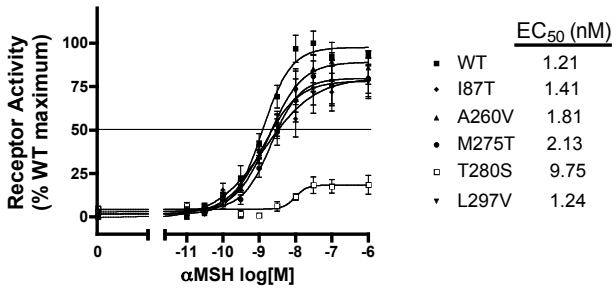


**Figure 2.** Functional analysis of mutant MC3Rs. α-MSH dose response curves of mutants identified in A) lean controls of Cohort I and Cohort II (n=932), and B) severely obese cases of Cohort I and Cohort II (n=889). Data points represent mean ±SEM of at least three experiments performed in triplicate. Mean ($CI_{95}$) of the $EC_{50}$ (nM) is indicated for each variant, when the variant response reached a maximum. For comparison purposes, the activities range from basal activity (0%) to the maximal activity (100%) of each receptor.

***In silico* analysis of severe adult obesity-associated *MC4R* and *MC3R* mutations.**

To determine whether *in silico* approaches could also be used to determine association of functionally significant mutations in MC4R and MC3R with obesity we used the computer mutation prediction programs, PolyPhen[137] and SNAP[138-140]. After classification of functional consequences, the prevalence of functionally altered MC4R mutations was significantly greater compared to controls for both the prediction tools, PolyPhen (p =0.001) and SNAP (p=0.002) (Figure 3). However, as with our *in vitro* analysis (p=0.625), the prevalence of MC3R variants with functional alterations by both *in silico* prediction methods was the same in cases and controls (PolyPhen p=0.442; SNAP p=0.277) (Figure 3). For both MC4R and MC3R there was no significant difference between the prevalence of mutations classified as having a functional alteration in the *in vitro* assay and *in silico*. However, there were a number of discrepancies between both methods, which indicates that at an individual mutation level *in silico* approaches cannot replace functional characterization (Table 1 and Figure 3).

**Figure 3.**

**A.**

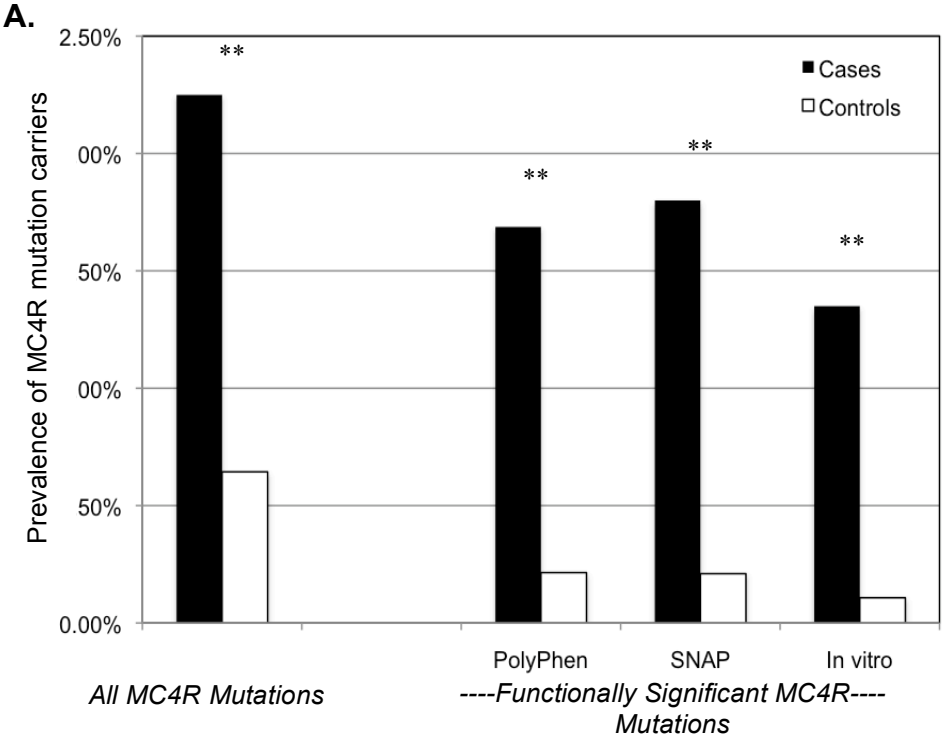
2.50%
00%
50%
00%
50%
0.00%
Prevalence of MC4R mutation carriers
Cases
Controls
**
**
**
**
PolyPhen
SNAP
In vitro
All MC4R Mutations
----Functionally Significant MC4R----
Mutations

**B.**

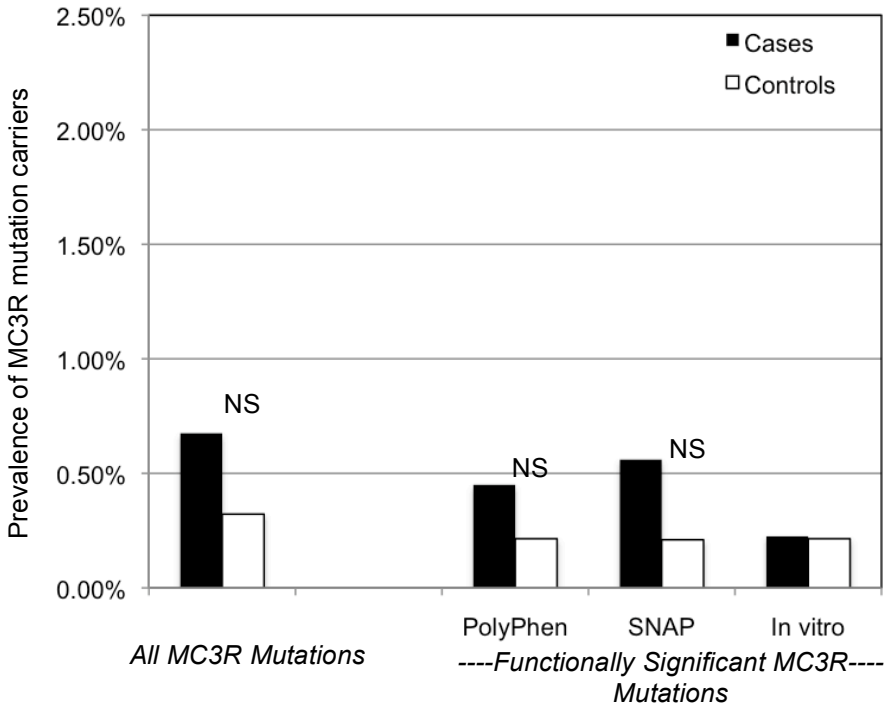
2.50%
2.00%
1.50%
1.00%
0.50%
0.00%
Prevalence of MC3R mutation carriers
Cases
Controls
NS
NS
NS
PolyPhen
SNAP
In vitro
All MC3R Mutations
----Functionally Significant MC3R----
Mutations

**Figure 3.** Prevalence of rare *MC4R* (A) and *MC3R* (B) mutation carriers in severely obese and lean subjects. Prevalence of carriers is determined by combining both Cohort I and Cohort II (a total of 889 cases and 932 controls). The prevalence of total rare mutation case carriers were compared to control carriers. These mutations were then grouped according to results of the funcitonal studies. Comparison of carriers between cases and controls were made using two-tailed Fisher's exact test. **: $p<0.005$, NS= not significant.

## DISCUSSION

This study confirms that mutations in *MC4R* are a significant cause of severe human obesity and extends this finding to severely obese North American adults. Indeed, we find the same combined prevalence of such mutations (2.25% ($CI_{95\%}$ of 1.44-3.47%)) in our severely obese adult patient populations as that previously described in French adults (2.35% (CI95 0.90-3.80%)) with severe obesity (BMI>35kg/$m^2$)[92] and in young adult Danish males (BMI≥31kg/$m^2$)[134]. This prevalence also matches the frequency of *MC4R* mutations detected in cohorts of patients with childhood obesity of different origins (1-6%)[97, 116-121, 134, 141]. Rare *MC4R* mutations are also found in non-obese controls albeit with a significantly lower frequency. The prevalence of such mutations in our control population (0.64%) is strikingly similar to that described for a very large population-based sample of adults from Germany (0.66% ($CI_{95\%}$ 0.44-0.96%))[142] and in most non-obese control populations. While the significant difference in the prevalence of rare *MC4R* mutations between cases and controls supports a causative role for such mutations in the severe obesity of these patients, this observation underlines the importance of systematically evaluating the functional consequences of such mutations. Indeed, restricting the association analysis to only mutations with a significant effect on the function of MC4R, significantly increases the odds ratio of association of rare MC4R mutations with severe obesity.

As compared to MC4R, the importance and role of MC3R mutations in the pathogenesis of obesity in rodents and humans has been less clear. As compared to *mc4r* -/- mice, *mc3r*-/- mice have a milder phenotype, limited to an increase in body fat, and unlike in heterozygous *mc4r+/-* mice, no energy homeostasis phenotype has been observed in heterozygous *mc3r+/-* mice[33, 128, 129, 143].

To date only two common variants[136] and four rare mutations in heterozygous carriers[131, 144] have been described in the coding region of the *MC3R*. The two common *MC3R* variants Thr6Lys and Val81Ile, which were also detected in the current study, were not associated with any obesity-related phenotypes, therefore likely representing benign polymorphisms[136, 145-148].

With respect to rare mutations in *MC3R*, one mutation, Ile183Asn, has been detected in one severely obese girl and her obese father, was absent in control subjects, and was characterized to be functionally inactive[130, 131]. More recently, 3 MC3R mutations were identified in a study of 290 severely obese Italian adults, mean BMI of 44.2±5.9kg/m$^2$. These three mutations were absent in 215 non-obese controls[144]. In that study, however, controls were only screened for mutations found in cases but the *MC3R* gene was not systematically sequenced in these controls. Two of these mutations were studied in the two families and segregated with obesity in the family members (total of four

relatives). Only one of the mutations, Ile335Ser, demonstrated *in vitro* functional abnormalities[144].

Our study, the largest yet to evaluate the prevalence of *MC3R* mutations in severe human obesity, does not support a significant role for mutations in this gene in this condition. The prevalence of such mutations in cases is 0.67% ($CI_{95\%}$ of 0.27-1.50) and is the same in controls. Systematic *in vitro* study of these mutations also demonstrates that functionally significant mutations are as frequent in both cohorts. Interestingly, the prevalence of rare MC3R variants found in both groups is also the same as the prevalence of rare MC4R variants (whether considering all or only restricted to functionally significant) found in controls or in the general population, further suggesting that it corresponds to the "background" frequency of rare mutations in these genes.

Our data does not eliminate a possible role for some of the individual *MC3R* mutations in the obesity of the carriers, in particular if some of these mutations have a pleiotropic or dominant negative effect. However, formal demonstration of the phenotypical effect of such specific mutations would require the study of very large multigenerational pedigrees to reach statistical significance. Such pedigrees are rarely available.

The recent completion of large genome scans has demonstrated that a certain number of common variants are associated with severe obesity but has

also strongly suggested that, in aggregate, such common variants will only account for a small portion of the overall genetic predisposition to this condition[113, 114, 149]. This observation has led to the re-visiting of the hypothesis that rare variants could account for the majority of one individual's predisposition to severe obesity and has led to the suggestion that large scale systematic sequencing of patients will be required to detect genes in which rare mutations predispose to the disease. Our results underline some of the possible limitations in the outcomes and interpretations of this approach. First, it is clear that the mere presence of rare heterozygous variants in cases is not sufficient to implicate a gene in the condition as such variant can be present at the same prevalence in controls, reflecting the background level of benign mutations in the gene. Second, differentiating functionally relevant mutations from functionally neutral mutations through specific *in vitro*/*in vivo* assays might be required to strengthen the association of rare mutations in a particular gene with a common phenotype. Finally, at an individual level, demonstration of the role of a specific mutation in a common condition might be limited.

## MATERIALS AND METHODS

***Subjects - US case-control study (Cohort I)***[132, 150]: Patients and controls were recruited through an ongoing study on the genetic determinants and clinical implications of severe obesity as well as from the Cardiovascular Research Institute Genomic Resource, a population-based investigation of cardio-vascular disease both established at the University of California, San Francisco (UCSF). Severely obese adult patients (n=510) were selected for a BMI≥40 kg/m$^2$. BMI was 47.9±8.3 kg/m$^2$, Age 48.3±12.1y, 73% female, 85% Caucasian. Controls (n=554) were chosen on the basis of a BMI≤25 (BMI 22.9±1.4 kg/m$^2$ and were matched for sex (68% female), Age (51.3±4.5y) and ethnicity (82% Caucasian).
The UCSF Committee on Human Research approved the protocols, and informed written consent was obtained from all patients. Genomic DNA was extracted from white blood cells by standard methods.

***Subjects - Canadian case-control study (Cohort II)***[100, 150]*:* Patients were recruited Ottawa Hospital Weight Management Clinic and controls were recruited from the Ottawa region. Severely obese Caucasian adult patients (n=379) were selected for a BMI≥40 kg/m$^2$. BMI was 49.0±8.8 kg/m$^2$, Age 49.5±10.7y, 63% female. Caucasian controls (n=378) were chosen on the basis of a BMI below the 10th percentile for age and sex (BMI 19.4±1.6 kg/m$^2$), and were matched for sex (64%female), and age (45.5±13.0y).

The institutional review boards of the University of Ottawa Heart Institute and the Ottawa Hospital approved this study and informed consent was obtained from all participants. Genomic DNA was extracted from white blood cells by standard methods. This cohort has previously been used to sequence for variants implicated in obesity[100].

***Sequencing*** - Two primers, MC4R-AF (5'-ATCAATTCAGGGGGACACTG-3') and MC4R-ER (5'-TGCATGTTCCTATATTGCGTG-3'), were used in PCR to amplify the entire coding region of the *MC4R* gene as described[35]. Two primers, MC3R-F (5'-AAGTTCTCCCTATGTCTCCAAGC -3') and MC3R-R (5'-CAAACGACAAGTACAATCATGGC -3'), were used in PCR to amplify the entire coding region of the *MC3R* gene. The sequencing reaction was performed with the BigDye terminator kit (Applied Biosystems, Foster City, CA) under the standard manufacturer's conditions. Each PCR product was sequenced using MC4R-AF, MC4R-ER, MC3R-F, MC3R-R, and two internal primers, MC4R-CF (5'-TGTAGCTCCTTGCTTGCATC-3') and MC4R-CR (5'-GGCCATCAGGAACATGTGGA-3'). Sequencing was performed on an ABIPRISM 3700 automated DNA sequencer (Applied Biosystems).

***In Vitro analysis of missense MC4R and MC3R mutations*** - *MC4R and MC3R expression vectors:* Wild type (WT) and mutant alleles of *MC4R* and *MC3R* gene were amplified and cloned directly from the genomic DNA of the patient. Both one exon genes were cloned in the vector pcDNA 3.1 (Invitrogen, San Diego,

CA). All expression vectors were sequenced to establish the presence of the mutation and the absence of any induced mutations.

***Assay of MC4R and MC3R activity*** - HEK 293 cells stably expressing or transiently transfected to express the luciferase reporter under the control of a cAMP responsive promoter[119, 132] were maintained in a-MEM supplemented with 10% calf serum (HYCLONE), L-glutamine, non-essential amino acids, and penicillin/streptomycin. Transfection and dose response assays were performed as previously described[119, 132]. Briefly, different concentrations of $\alpha$-MSH (SIGMA, St. Louis, Missouri, USA) were added to the medium at the desired concentration. Luciferase activity, representing the cAMP production through MC4R or MC3R activation, was assessed using the Steady-Glo Luciferase Assay System (Promega, Madison, WI) and a microplate luminescence counter (Packard Instrument, Downers Grove, IL). Luciferase activity upon MC4R or MC3R activation was normalized over the transfection efficiency and the results were finally normalized as a percentage of the maximum stimulation observed for the wild type receptors.

***In silico prediction of missense mutation effects*** - *PolyPhen Prediction:* Missense variants identified by sequencing were classified based on their potential impact on protein function or structure (benign, possibly damaging, or probably damaging) using a new version of the PolyPhen method[137]. These predictions are based on the analysis of multiple sequence alignments of

homologous proteins, functional annotation, and structural information if available[137]. The new version of PolyPhen constructs multiple sequence alignment using a pipeline of several existing programs for aligning sequences, alignment quality control, and clustering of sequences. PolyPhen defines the predictions of the mutations as follows: 1) probably damaging: it is with high confidence that it is suppose to affect protein function or structure, 2) possibly damaging: it is suppose to affect protein function or structure, 3) benign: it is most likely that it lacks any phenotypic effect.
(http://genetics.bwh.harvard.edu/pph)

***SNAP Prediction*** - SNAP (Screening for Non-Acceptable Polymorphisms) is a neural-network based method[140] that uses, among other things, information about sequence conservation, per residue predictions of secondary structure, solvent accessibility, and flexibility, and, if available, experimental functional annotations. The server output is a binary classification of the mutation's functional effect (neutral/non-neutral) in combination with the reliability index (RI) of prediction (integer score ranging from zero to nine)[138], which correlates well with the expected accuracy of the prediction[139].

***Statistical Analysis*** - Prevalence and confidence intervals were calculated using GraphPad Statistics Software. Common variants and haplotype associations with obesity were analyzed by performing a Chi-square analysis-of-contingency table with Yates' correction. The prevalence of rare mutation carriers and the

prevalence of functionally significant rare mutation carriers (as defined by *in silico* and *in vitro* experiments) in severely obese subjects compared to those prevalences in lean subjects were analyzed for a significant difference ($p<0.05$) by two-tailed Fisher's exact test. Best-fit estimates of the EC50s (the concentration of ligand needed to achieve 50% of maximum effect) and the 95% confidence intervals were obtained by non-linear regression fitting of the sigmoidal dose response curves using Prism 4. Mutant receptor EC50s were compared to wild type receptor EC50 and significance ($p<0.05$) was determined by ANOVA followed by Dunnett's post-test.

# CHAPTER IV

## Mutational Analysis of the Pro-opiomelanocortin Gene in French Obese Children Led to the Identification of a Novel Deleterious Heterozygous Mutation Located in the α-Melanocyte Stimulating Hormone Domain*.

**in collaboration with Beatrice Dubern*

**SUMMARY**

The pro-opiomelanocotin (POMC) plays a key role in body weight regulation, where its derived peptides mediate leptin action *via* the hypothalamic melanocortin 4 receptor (MC4R). The pathogenic effects of POMC mutations have been challenged in obesity. Our aim was to assess the relevance of POMC mutations in a cohort of French obese and nonobese children. Direct sequencing of the POMC gene was performed in 322 obese and 363 control unrelated children. Functional studies for the novel Phe144Leu mutation included the response to α-melanocyte stimulating hormone (αMSH) and a competitive binding assay. POMC mutations were identified in 3.72% of obese [95% confidence interval (CI): 1.66-5.80] and 2.20% of control (95% CI: 0.69-3.71) subjects. The novel mutation located in the αMSH region of the POMC gene (Phe144Leu) was found in one obese child and was transmitted by the obese father. Functional studies showed that MC4R activation in response to Leu144αMSH was almost completely abolished due to a dramatically altered binding of Leu144αMSH to MC4R. The frequency of POMC mutations is not significantly different between obese and control children in our cohort. The novel heterozygous mutation Phe144Leu leading to the absence of melanocortin signaling was associated with early-onset obesity suggesting its pathogenic role.

## INTRODUCTION

The proopiomelanocortin (POMC) is a complex propeptide encoding a number of melanocortin peptides that are released by tissue-specific proteolytic processing. These peptides have important roles in a range of functions such as skin pigmentation, control of adrenal function, and body weight regulation *via* the leptin/melanocortin pathway[151]. The production of POMC in the central nervous system is stimulated by leptin and its posttranslational process leads to the generation of different peptides[152]. The nature of POMC-derived peptides depends on the type of endoproteolytic enzymes present in specific brain areas. In the anterior pituitary, the presence of the proconvertase (PC) 1 enzyme allows the production of adrenocorticotropic hormone (ACTH) and β-lipotropin peptides, while the simultaneous presence of PC1 and PC2 in the hypothalamus determines the production of α-, β-, γ-melanocyte-stimulating hormone (α-, β-, γMSH) and β-endorphins. POMC knockout mice become obese due to the loss of the anorexigenic action of αMSH on melanocortin-4 receptor (MC4R) expressing neurons. They have no adrenal function because of the lack of ACTH production and present variable alterations in coat pigmentation due to the absence of αMSH in the skin[153]. The phenotype of POMC-deficient mice resembles that of patients with rare mutations that completely prevent POMC-derived peptide production. To date, six families with children carrying homozygous or compound heterozygous loss-of-function mutations in POMC have been described. The children in these families display a hypocortisolism,

early-onset obesity, and variable alterations of skin and hair pigmentation, thereby defining a new rare syndrome of obesity associated with POMC deficiency[154, 155].

The POMC gene is located in the human chromosome 2, which is a region strongly linked with leptin levels and to a lesser extent with obesity[156-159]. It was considered a strong positional candidate, and direct gene screening revealed several polymorphisms, generally with low frequency, located in both coding and noncoding regions[160]. Variants of the POMC gene were found in German[161, 162], Danish[163], Swedish[164], Italian[165, 166], and English[167, 168] obese children and young adults and in French diabetic and obese adults[169]. These variations included base insertion or deletion, missense, or silent mutations and were generally uncommon. Most of these variants were not associated with obesity-related phenotypes and generally had no functional consequences, except for mutations involving βMSH domain (Arg236Gly and Tyr221Cys)[162, 167, 168]. The frequency of the Arg236Gly mutation was shown to be mildly increased in U.K. obese children, and functional analyses revealed that this mutation prevents the normal processing of βMSH and β-endorphin, resulting in a fusion protein[167]. Able to bind MC4R, this aberrant peptide leads to a decreased activation of the receptor. Recently, the mutation Tyr221Cys, also located in the βMSH domain of POMC, was implicated in early-onset obesity with deleterious *in vitro* functional effects[162, 168]. Those findings suggested that βMSH might play a critical role in weight regulation in humans. Thus, further investigations of the POMC gene in obese and nonobese populations are needed to determine the contributing role of

POMC gene variants in human obesity.

In the present study, we report the mutational analysis of the POMC gene in a French cohort of 322 obese children and 363 controls. We also describe a novel heterozygous mutation in the αMSH domain of the POMC gene associated with early-onset obesity and with deleterious *in vitro* functional effects.

## RESULTS

### *Frequency of POMC mutations in obese and lean French children and identification of a patient carrying the Phe144Leu POMC mutation.*

By screening 322 severely obese children for POMC mutations, nine mutations were identified (Asp53Gly, Gly96Cys, Pro132Ala, Arg236Gly, Glu214Gly, Ala195Thr, Leu209Pro, Phe87Leu, Phe144Leu) in 12 unrelated individuals (3.72%, 95% CI: 1.66-5.80]). Among them, six have not been previously reported (Asp53Gly, Phe87Leu, Gly96Cys, Pro132Ala, Phe144Leu, Leu209Pro). In the control group, two novel mutations (Asn91Ser, Glu57Lys) were uniquely detected, whereas two mutations (Glu214Gly, Ala195Thr) were found in both obese and control populations (Table 1 and figure 1). Four obese patients and one lean control were carriers of the Asp53Gly mutation (1.24%). Overall, the frequency of POMC gene variations was not significantly different between obese (3.72%, 95% CI: 1.66-5.80) and controls [2.20%, 95% CI: 0.69-3.71, $p$ = not significant (NS)] in this group of French children. Clinical and biological characteristics of POMC mutation carriers (obese and controls) are shown in Table 2. No difference in weight and BMI *Z* score was observed between POMC genetic variant carriers and noncarriers in the obese and lean groups, respectively (data not shown).

**Table 1.**

| Nucleotide change | Amino acid change | Obese (n=322) | Controls (n=373) | $\chi^2$ |
|---|---|---|---|---|
| 158 a>g | Asp53Gly | 4 (1.24%) | 1 (0.27%) | NS |
| 287 c>t | Gly96Cys | 1 (0.31%) | 0 | |
| 395 c>g | Pro132Ala | 1 (0.31%) | 0 | |
| 707 c>g | Arg236Gly | 1 (0.31%) | 0 | |
| 642 a>g | Glu214Gly | 1 (0.31%) | 4 (1.07%) | |
| 584 g>a | Ala195Thr | 1 (0.31%) | 1 (0.27%) | |
| 627 t>c | Leu209Pro | 1 (0.31%) | 0 | |
| 262 c>a | Phe87Leu | 1 (0.31%) | 0 | |
| 273 a>g | Asn91Ser | 0 | 1 (0.27%) | |
| 169 g>a | Gln57Lys | 0 | 1 (0.27%) | |
| 431 t>c | Phe144Leu | 1 (0.31%) | 0 | |
| **POMC gene variations frequency** | | **3.72% $CI_{95\%}$[1.66-5.80]** | **2.20% $CI_{95\%}$[0.69-3.71]** | **NS** |

**Table 1.** Frequency of POMC gene variations in obese and control children.

**Figure 1.**

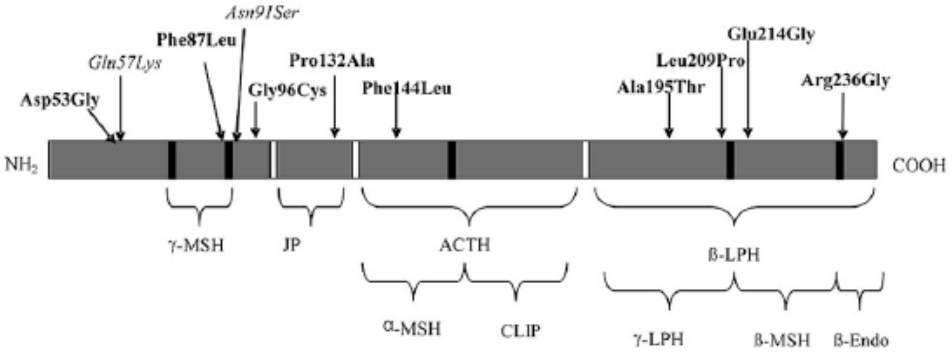


**Figure 1.** POMC protein and location of the variants in obese and lean children. White and black boxes are for the cut sites for PCs. Italics: mutations identified only in controls. JP, joint peptide; CLIP, corticotropin-like intermediate peptide; LPH, lipoprotein hormone; Endo, endorphin.

**Table 2.**

| Subjects | POMC mutation | Age (y) | Sex | BMI Z (SD) | Age at obesity onset (y) | Ins T0 (μU/mL) | Gly T0 (mmol/L) | HOMA | TG (mmol/L) | Chol (g/L) | Leptin (ng/mL) |
|---|---|---|---|---|---|---|---|---|---|---|---|
| Obese | | | | | | | | | | | |
| 1 | Asp53Gly | 5 | F | 4.7 | 5 | 4.1 | 4.3 | 0.8 | 0.5 | 0.7 | ND |
| 2 | Asp53Gly | 7 | M | 6.7 | 0.5 | 13.0 | 5.1 | 3.0 | 0.6 | 1.7 | 17.5 |
| 3 | Asp53Gly | 8 | M | 5.2 | 4 | 14.0 | 4.8 | 3.0 | 0.5 | 1.5 | 16.0 |
| 4 | Asp53Gly | 10 | F | 4.7 | 6 | 19.8 | 4.8 | 4.2 | 1.3 | 2.1 | 26.0 |
| 5 | Gly96Cys | 13 | F | 3.6 | ? | 14.0 | 4.9 | 3.0 | 0.8 | 1.4 | 21.0 |
| 6 | Pro132Ala | 17 | F | 3.8 | ? | 16.9 | 5.0 | 3.7 | 0.9 | 1.5 | ND |
| 7 | Arg236Gly | 15 | F | 1.7 | 5 | ND | ND | ND | ND | ND | ND |
| 8 | Glu214Gly | 11 | F | 3.3 | 2 | 26.0 | 4.9 | 5.7 | 0.8 | 0.9 | 12.0 |
| 9 | Ala195Thr | 12 | F | 5.8 | ? | ND | ND | ND | ND | ND | ND |
| 10 | Leu209Pro | 14 | M | 3.9 | 3.2 | 18.0 | 5.1 | 4.1 | 0.8 | 1.5 | 19.4 |
| 11 | Phe87Leu | 7 | F | 6.2 | ? | 15.0 | 5.0 | 3.3 | 0.6 | 1.8 | 21.0 |
| 12 | Phe144Leu | 12 | F | 2.7 | 4.5 | 8.3 | 5.5 | 2.0 | 0.9 | 1.7 | 20.0 |
| Controls | | | | | | | | | | | |
| 13 | Asn91Ser | 11 | M | −1.1 | — | 5.9 | 4.8 | 1.3 | 0.4 | 1.2 | 3.9 |
| 14 | Glu57Lys | 11 | M | 0.3 | — | 15.5 | 4.1 | 2.9 | 0.8 | 1.1 | 3.5 |
| 15 | Asp53Gly | 12 | M | 0.9 | — | ND | ND | ND | ND | 1.2 | 4.2 |
| 16 | Glu214Gly | 13 | M | 1.6 | — | 15.0 | 5.7 | 3.8 | 1.1 | 1.4 | 21.4 |
| 17 | Glu214Gly | 12 | F | 0.1 | — | 4.2 | 4.7 | 0.9 | 0.8 | 1.5 | 8.6 |
| 18 | Glu214Gly | 11 | F | 3.9 | — | 23.2 | 5.1 | 5.2 | 1.3 | 1.1 | 40.8 |
| 19 | Glu214Gly | 12 | M | −1.2 | — | 5.2 | 4.9 | 1.1 | 0.4 | 1.7 | 0.8 |
| 20 | Ala195Thr | 14 | F | 0.8 | — | ND | ND | ND | ND | ND | 16.8 |

**Table 2.** Characteristics of POMC mutations carriers.

M, male, F, female; age at obesity onset is defined as age with BMI above the 97th percentile; Ins T0, fasting insulinemia; Gly T0: fasting glucose; HOMA, homeostasis model assessment index defined as (fasting insulin level _ fasting glucose level) divided by 22.5; TG, triacylglycerol; Chol, total cholesterol; ?, data not available; ND, not determined.

Biological parameters were measured according to methods described in Materials and Methods section.

Because most of the detected mutations occurred in regions of the POMC propeptide with uncertain biological functions, we concentrated our study on the novel heterozygous missense mutation Phe144Leu located in the αMSH coding region of POMC gene. The Phe144Leu mutation was detected in only one obese child and was absent in the control population. Segregation analysis of the mutation in the family showed that the mutation was present in the obese father (figure 2A). The other available family members were not carriers of the mutation and were neither overweight nor obese.

**Figure 2.**

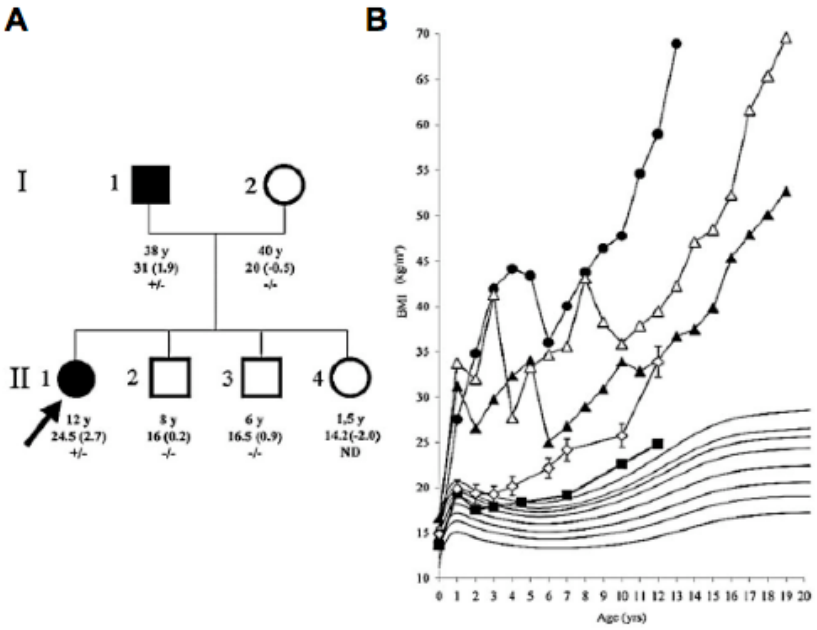


**Figure 2.** Pedigree, genotype, and clinical characteristics of the Phe144Leu POMC mutation carrier. (*A*) Pedigree and genotypes. The proband II1 is a 12-y-old female with a BMI of 22.5 kg/m$^2$ (BMI *Z* score = 2.7 SDs). She is heterozygous for a Phe144Leu (t > c 431) mutation. The mutated allele was

transmitted by her father who is moderately obese (BMI, 31 kg/m$^2$ at age 38 y, BMI *Z* score = 1.9 SDs). Subjects I2 (BMI, 21 kg/m$^2$ at age 40 y, BMI *Z* score = -0.5 SD), II2 (age, 8 y; BMI *Z* score = 0.2 SD) and II3 (age, 6 y; BMI *Z* score = 0.9 SD) are nonobese carriers of two normal alleles. Obese individuals (*solid circles and squares*). Age, BMI *Z* score, and genotype (+, normal; -, mutated) are indicated on the pedigree; ND, not determined. (*B*) BMI curves of the proband (HetPOMC), six heterozygous MC4R mutation carriers (HetMC4R), and three homozygous null leptin receptor mutants (LepR 1, 2, 3). HetPOMC (*solid squares*); LepR 1 (*solid circles*); LepR 2 (*open triangles*); LepR 3 (*solid triangles*); HetMC4R (*open diamonds*).

***Clinical and biologic phenotype of the phe144leu mutation carrier.***

The Phe144Leu mutation carrier was a 12-y-old obese girl from a nonconsanguineous family. She was born at term and had a normal birth weight (3000 g). She had no red hair and no clinical evidence of adrenal impairment. At age 12 y, the patient's BMI *Z* score was 2.7 SDs with normal puberty (Tanner stage 4). Her fat mass was 31.45% (18.7 kg) of her total body mass. The BMI curve showed a preserved but early (at age 2 y) adiposity rebound in the absence of any dietary intervention (figure 2B). The age at obesity onset, defined as age with BMI above the 97th percentile, was 4.5 y. We compared the BMI evolution of the proband with that of subjects lacking leptin receptor (LEPR) signaling and with that of subjects heterozygous for MC4R mutations[170] (figure 2B). In contrast to LEPR-deficient patients, the BMI curve of the proband did not

show a dramatic augmentation. When compared with young MC4R mutation carriers[116] (unpublished data), the BMI curves were close during the first 4 y of life between MC4R mutation carriers and the girl carrying the Phe144Leu mutation. Differences in BMI evolution markedly appeared after the age of 5 y because the BMI of the POMC mutation carrier showed only minor aggravation compared with MC4R subjects displaying a rapid increase in BMI in the absence of any dietary intervention.

Endocrine and metabolic explorations in the proband showed only a moderate hyperinsulinemia with a plasma insulin level of 16.9 µUI/mL 120 min after glucose ingestion with normal glucose levels (Table 3). Hypothalamic-pituitary-adrenal axis explorations were normal (urinary free cortisol, dynamic test of adrenal axis), as well as thyroid axis explorations (free $T_4$ and TSH) (Table 3). Circulating leptin measurement (leptin 20 ng/mL) was in agreement with her corpulence (leptin/kg fat mass, 1.1). Lipid metabolism was unremarkable (total cholesterol, 1.7 g/L; triacylglycerol, 0.9 mM). At age 12 y, the resting metabolic rate evaluated by indirect calorimetry was normal for her body composition (1260 kcal /24 h, 39 kg fat-free mass).

**Table 3.**

| | Phe144Leu | Normal range |
|---|---|---|
| UFC ($\mu$g/24 h) | 17.5 | 23 ± 11 |
| CRF test | | |
| Cortisol (ng/mL) (0–60 min) | 53–146 | 104 ± 48–184 ± 29 |
| ACTH (pg/mL) (0–60 min) | 25–76 | <40–77 ± 27 |
| LPH (pg/mL) (0–60 min) | 124–218 | 87 ± 38–167 ± 49 |
| TSH ($\mu$U/mL) | 3.0 | 1.78 (0.2–3.5) |
| Free $T_4$ (pg/mL) | 7.2 | 8.5 (5.8–11.5) |
| OGTT | | |
| Glucose (mmol/L) (0–30–120 min) | 5.0–7.2–6.5 | T0: 3.3–5.8; T120: <7.8 |
| Insulinemia ($\mu$UI/mL) (0–30–120 min) | 8.3–32.2–16.9 | T0: <5 |

**Table 3.** Endocrine characteristics of the proband with the Phe144Leu mutation. UFC, urinary free cortisol; CRF, corticotropin releasing factor; LPH, lipoprotein hormone; OGTT, oral glucose tolerance test.

***Functional effect of the Phe144leu POMC mutation.***

We evaluated the ability of Leu144αMSH (mutated POMC allele) to activate hMC4R by comparing both cAMP production and the binding to the receptor with that of Phe144αMSH (wild-type allele). In our assay, hMC4R activation in response to Leu144αMSH was almost completely abolished ($EC_{50}$ not determinable) compared with that with Phe144αMSH ($EC_{50}$ ± SD = 1.5 ± 0.7 nM) (Figure 3A). This result was due, at least partially, to the dramatically altered binding of Leu144αMSH to hMC4R (figure 3B).

**Figure 3.**

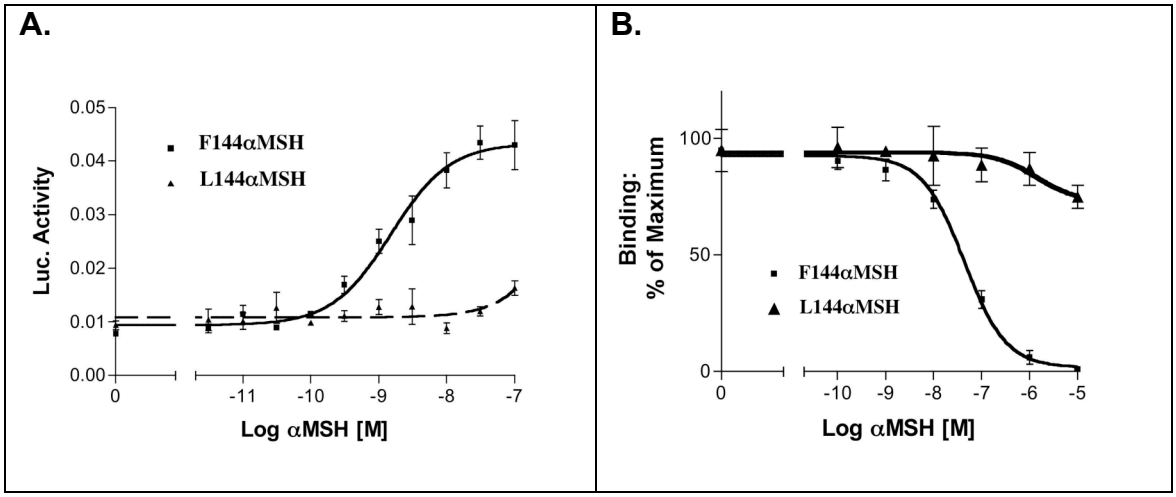


**Figure 3.** Impaired activation and binding of MC4R by the αMSH product of Phe144Leu POMC. Leu144αMSH (Leu at position 7 of αMSH corresponding to the mutated POMC allele) and Phe144αMSH (Phe at position 7 corresponding to wild type) were synthesized and purified by high-performance liquid chromatography. *A*) MC4R activity in response of Phe144αMSH or Leu144αMSH. Data points represent means of five determinations and error bars indicate SDs. The $EC_{50}$ ± SDs for αMSH activation is 1.5 ± 0.7 nM. *B*) Competition binding assay of Phe144αMSH or Leu144αMSH on the human MC4R. Each point is the mean of triplicate values and error bars indicate SDs. The $IC_{50}$ for Phe144αMSH in this experiment is 29.6 ± 7.52 nM. Phe144αMSH (*solid squares*); Leu144αMSH (*solid triangles*).

## DISCUSSION

We report here the screening of the POMC gene in a cohort of obese and nonobese French children. A novel mutation (Phe144Leu) located in the αMSH domain of the POMC gene associated with early-onset obesity was detected. *In vitro* studies revealed that the Phe144Leu amino acid substitution resulted in a deleterious functional effect with a complete lack of hMC4R activation due to a dramatic impairment of mutant αMSH binding. The Phe144Leu mutation was found in a 12-y-old girl with early-onset obesity. No other associated phenotypes such as adrenal insufficiency and hypopigmentation were noted in contrast to the phenotype in patients with POMC-null homozygous mutation[154]. This may be explained by the complex regulation of pigmentation characterized by high interindividual variability. More specifically, pigmentation in humans varies greatly between individuals and particularly among ethnic groups, primarily because of several differences in melanin (*e.g.* size, shape, density, and type) and the multiple polymorphisms in melanocortin 1 receptor that are capable of modulating its basal activity[160]. Several observations, including this one, suggest that the skin and hair phenotype might vary according to the ethnic origin of POMC mutation carriers[155, 167]. Precise chemical analysis measuring hair melanin peptide and skin pigmentation would be necessary to firmly conclude. We also observed normal results in hypothalamic-pituitary-adrenal axis explorations in the Phe144Leu carrier, which could be explained by the fact that the mutation does not alter the effect of ACTH on melanocortin 2 receptor. This is in agreement with

previous findings observed in heterozygous carriers of POMC mutations[155, 162, 167, 168]. However, this would need further *in vitro* functional investigation.

The BMI curve of this subject shows several interesting findings. Obesity starts as early as in the MC4R mutant carriers, suggesting a very early effect of the functionally relevant Phe144leu mutation on weight gain after birth. However, it is less severe over time. This is not due to a change in diet because both MC4R and POMC mutated subjects did not undergo any dietary intervention until the age of 10 y. This observation suggests that, in humans, deleterious heterozygous mutations in the αMSH domain of the POMC gene might lead to a less severe obese phenotype than heterozygous mutations in MC4R gene. While the central melanocortin system is intolerant to the loss of a single MC4R allele, it appears to be able to tolerate the loss of one copy of the POMC gene, except for mutations in βMSH. The Phe144Leu mutation in αMSH, as the one recently reported by Lee *et al.*[168], appears to have only a moderate effect on the obese phenotype when compared with the effect of βMSH mutations. Our findings provide additional support for a more critical role of βMSH than of αMSH in the control of human energy balance[162, 167, 168]. Because βMSH is present in the human hypothalamus [171] and seems to have higher affinity for the hMC4R[172], it is likely to be the more physiologically relevant endogenous ligand for the hMC4R (when compared with αMSH). The obese phenotype associated with the POMC mutation reported here could also be modulated by other variants in modifier genes, intrinsic and/or extrinsic to the melanocortin pathway. Co-segregation analysis also showed that the obese father carrying the mutation has a

comparatively less pronounced form of obesity. Gene-environment interactions are a plausible explanation, as the younger generation is growing up in a much more obesogenic environment compared with the older generation. This family pedigree with the POMC mutation further illustrates the complex nature of human obesity when variant alleles in certain thrifty genes might interact together to favor weight gain in a predisposing environment.

In our study, the frequency of POMC gene variations was not significantly different between obese and control children. In contrast to MC4R mutations that [167, 168]are significantly more frequent in obese populations[92, 142], it suggests that the implication of POMC mutations in the development of obesity remains to be discussed. Although carriers of POMC mutations have been described in several studies[154, 155, 161-164, 166-168], the effect of the mutations on the obesity phenotype appears to be variable and the study of the functional consequences of POMC mutations are still rare but necessary to demonstrate their pathogenic role. Up to now, only a few POMC mutations may be considered a cause of monogenic obesity [154, 162, 167, 168].

In conclusion, we found a similar frequency of POMC mutations in lean and obese children. Only rare deleterious mutations, such as the Phe144Leu described here, might contribute to early-onset obesity[161-163, 166-168]. In addition to previous studies, our findings confirm the less critical role of the POMC gene mutations in the complex determinism of human obesity when compared with MC4R mutations that are involved in 2%-3% of human obesity[92, 142]. In addition, they may confirm the more critical role of βMSH than αMSH in the control of

human energy balance because mutations in αMSH appear to have only a moderate effect on the obese phenotype when compared with the effect of βMSH mutations and support the physiologic role of the melanocortin pathway in human weight regulation.

## MATERIALS AND METHODS

***Direct POMC gene sequencing*** - This study was approved by the local ethics committee, and informed consent was obtained from all participating subjects. The genomic DNA of all subjects was isolated from 10 mL of venous whole blood (Wizard Genomic DNA Purification Kit, Promega Madison, WI). Direct sequencing (Sequencer Applied Biosystem) of the coding region of the POMC gene was performed in 322 unrelated obese children and in 363 nonobese children. Obese children [mean age, 12.8 y ± 2.8 standard deviations (SDs); mean body mass index (BMI) *Z* score = 4.3 ± 1.2 SDs; BMI *Z* score range, 2.0-10.2 SDs] were prospectively recruited between 2001 and 2004 in three different departments of pediatric nutrition located in Paris, Caen, and Margency, France [as described in Dubern *et al.*[116]]. In the present study, obesity was defined as a BMI *Z* score at least 2 SDs above the mean age and sex-specific BMI values in children in France[173]. The control group included 363 nonobese children (mean age, 11.5 y ± 0.6 SD; mean BMI *Z* score = 0.2 ± 1.0 SD; BMI *Z* score range, -2.96 to 1.93 SDs). These children were part of a randomized, controlled ongoing field trial (ICAPS) in middle school's first-level adolescents from eight randomly selected schools in the department of the Bas-Rhin (Eastern France) [174].

Genotyping of the Phe144Leu POMC mutation in the proband's family was also performed by direct sequencing (Sequencer Applied Biosystem) of the coding regions of the POMC gene. Primers and conditions can be provided upon request. Nucleotides and amino acids were numbered according to GenBank

accession numbers V01510 and NP 000930, respectively.

***Clinical and biochemical data*** - All obese patients underwent a physical examination with anthropometric measurements and Tanner stage evaluation by the same investigator in each center. Height and weight curves were obtained from the medical health records of the subjects.

In the patient carrying the Phe144Leu mutation, body composition (fat-free mass and body fat) was measured using whole-body dual-energy x-ray absorptiometry (Hologic QDR 2000 unit, Waltham, MA). The percentage body fat was calculated as the ratio of total body fat mass over total body mass. Blood samples were collected in the morning after an overnight fast. Total cholesterol and triacylglycerol were measured using an enzymatic assay (Boerhinger, Mannheim, Germany). Plasma leptin concentrations were measured by radioimmunoassay (RIA) (LINCO Research, Inc., St. Louis, MO). Oral glucose tolerance test was performed by giving 1.75 g glucose/kg body weight (maximum, 75 g). Plasma glucose and insulin concentrations were measured in the fasting state and 30 and 120 min after glucose ingestion using the glucose oxidase method and a RIA with polyclonal antibodies (INSI-PR, CIS Bio International, Gif-sur-Yvette, France), respectively. Hypothalamic-pituitary-adrenal axis exploration included urinary free cortisol and a dynamic test of adrenal axis with measurements of serum cortisol and ACTH by standard immunoassays. To explore thyroid axis, serum free thyroxine ($T_4$) and thyroid-stimulating hormone (TSH) were measured by standard immunoassays. Basal

resting metabolic rate was performed using indirect calorimetry (Deltatrac II monitor, Datex Instrumentarium Corp., Helsinki, Finland).

***Human MC4R (hMC4R) activation by the αMSH product of Phe144leu POMC*** - Leu144αMSH (Leu at position 7 of αMSH) and Phe144αMSH (Phe at position 7) were synthesized and purified by high-performance liquid chromatography (Genemed Synthesis Inc., South San Francisco, CA). MC4R activity was measured by analyzing its ability to activate expression of a cyclic adenosine monophosphate (cAMP)-inducible luciferase gene in HEK 293[119]. HEK 293 cells stably expressing a cAMP-inducible luciferase gene were transiently transfected with the hMC4R and stimulated for 6 h with medium alone, increasing amounts of Phe144αMSH or Leu144αMSH, after which luciferase activity was measured as previously described[119]. Data points represent means of five determinations and error bars indicate SDs.

***Competitive binding assay*** - HEK 293 cells stably transfected with the hMC4R were incubated with [$^{125}$I]NDP αMSH in the presence of increasing concentrations of Phe144αMSH or Leu144αMSH. Results are expressed as a percentage of total specific binding (Bmax). The curve is fitted using nonlinear regression analysis and one-site competition model (GraphPad Prism, graph software, San Diego, CA). Each point is the mean of triplicate values. Error bars indicate SDs.

# SUPPORTING MATERIAL

1 Flegal, K.M., Carroll, M.D., Ogden, C.L. & Johnson, C.L. (2002) Prevalence and trends in obesity among US adults, 1999-2000. *Jama* **288**, 1723-1727.

2 Calle, E.E., Thun, M.J., Petrelli, J.M., Rodriguez, C. & Heath, C.W., Jr. (1999) Body-mass index and mortality in a prospective cohort of U.S. adults. *N Engl J Med* **341**, 1097-1105.

3 Eckel, R.H. & Krauss, R.M. (1998) American Heart Association call to action: obesity as a major risk factor for coronary heart disease. AHA Nutrition Committee. *Circulation* **97**, 2099-2100.

4 Hill, J.O., Wyatt, H.R., Reed, G.W. & Peters, J.C. (2003) Obesity and the environment: where do we go from here? *Science* **299**, 853-855.

5 Kopelman, P.G. (2000) Obesity as a medical problem. *Nature* **404**, 635-643.

6 Must, A., Spadano, J., Coakley, E.H., Field, A.E., Colditz, G. & Dietz, W.H. (1999) The disease burden associated with overweight and obesity. *Jama* **282**, 1523-1529.

7 Friedman, J.M. & Halaas, J.L. (1998) Leptin and the regulation of body weight in mammals. *Nature* **395**, 763-770.

8 Thornton, J.E., Cheung, C.C., Clifton, D.K. & Steiner, R.A. (1997) Regulation of hypothalamic proopiomelanocortin mRNA by leptin in ob/ob mice. *Endocrinology* **138**, 5063-5066.

9 Schwartz, M.W., Seeley, R.J., Woods, S.C., Weigle, D.S., Campfield, L.A., Burn, P. & Baskin, D.G. (1997) Leptin increases hypothalamic pro-opiomelanocortin mRNA expression in the rostral arcuate nucleus. *Diabetes* **46**, 2119-2123.

10 Cheung, C.C., Clifton, D.K. & Steiner, R.A. (1997) Proopiomelanocortin neurons are direct targets for leptin in the hypothalamus. *Endocrinology* **138**, 4489-4492.

11 Mizuno, T.M. & Mobbs, C.V. (1999) Hypothalamic agouti-related protein messenger ribonucleic acid is inhibited by leptin and stimulated by fasting. *Endocrinology* **140**, 814-817.

12 Wilson, B.D., Bagnol, D., Kaelin, C.B., Ollmann, M.M., Gantz, I., Watson, S.J. & Barsh, G.S. (1999) Physiological and anatomical circuitry between Agouti-related protein and leptin signaling. *Endocrinology* **140**, 2387-2397.

13 Seeley, R.J., Yagaloff, K.A., Fisher, S.L., Burn, P., Thiele, T.E., van Dijk, G., Baskin, D.G. & Schwartz, M.W. (1997) Melanocortin receptors in leptin effects. *Nature* **390**, 349.

14 Mizuno, T.M., Kleopoulos, S.P., Bergen, H.T., Roberts, J.L., Priest, C.A. & Mobbs, C.V. (1998) Hypothalamic pro-opiomelanocortin mRNA is reduced by fasting and [corrected] in ob/ob and db/db mice, but is stimulated by leptin. *Diabetes* **47**, 294-297.

15 Baskin, D.G., Hahn, T.M. & Schwartz, M.W. (1999) Leptin sensitive neurons in the hypothalamus. *Horm Metab Res* **31**, 345-350.

16 Haskell-Luevano, C., Chen, P., Li, C., Chang, K., Smith, M.S., Cameron, J.L. & Cone, R.D. (1999) Characterization of the neuroanatomical distribution of agouti-related protein immunoreactivity in the rhesus monkey and the rat. *Endocrinology* **140**, 1408-1415.

17 Marsh, D.J., Hollopeter, G., Huszar, D., Laufer, R., Yagaloff, K.A., Fisher, S.L., Burn, P. & Palmiter, R.D. (1999) Response of melanocortin-4 receptor-deficient mice to anorectic and orexigenic peptides. *Nat Genet* **21**, 119-122.

18 Rouille, Y., Duguay, S.J., Lund, K., Furuta, M., Gong, Q., Lipkind, G., Oliva, A.A., Jr., Chan, S.J. & Steiner, D.F. (1995) Proteolytic processing mechanisms in the biosynthesis of neuroendocrine peptides: the subtilisin-like proprotein convertases. *Front Neuroendocrinol* **16**, 322-361.

19 Gantz, I., Miwa, H., Konda, Y., Shimoto, Y., Tashiro, T., Watson, S.J., DelValle, J. & Yamada, T. (1993) Molecular cloning, expression, and gene localization of a fourth melanocortin receptor. *J Biol Chem* **268**, 15174-15179.

20 Tota, M.R., Smith, T.S., Mao, C., MacNeil, T., Mosley, R.T., Van der Ploeg, L.H. & Fong, T.M. (1999) Molecular interaction of Agouti protein and Agouti-related protein with human melanocortin receptors. *Biochemistry* **38**, 897-904.

21 Yang, Y.K., Thompson, D.A., Dickinson, C.J., Wilken, J., Barsh, G.S., Kent, S.B. & Gantz, I. (1999) Characterization of Agouti-related protein binding to melanocortin receptors. *Mol Endocrinol* **13**, 148-155.

22 Ollmann, M.M., Wilson, B.D., Yang, Y.K., Kerns, J.A., Chen, Y., Gantz, I. & Barsh, G.S. (1997) Antagonism of central melanocortin receptors in vitro and in vivo by agouti-related protein. *Science* **278**, 135-138.

23 Fan, W., Boston, B.A., Kesterson, R.A., Hruby, V.J. & Cone, R.D. (1997) Role of melanocortinergic neurons in feeding and the agouti obesity syndrome. *Nature* **385**, 165-168.

24 Nijenhuis, W.A., Oosterom, J. & Adan, R.A. (2001) AgRP(83-132) acts as an inverse agonist on the human-melanocortin-4 receptor. *Mol. Endocrinol.* **15**, 164-171.

25 Strobel, A., Issad, T., Camoin, L., Ozata, M. & Strosberg, A.D. (1998) A leptin missense mutation associated with hypogonadism and morbid obesity. *Nat Genet* **18**, 213-215.

26 Montague, C.T., Farooqi, I.S., Whitehead, J.P., Soos, M.A., Rau, H., Wareham, N.J., Sewter, C.P., Digby, J.E., Mohammed, S.N., Hurst, J.A., Cheetham, C.H., Earley, A.R., Barnett, A.H., Prins, J.B. & O'Rahilly, S. (1997) Congenital leptin deficiency is associated with severe early-onset obesity in humans. *Nature* **387**, 903-908.

27 Ozata, M., Ozdemir, I.C. & Licinio, J. (1999) Human leptin deficiency caused by a missense mutation: multiple endocrine defects, decreased sympathetic tone, and immune system dysfunction indicate new targets for leptin action, greater central than peripheral resistance to the effects of leptin, and spontaneous correction of leptin-mediated defects. *J Clin Endocrinol Metab* **84**, 3686-3695.

28 Kowalski, T.J., Liu, S.M., Leibel, R.L. & Chua, S.C., Jr. (2001) Transgenic complementation of leptin-receptor deficiency. I. Rescue of the obesity/diabetes phenotype of LEPR-null mice expressing a LEPR-B transgene. *Diabetes* **50**, 425-435.

29 Clement, K., Vaisse, C., Lahlou, N., Cabrol, S., Pelloux, V., Cassuto, D., Gourmelen, M., Dina, C., Chambaz, J., Lacorte, J.M., Basdevant, A., Bougneres, P., Lebouc, Y., Froguel, P. & Guy-Grand, B. (1998) A mutation in the human leptin receptor gene causes obesity and pituitary dysfunction. *Nature* **392**, 398-401.

30 Challis, B.G., Coll, A.P., Yeo, G.S., Pinnock, S.B., Dickson, S.L., Thresher, R.R., Dixon, J., Zahn, D., Rochford, J.J., White, A., Oliver, R.L., Millington, G., Aparicio, S.A., Colledge, W.H., Russ, A.P., Carlton, M.B. & O'Rahilly, S. (2004) Mice lacking pro-opiomelanocortin are sensitive to high-fat feeding but respond normally to the acute anorectic effects of peptide-YY(3-36). *Proc Natl Acad Sci U S A* **101**, 4695-4700.

31 Jackson, R.S., Creemers, J.W., Ohagi, S., Raffin-Sanson, M.L., Sanders, L., Montague, C.T., Hutton, J.C. & O'Rahilly, S. (1997) Obesity and impaired prohormone processing associated with mutations in the human prohormone convertase 1 gene. *Nat. Genet.* **16**, 303-306.

32 Krude, H., Biebermann, H., Luck, W., Horn, R., Brabant, G. & Gruters, A. (1998) Severe early-onset obesity, adrenal insufficiency and red hair pigmentation caused by POMC mutations in humans. *Nat. Genet.* **19**, 155-157.

33 Huszar, D., Lynch, C.A., Fairchild-Huntress, V., Dunmore, J.H., Fang, Q., Berkemeier, L.R., Gu, W., Kesterson, R.A., Boston, B.A., Cone, R.D., Smith, F.J., Campfield, L.A., Burn, P. & Lee, F. (1997) Targeted disruption of the melanocortin-4 receptor results in obesity in mice. *Cell* **88**, 131-141.

34 Vaisse, C., Clement, K., Guy-Grand, B. & Froguel, P. (1998) A frameshift mutation in human MC4R is associated with a dominant form of obesity. *Nat Genet* **20**, 113-114.

35 Vaisse, C., Clement, K., Durand, E., Hercberg, S., Guy-Grand, B. & Froguel, P. (2000) Melanocortin-4 receptor mutations are a frequent and heterogeneous cause of morbid obesity. *J Clin Invest* **106**, 253-262.

36 Nijenhuis, W.A., Garner, K.M., van Rozen, R.J. & Adan, R.A. (2003) Poor cell surface expression of human melanocortin-4 receptor mutations associated with obesity. *J Biol Chem* **278**, 22939-22945.

37 Lubrano-Berthelier, C., Cavazos, M., Dubern, B., Shapiro, A., Stunff, C.L., Zhang, S., Picart, F., Govaerts, C., Froguel, P., Bougneres, P., Clement, K. & Vaisse, C. (2003) Molecular genetics of human obesity-associated MC4R mutations. *Ann N Y Acad Sci* **994**, 49-57.

38 Farooqi, I.S., Keogh, J.M., Yeo, G.S., Lank, E.J., Cheetham, T. & O'Rahilly, S. (2003) Clinical spectrum of obesity and mutations in the melanocortin 4 receptor gene. *N Engl J Med* **348**, 1085-1095.

39 MacNeil, D.J., Howard, A.D., Guan, X., Fong, T.M., Nargund, R.P., Bednarek, M.A., Goulet, M.T., Weinberg, D.H., Strack, A.M., Marsh, D.J., Chen, H.Y., Shen, C.P., Chen, A.S., Rosenblum, C.I., MacNeil, T., Tota, M., MacIntyre, E.D. & Van der Ploeg, L.H. (2002) The role of melanocortins in body weight regulation: opportunities for the treatment of obesity. *Eur J Pharmacol* **440**, 141-157.

40 Elmquist, J.K., Maratos-Flier, E., Saper, C.B. & Flier, J.S. (1998) Unraveling the central nervous system pathways underlying responses to leptin. *Nat Neurosci* **1**, 445-450.

41 Civelli, O. (2005) GPCR deorphanizations: the novel, the known and the unexpected transmitters. *Trends Pharmacol Sci* **26**, 15-19.

42 Hopkins, A.L. & Groom, C.R. (2002) The druggable genome. *Nature reviews Drug discovery* **1**, 727-730.

43 Alberts, B.r.u.c.e., Johnson, A.l.e.x.a.n.d.e.r., Lewis, J.u.l.i.a.n., Walter, P.e.t.e.r., Raff, M.a.r.t.i.n. & Roberts, K.e.i.t.h. (2002) Molecular Biology of the Cell 4th Edition. 1616.

44 Schramm, M. & Selinger, Z. (1984) Message transmission: receptor controlled adenylate cyclase system. *Science* **225**, 1350-1356.

45 Guy-Grand, B., Apfelbaum, M., Crepaldi, G., Gries, A., Lefebvre, P. & Turner, P. (1989) International trial of long-term dexfenfluramine in obesity. *Lancet* **2**, 1142-1145.

46 Renshaw, D. & Batterham, R.L. (2005) Peptide YY: a potential therapy for obesity. *Current drug targets* **6**, 171-179.

47 Boggiano, M.M., Chandler, P.C., Oswald, K.D., Rodgers, R.J., Blundell, J.E., Ishii, Y., Beattie, A.H., Holch, P., Allison, D.B., Schindler, M., Arndt, K., Rudolf, K., Mark, M., Schoelch, C., Joost, H.G., Klaus, S., Thöne-Reineke, C., Benoit, S.C., Seeley, R.J., Beck-Sickinger, A.G., Koglin, N., Raun, K., Madsen, K., Wulff, B.S., Stidsen, C.E., Birringer, M., Kreuzer, O.J., Deng, X.Y., Whitcomb, D.C., Halem, H., Taylor, J., Dong, J., Datta, R., Culler, M., Ortmann, S., Castañeda, T.R. & Tschöp, M. (2005) PYY3-36 as an anti-obesity drug target. *Obesity reviews : an official journal of the International Association for the Study of Obesity* **6**, 307-322.

48 Zorrilla, E.P., Iwasaki, S., Moss, J.A., Chang, J., Otsuji, J., Inoue, K., Meijler, M.M. & Janda, K.D. (2006) Vaccination against weight gain. *Proc Natl Acad Sci USA* **103**, 13226-13231.

49 Sun, Y., Wang, P., Zheng, H. & Smith, R.G. (2004) Ghrelin stimulation of growth hormone release and appetite is mediated through the growth hormone secretagogue receptor. *Proc Natl Acad Sci USA* **101**, 4679-4684.

50 Abbott, C.R., Small, C.J., Kennedy, A.R., Neary, N.M., Sajedi, A., Ghatei, M.A. & Bloom, S.R. (2005) Blockade of the neuropeptide Y Y2 receptor with the specific antagonist BIIE0246 attenuates the effect of endogenous and exogenous peptide YY(3-36) on food intake. *Brain Res* **1043**, 139-144.

51 Batterham, R.L., Cowley, M.A., Small, C.J., Herzog, H., Cohen, M.A., Dakin, C.L., Wren, A.M., Brynes, A.E., Low, M.J., Ghatei, M.A., Cone, R.D. & Bloom, S.R. (2002) Gut hormone PYY(3-36) physiologically inhibits food intake. *Nature* **418**, 650-654.

52 Ellacott, K.L. & Cone, R.D. (2004) The central melanocortin system and the integration of short- and long-term regulators of energy homeostasis. *Recent Prog Horm Res* **59**, 395-408.

53 Heisler, L.K., Jobst, E.E., Sutton, G.M., Zhou, L., Borok, E., Thornton-Jones, Z., Liu, H.Y., Zigman, J.M., Balthasar, N., Kishi, T., Lee, C., Aschkenasi, C.J., Zhang, C., Yu, J., Boss, O., Mountjoy, K.G., Clifton, P.G., Lowell, B., Friedman, J.M., Horvath, T., Butler, A.A., Elmquist, J. & Cowley, M.A. (2006)

Serotonin reciprocally regulates melanocortin neurons to modulate food intake. *Neuron* **51**, 239-249.

54 Xu, Y., Jones, J.E., Kohno, D., Williams, K.W., Lee, C., Choi, M.J., Anderson, J.G., Heisler, L.K., Zigman, J.M., Lowell, B. & Elmquist, J. (2008) 5-HT2CRs expressed by pro-opiomelanocortin neurons regulate energy homeostasis. *Neuron* **60**, 582-589.

55 Nonogaki, K., Abdallah, L., Goulding, E.H., Bonasera, S.J. & Tecott, L.H. (2003) Hyperactivity and reduced energy cost of physical activity in serotonin 5-HT(2C) receptor mutant mice. *Diabetes* **52**, 315-320.

56 Vickers, S.P., Clifton, P.G., Dourish, C.T. & Tecott, L.H. (1999) Reduced satiating effect of d-fenfluramine in serotonin 5-HT(2C) receptor mutant mice. *Psychopharmacology (Berl)* **143**, 309-314.

57 Gierschik, P. (1992) ADP-ribosylation of signal-transducing guanine nucleotide-binding proteins by pertussis toxin. *Curr Top Microbiol Immunol* **175**, 69-96.

58 Regard, J.B., Kataoka, H., Cano, D.A., Camerer, E., Yin, L., Zheng, Y.W., Scanlan, T.S., Hebrok, M. & Coughlin, S.R. (2007) Probing cell type-specific functions of Gi in vivo identifies GPCR regulators of insulin secretion. *J Clin Invest* **117**, 4034-4043.

59 Soriano, P. (1999) Generalized lacZ expression with the ROSA26 Cre reporter strain. *Nat Genet* **21**, 70-71.

60 Xu, A.W., Kaelin, C.B., Takeda, K., Akira, S., Schwartz, M.W. & Barsh, G.S. (2005) PI3K integrates the action of insulin and leptin on hypothalamic neurons. *J Clin Invest* **115**, 951-958.

61 Xu, A.W., Kaelin, C.B., Morton, G.J., Ogimoto, K., Stanhope, K., Graham, J., Baskin, D.G., Havel, P., Schwartz, M.W. & Barsh, G.S. (2005) Effects of Hypothalamic Neurodegeneration on Energy Balance. *PLOS Biology* **3**, 9.

62 Ryohichi Banno, D.Z., Maybless Atienza, and Kendra K. Bence (2008) Mice with POMC neuron-specific deletion of protein tyrosine phophatase 1B (PTP1B) show mild protection from diet-induced obesity and significantly improved glucose homeostasis. *Keystone Symposia Abstract Book: Neuronal*

*Mechanism Controlling Food Intake, Glucose Metabolism and Body weight.* **Abstract number: 108**, 1.

63 Shi, H., Strader, A.D., Sorrell, J.E., Chambers, J.B., Woods, S.C. & Seeley, R.J. (2008) Sexually different actions of leptin in proopiomelanocortin neurons to regulate glucose homeostasis. *Am J Physiol Endocrinol Metab* **294**, E630-639.

64 Balthasar, N., Coppari, R., McMinn, J., Liu, S.M., Lee, C., Tang, V., Kenny, C.D., McGovern, R.A., Chua, S.C., Elmquist, J. & Lowell, B. (2004) Leptin receptor signaling in POMC neurons is required for normal body weight homeostasis. *Neuron* **42**, 983-991.

65 Könner, A.C., Janoschek, R., Plum, L., Jordan, S.D., Rother, E., Ma, X., Xu, C., Enriori, P., Hampel, B., Barsh, G.S., Kahn, C.R., Cowley, M.A., Ashcroft, F.M. & Brüning, J.C. (2007) Insulin action in AgRP-expressing neurons is required for suppression of hepatic glucose production. *Cell Metabolism* **5**, 438-449.

66 Belgardt, B.F., Husch, A., Rother, E., Ernst, M.B., Wunderlich, F.T., Hampel, B., Klöckener, T., Alessi, D., Kloppenburg, P. & Brüning, J.C. (2008) PDK1 deficiency in POMC-expressing cells reveals FOXO1-dependent and -independent pathways in control of energy homeostasis and stress response. *Cell Metabolism* **7**, 291-301.

67 Claret, M., Smith, M.A., Batterham, R.L., Selman, C., Choudhury, A.I., Fryer, L.G.D., Clements, M., Al-Qassab, H., Heffron, H., Xu, A.W., Speakman, J.R., Barsh, G.S., Viollet, B., Vaulont, S., Ashford, M.L.J., Carling, D. & Withers1, D.J. (2007) AMPK is essential for energy homeostasis regulation and glucose sensing by POMC and AgRP neurons. *The Journal of Clinical Investigation* **117**, 12.

68 Choudhury, A.I., Heffron, H., Smith, M.A., Al-Qassab, H., Xu, A.W., Selman, C., Simmgen, M., Clements, M., Claret, M., Maccoll, G., Bedford, D.C., Hisadome, K., Diakonov, I., Moosajee, V., Bell, J.D., Speakman, J.R., Batterham, R.L., Barsh, G.S., Ashford, M.L. & Withers, D.J. (2005) The role of insulin

receptor substrate 2 in hypothalamic and beta cell function. *J Clin Invest* **115**, 940-950.

69 Kievit, P., Howard, J.K., Badman, M.K., Balthasar, N., Coppari, R., Mori, H., Lee, C., Elmquist, J., Yoshimura, A. & Flier, J.S. (2006) Enhanced leptin sensitivity and improved glucose homeostasis in mice lacking suppressor of cytokine signaling-3 in POMC-expressing cells. *Cell Metabolism* **4**, 123-132.

70 Plum, L., Ma, X., Hampel, B., Balthasar, N., Coppari, R., Münzberg, H., Shanabrough, M., Burdakov, D., Rother, E., Janoschek, R., Alber, J., Belgardt, B.F., Koch, L., Seibler, J., Schwenk, F., Fekete, C., Suzuki, A., Mak, T.W., Krone, W., Horvath, T.L., Ashcroft, F.M. & Brüning, J.C. (2006) Enhanced PIP3 signaling in POMC neurons causes KATP channel activation and leads to diet-sensitive obesity. *J Clin Invest* **116**, 1886-1901.

71 Janoschek, R., Plum, L., Koch, L., Münzberg, H., Diano, S., Shanabrough, M., Müller, W., Horvath, T.L. & Brüning, J.C. (2006) gp130 signaling in proopiomelanocortin neurons mediates the acute anorectic response to centrally applied ciliary neurotrophic factor. *Proc Natl Acad Sci USA* **103**, 10707-10712.

72 Xu, A.W., Ste-Marie, L., Kaelin, C.B. & Barsh, G.S. (2007) Inactivation of signal transducer and activator of transcription 3 in proopiomelanocortin (Pomc) neurons causes decreased pomc expression, mild obesity, and defects in compensatory refeeding. *Endocrinology* **148**, 72-80.

73 Yaswen, L., Diehl, N., Brennan, M.B. & Hochgeschwender, U. (1999) Obesity in the mouse model of pro-opiomelanocortin deficiency responds to peripheral melanocortin. *Nat Med* **5**, 1066-1070.

74 Gropp, E., Shanabrough, M., Borok, E., Xu, A.W., Janoschek, R., Buch, T., Plum, L., Balthasar, N., Hampel, B., Waisman, A., Barsh, G.S., Horvath, T.L. & Brüning, J.C. (2005) Agouti-related peptide-expressing neurons are mandatory for feeding. *Nat Neurosci* **8**, 1289-1291.

75 Döring, H., Schwarzer, K., Nuesslein-Hildesheim, B. & Schmidt, I. (1998) Leptin selectively increases energy expenditure of food-restricted lean mice. *Int J Obes Relat Metab Disord* **22**, 83-88.

76 Balthasar, N., Dalgaard, L.T., Lee, C., Yu, J., Funahashi, H., Williams, T., Ferreira, M., Tang, V., McGovern, R.A., Kenny, C.D., Christiansen, L.M., Edelstein, E., Choi, B., Boss, O., Aschkenasi, C., Zhang, C., Mountjoy, K., Kishi, T., Elmquist, J. & Lowell, B. (2005) Divergence of melanocortin pathways in the control of food intake and energy expenditure. *Cell* **123**, 493-505.

77 Chen, A.S., Metzger, J.M., Trumbauer, M.E., Guan, X.M., Yu, H., Frazier, E.G., Marsh, D.J., Forrest, M.J., Gopal-Truter, S., Fisher, J., Camacho, R.E., Strack, A.M., Mellin, T.N., MacIntyre, D.E., Chen, H.Y. & Van der Ploeg, L.H. (2000) Role of the melanocortin-4 receptor in metabolic rate and food intake in mice. *Transgenic Res* **9**, 145-154.

78 Ste Marie, L., Miura, G.I., Marsh, D.J., Yagaloff, K. & Palmiter, R.D. (2000) A metabolic defect promotes obesity in mice lacking melanocortin-4 receptors. *Proc Natl Acad Sci USA* **97**, 12339-12344.

79 Bjørbaek, C. & Kahn, B.B. (2004) Leptin signaling in the central nervous system and the periphery. *Recent Prog Horm Res* **59**, 305-331.

80 Kristiansen, K. (2004) Molecular mechanisms of ligand binding, signaling, and regulation within the superfamily of G-protein-coupled receptors: molecular modeling and mutagenesis approaches to receptor structure and function. *Pharmacol Ther* **103**, 21-80.

81 Kobilka, B.K. (2007) G protein coupled receptor structure and activation. *Biochim Biophys Acta* **1768**, 794-807.

82 Lagerström, M.C. & Schiöth, H.B. (2008) Structural diversity of G protein-coupled receptors and significance for drug discovery. *Nature reviews Drug discovery* **7**, 339-357.

83 Coughlin, S.R. (1999) How the protease thrombin talks to cells. *Proc Natl Acad Sci USA* **96**, 11023-11027.

84 Nijenhuis, W. (2003) Poor Cell Surface Expression of Human Melanocortin-4 Receptor Mutations Associated with Obesity. *Journal of Biological Chemistry* **278**, 22939-22945.

85 Tolle, V. & Low, M.J. (2008) In vivo evidence for inverse agonism of Agouti-related peptide in the central nervous system of proopiomelanocortin-deficient mice. *Diabetes* **57**, 86-94.

86 Srinivasan, S. (2004) Constitutive activity of the melanocortin-4 receptor is maintained by its N-terminal domain and plays a role in energy homeostasis in humans. *Journal of Clinical Investigation* **114**, 1158-1164.

87 Ollmann, M. (1997) Antagonism of Central Melanocortin Receptors in Vitro and in Vivo by Agouti-Related Protein. *Science* **278**, 135-138.

88 Fan, W., Boston, B.A., Kesterson, R.A., Hruby, V.J. & Cone, R.D. (1997) Role of melanocortinergic neurons in feeding and the agouti obesity syndrome. *Nature* **385**, 165-168.

89 Nijenhuis, W.A., Oosterom, J. & Adan, R.A. (2001) AgRP(83-132) acts as an inverse agonist on the human-melanocortin-4 receptor. *Mol Endocrinol* **15**, 164-171.

90 Haskell-Luevano, C. & Monck, E.K. (2001) Agouti-related protein functions as an inverse agonist at a constitutively active brain melanocortin-4 receptor. *Regul Pept* **99**, 1-7.

91 Scarborough, R.M., Naughton, M.A., Teng, W., Hung, D.T., Rose, J., Vu, T.K., Wheaton, V.I., Turck, C.W. & Coughlin, S.R. (1992) Tethered ligand agonist peptides. Structural requirements for thrombin receptor activation reveal mechanism of proteolytic unmasking of agonist function. *J Biol Chem* **267**, 13146-13149.

92 Lubrano-Berthelier, C., Dubern, B., Lacorte, J.M., Picard, F., Shapiro, A., Zhang, S., Bertrais, S., Hercberg, S., Basdevant, A., Clement, K. & Vaisse, C. (2006) Melanocortin 4 receptor mutations in a large cohort of severely obese adults: prevalence, functional classification, genotype-phenotype relationship, and lack of association with binge eating. *J Clin Endocrinol Metab* **91**, 1811-1818.

93 Peter, J.C., Nicholson, J.R., Heydet, D., Lecourt, A.C., Hoebeke, J. & Hofbauer, K.G. (2007) Antibodies against the melanocortin-4 receptor act as

inverse agonists in vitro and in vivo. *Am J Physiol Regul Integr Comp Physiol* **292**, R2151-2158.

94 Tao, Y.X. & Segaloff, D.L. (2005) Functional analyses of melanocortin-4 receptor mutations identified from patients with binge eating disorder and nonobese or obese subjects. *J Clin Endocrinol Metab* **90**, 5632-5638.

95 Xiang, Z., Litherland, S.A., Sorensen, N.B., Proneth, B., Wood, M.S., Shaw, A.M., Millard, W.J. & Haskell-Luevano, C. (2006) Pharmacological characterization of 40 human melanocortin-4 receptor polymorphisms with the endogenous proopiomelanocortin-derived agonists and the agouti-related protein (AGRP) antagonist. *Biochemistry* **45**, 7277-7288.

96 Lubrano-Berthelier, C. (2003) Intracellular retention is a common characteristic of childhood obesity-associated MC4R mutations. *Human Molecular Genetics* **12**, 145-153.

97 Hinney, A., Hohmann, S., Geller, F., Vogel, C., Hess, C., Wermter, A.K., Brokamp, B., Goldschmidt, H., Siegfried, W., Remschmidt, H., Schäfer, H., Gudermann, T. & Hebebrand, J. (2003) Melanocortin-4 receptor gene: case-control study and transmission disequilibrium test confirm that functionally relevant mutations are compatible with a major gene effect for extreme obesity. *J Clin Endocrinol Metab* **88**, 4258-4267.

98 Valli-Jaakola, K., Lipsanen-Nyman, M., Oksanen, L., Hollenberg, A.N., Kontula, K., Bjørbaek, C. & Schalin-Jäntti, C. (2004) Identification and characterization of melanocortin-4 receptor gene mutations in morbidly obese finnish children and adults. *J Clin Endocrinol Metab* **89**, 940-945.

99 Lubrano-Berthelier, C., Le Stunff, C., Bougnères, P. & Vaisse, C. (2004) A homozygous null mutation delineates the role of the melanocortin-4 receptor in humans. *J Clin Endocrinol Metab* **89**, 2028-2032.

100 Ahituv, N., Kavaslar, N., Schackwitz, W., Ustaszewska, A., Martin, J., Hebert, S., Doelle, H., Ersoy, B., Kryukov, G., Schmidt, S., Yosef, N., Ruppin, E., Sharan, R., Vaisse, C., Sunyaev, S., Dent, R., Cohen, J., McPherson, R. & Pennacchio, L.A. (2007) Medical sequencing at the extremes of human body mass. *Am J Hum Genet* **80**, 779-791.

101 Calton, M.A., Ersoy, B.A., Zhang, S., Kane, J.P., Malloy, M.J., Pullinger, C.R., Bromberg, Y., Pennacchio, L.A., Dent, R., McPherson, R., Ahituv, N. & Vaisse, C. (2009) Association of functionally significant Melanocortin-4 but not Melanocortin-3 receptor mutations with severe adult obesity in a large North American case-control study. *Human Molecular Genetics* **18**, 1140-1147.

102 Rasmussen, S.G., Choi, H.J., Rosenbaum, D.M., Kobilka, T.S., Thian, F.S., Edwards, P.C., Burghammer, M., Ratnala, V.R., Sanishvili, R., Fischetti, R.F., Schertler, G.F., Weis, W.I. & Kobilka, B.K. (2007) Crystal structure of the human beta2 adrenergic G-protein-coupled receptor. *Nature* **450**, 383-387.

103 Cherezov, V., Rosenbaum, D.M., Hanson, M.A., Rasmussen, S.G., Thian, F.S., Kobilka, T.S., Choi, H.J., Kuhn, P., Weis, W.I., Kobilka, B.K. & Stevens, R.C. (2007) High-resolution crystal structure of an engineered human beta2-adrenergic G protein-coupled receptor. *Science* **318**, 1258-1265.

104 Yang, Y.K., Fong, T.M., Dickinson, C.J., Mao, C., Li, J.Y., Tota, M.R., Mosley, R., Van der Ploeg, L.H. & Gantz, I. (2000) Molecular determinants of ligand binding to the human melanocortin-4 receptor. *Biochemistry* **39**, 14900-14911.

105 Kobilka, B.K. & Deupi, X. (2007) Conformational complexity of G-protein-coupled receptors. *Trends Pharmacol Sci* **28**, 397-406.

106 Yang, Y., Cai, M., Chen, M., Qu, H., McPherson, D., Hruby, V. & Harmon, C.M. (2009) Key amino acid residues in the Melanocortin-4 Receptor for nonpeptide THIQ Specific Binding and Signaling. *Regul Pept*.

107 Holst, B., Elling, C.E. & Schwartz, T.W. (2002) Metal ion-mediated agonism and agonist enhancement in melanocortin MC1 and MC4 receptors. *J Biol Chem* **277**, 47662-47670.

108 Schwartz, T.W., Frimurer, T.M., Holst, B., Rosenkilde, M.M. & Elling, C.E. (2006) Molecular mechanism of 7TM receptor activation--a global toggle switch model. *Annu Rev Pharmacol Toxicol* **46**, 481-519.

109 Vassart, G., Pardo, L. & Costagliola, S. (2004) A molecular dissection of the glycoprotein hormone receptors. *Trends Biochem Sci* **29**, 119-126.

110 Toyooka, M., Tujii, T. & Takeda, S. (2009) The N-terminal domain of GPR61, an orphan G-protein-coupled receptor, is essential for its constitutive activity. *J Neurosci Res* **87**, 1329-1333.

111 Ballesteros, J.A. & Weinstein, H. (1995) [19] Integrated methods for the construction of three-dimensional models and computational probing of structure-function relations in G protein-coupled receptors. *Methods in Neurosciences* **25**, 366-428.

112 Swarbrick, M.M. & Vaisse, C. (2003) Emerging trends in the search for genetic variants predisposing to human obesity. *Current opinion in clinical nutrition and metabolic care* **6**, 369-375.

113 Loos, R.J., Lindgren, C.M., Li, S., Wheeler, E., Zhao, J.H., Prokopenko, I., Inouye, M., Freathy, R.M., Attwood, A.P., Beckmann, J.S., Berndt, S.I., Prostate, L., Colorectal, and Ovarian (PLCO) Cancer Screening Trial, Jacobs, K.B., Chanock, S.J., Hayes, R.B., Bergmann, S., Bennett, A.J., Bingham, S.A., Bochud, M., Brown, M., Cauchi, S., Connell, J.M., Cooper, C., Smith, G.D., Day, I., Dina, C., De, S., Dermitzakis, E.T., Doney, A.S., Elliott, K.S., Elliott, P., Evans, D.M., Sadaf Farooqi, I., Froguel, P., Ghori, J., Groves, C.J., Gwilliam, R., Hadley, D., Hall, A.S., Hattersley, A.T., Hebebrand, J., Heid, I.M., KORA, Lamina, C., Gieger, C., Illig, T., Meitinger, T., Wichmann, H.E., Herrera, B., Hinney, A., Hunt, S.E., Jarvelin, M.R., Johnson, T., Jolley, J.D., Karpe, F., Keniry, A., Khaw, K.T., Luben, R.N., Mangino, M., Marchini, J., McArdle, W.L., McGinnis, R., Meyre, D., Munroe, P.B., Morris, A.D., Ness, A.R., Neville, M.J., Nica, A.C., Ong, K.K., O'Rahilly, S., Owen, K.R., Palmer, C.N., Papadakis, K., Potter, S., Pouta, A., Qi, L., Study, N.H., Randall, J.C., Rayner, N.W., Ring, S.M., Sandhu, M.S., Scherag, A., Sims, M.A., Song, K., Soranzo, N., Speliotes, E.K., Initiative, D.G., Syddall, H.E., Teichmann, S.A., Timpson, N.J., Tobias, J.H., Uda, M., Study, S., Vogel, C.I., Wallace, C., Waterworth, D.M., Weedon, M.N., Consortium, W.T.C.C., Willer, C.J., FUSION, Wraight, Yuan, X., Zeggini, E., Hirschhorn, J.N., Strachan, D.P., Ouwehand, W.H., Caulfield, M.J., Samani, N.J., Frayling, T.M., Vollenweider, P., Waeber, G., Mooser, V., Deloukas, P., McCarthy, M.I., Wareham, N.J., Barroso, I., Jacobs, K.B., Chanock, S.J., Hayes, R.B., Lamina,

C., Gieger, C., Illig, T., Meitinger, T., Wichmann, H.E., Kraft, P., Hankinson, S.E., Hunter, D.J., Hu, F.B., Lyon, H.N., Voight, B.F., Ridderstrale, M., Groop, L., Scheet, P., Sanna, S., Abecasis, G.R., Albai, G., Nagaraja, R., Schlessinger, D., Jackson, A.U., Tuomilehto, J., Collins, F.S., Boehnke, M. & Mohlke, K.L. (2008) Common variants near MC4R are associated with fat mass, weight and risk of obesity. *Nat Genet* **40**, 768-775.

114 Frayling, T.M., Timpson, N.J., Weedon, M.N., Zeggini, E., Freathy, R.M., Lindgren, C.M., Perry, J.R., Elliott, K.S., Lango, H., Rayner, N.W., Shields, B., Harries, L.W., Barrett, J.C., Ellard, S., Groves, C.J., Knight, B., Patch, A.M., Ness, A.R., Ebrahim, S., Lawlor, D.A., Ring, S.M., Ben-Shlomo, Y., Jarvelin, M.R., Sovio, U., Bennett, A.J., Melzer, D., Ferrucci, L., Loos, R.J., Barroso, I., Wareham, N.J., Karpe, F., Owen, K.R., Cardon, L.R., Walker, M., Hitman, G.A., Palmer, C.N., Doney, A.S., Morris, A.D., Smith, G.D., Hattersley, A.T. & McCarthy, M.I. (2007) A common variant in the FTO gene is associated with body mass index and predisposes to childhood and adult obesity. *Science* **316**, 889-894.

115 Ranadive, S.A. & Vaisse, C. (2008) Lessons from extreme human obesity: monogenic disorders. *Endocrinol Metab Clin North Am* **37**, 733-751, x.

116 Dubern, B., Clément, K., Pelloux, V., Froguel, P., Girardet, J.P., Guy-Grand, B. & Tounian, P. (2001) Mutational analysis of melanocortin-4 receptor, agouti-related protein, and alpha-melanocyte-stimulating hormone genes in severely obese children. *J Pediatr* **139**, 204-209.

117 Mergen, M., Mergen, H., Ozata, M., Oner, R. & Oner, C. (2001) A novel melanocortin 4 receptor (MC4R) gene mutation associated with morbid obesity. *J Clin Endocrinol Metab* **86**, 3448.

118 Sina, M., Hinney, A., Ziegler, A., Neupert, T., Mayer, H., Siegfried, W., Blum, W.F., Remschmidt, H. & Hebebrand, J. (1999) Phenotypes in three pedigrees with autosomal dominant obesity caused by haploinsufficiency mutations in the melanocortin-4 receptor gene. *Am J Hum Genet* **65**, 1501-1507.

119 Lubrano-Berthelier, C., Durand, E., Dubern, B., Shapiro, A., Dazin, P., Weill, J., Ferron, C., Froguel, P. & Vaisse, C. (2003) Intracellular retention is a

common characteristic of childhood obesity-associated MC4R mutations. *Human Molecular Genetics* **12**, 145-153.

120 Jacobson, P., Ukkola, O., Rankinen, T., Snyder, E.E., Leon, A.S., Rao, D.C., Skinner, J.S., Wilmore, J.H., Lönn, L., Cowan, G.S., Sjöström, L. & Bouchard, C. (2002) Melanocortin 4 receptor sequence variations are seldom a cause of human obesity: the Swedish Obese Subjects, the HERITAGE Family Study, and a Memphis cohort. *J Clin Endocrinol Metab* **87**, 4442-4446.

121 Miraglia Del Giudice, E., Cirillo, G., Nigro, V., Santoro, N., D'Urso, L., Raimondo, P., Cozzolino, D., Scafato, D. & Perrone, L. (2002) Low frequency of melanocortin-4 receptor (MC4R) mutations in a Mediterranean population with early-onset obesity. *Int J Obes Relat Metab Disord* **26**, 647-651.

122 Mountjoy, K.G., Mortrud, M.T., Low, M.J., Simerly, R.B. & Cone, R.D. (1994) Localization of the melanocortin-4 receptor (MC4-R) in neuroendocrine and autonomic control circuits in the brain. *Mol Endocrinol* **8**, 1298-1308.

123 Lu, D., Willard, D., Patel, I.R., Kadwell, S., Overton, L., Kost, T., Luther, M., Chen, W., Woychik, R.P. & Wilkison, W.O. (1994) Agouti protein is an antagonist of the melanocyte-stimulating-hormone receptor. *Nature* **371**, 799-802.

124 Schwartz, M.W., Woods, S.C., Porte, D., Seeley, R.J. & Baskin, D.G. (2000) Central nervous system control of food intake. *Nature* **404**, 661-671.

125 Hirschhorn, J.N. & Altshuler, D. (2002) Once and again-issues surrounding replication in genetic association studies. *J Clin Endocrinol Metab* **87**, 4438-4441.

126 Ma, L., Tataranni, P.A., Bogardus, C. & Baier, L.J. (2004) Melanocortin 4 receptor gene variation is associated with severe obesity in Pima Indians. *Diabetes* **53**, 2696-2699.

127 Roselli-Rehfuss, L., Mountjoy, K.G., Robbins, L.S., Mortrud, M.T., Low, M.J., Tatro, J.B., Entwistle, M.L., Simerly, R.B. & Cone, R.D. (1993) Identification of a receptor for gamma melanotropin and other proopiomelanocortin peptides in the hypothalamus and limbic system. *Proc Natl Acad Sci USA* **90**, 8856-8860.

128 Chen, A.S., Marsh, D.J., Trumbauer, M.E., Frazier, E.G., Guan, X.M., Yu, H., Rosenblum, C.I., Vongs, A., Feng, Y., Cao, L., Metzger, J.M., Strack, A.M., Camacho, R.E., Mellin, T.N., Nunes, C.N., Min, W., Fisher, J., Gopal-Truter, S., MacIntyre, D.E., Chen, H.Y. & Van der Ploeg, L.H. (2000) Inactivation of the mouse melanocortin-3 receptor results in increased fat mass and reduced lean body mass. *Nat Genet* **26**, 97-102.

129 Butler, A.A., Kesterson, R.A., Khong, K., Cullen, M.J., Pelleymounter, M.A., Dekoning, J., Baetscher, M. & Cone, R.D. (2000) A unique metabolic syndrome causes obesity in the melanocortin-3 receptor-deficient mouse. *Endocrinology* **141**, 3518-3521.

130 Tao, Y.X. & Segaloff, D.L. (2004) Functional characterization of melanocortin-3 receptor variants identify a loss-of-function mutation involving an amino acid critical for G protein-coupled receptor activation. *J Clin Endocrinol Metab* **89**, 3936-3942.

131 Lee, Y.S., Poh, L.K. & Loke, K.Y. (2002) A novel melanocortin 3 receptor gene (MC3R) mutation associated with severe obesity. *J Clin Endocrinol Metab* **87**, 1423-1426.

132 Lubrano-Berthelier, C., Cavazos, M., Le Stunff, C., Haas, K., Shapiro, A., Zhang, S., Bougneres, P. & Vaisse, C. (2003) The human MC4R promoter: characterization and role in obesity. *Diabetes* **52**, 2996-3000.

133 Branson, R., Potoczna, N., Kral, J.G., Lentes, K.U., Hoehe, M.R. & Horber, F.F. (2003) Binge eating as a major phenotype of melanocortin 4 receptor gene mutations. *N Engl J Med* **348**, 1096-1103.

134 Larsen, L.H., Echwald, S.M., Sørensen, T.I., Andersen, T., Wulff, B.S. & Pedersen, O. (2005) Prevalence of mutations and functional analyses of melanocortin 4 receptor variants identified among 750 men with juvenile-onset obesity. *J Clin Endocrinol Metab* **90**, 219-224.

135 Heid, I.M., Vollmert, C., Kronenberg, F., Huth, C., Ankerst, D.P., Luchner, A., Hinney, A., Brönner, G., Wichmann, H.E., Illig, T., Döring, A. & Hebebrand, J. (2008) Association of the MC4R V103I polymorphism with the metabolic syndrome: the KORA Study. *Obesity (Silver Spring)* **16**, 369-376.

136 Li, W.D., Joo, E.J., Furlong, E.B., Galvin, M., Abel, K., Bell, C.J. & Price, R.A. (2000) Melanocortin 3 receptor (MC3R) gene variants in extremely obese women. *Int J Obes Relat Metab Disord* **24**, 206-210.

137 Ramensky, V., Bork, P. & Sunyaev, S. (2002) Human non-synonymous SNPs: server and survey. *Nucleic Acids Res* **30**, 3894-3900.

138 Bromberg, Y., Yachdav, G. & Rost, B. (2008) SNAP predicts effect of mutations on protein function. *Bioinformatics* **24**, 2397-2398.

139 Bromberg, Y. & Rost, B. (2008) Comprehensive in silico mutagenesis highlights functionally important residues in proteins. *Bioinformatics* **24**, i207-212.

140 Bromberg, Y. & Rost, B. (2007) SNAP: predict effect of non-synonymous polymorphisms on function. *Nucleic Acids Res* **35**, 3823-3835.

141 Farooqi, I.S., Wangensteen, T., Collins, S., Kimber, W., Matarese, G., Keogh, J.M., Lank, E., Bottomley, B., Lopez-Fernandez, J., Ferraz-Amaro, I., Dattani, M.T., Ercan, O., Myhre, A.G., Retterstol, L., Stanhope, R., Edge, J.A., McKenzie, S., Lessan, N., Ghodsi, M., De Rosa, V., Perna, F., Fontana, S., Barroso, I., Undlien, D.E. & O'Rahilly, S. (2007) Clinical and molecular genetic spectrum of congenital deficiency of the leptin receptor. *N Engl J Med* **356**, 237-247.

142 Hinney, A., Bettecken, T., Tarnow, P., Brumm, H., Reichwald, K., Lichtner, P., Scherag, A., Nguyen, T.T., Schlumberger, P., Rief, W., Vollmert, C., Illig, T., Wichmann, H.E., Schäfer, H., Platzer, M., Biebermann, H., Meitinger, T. & Hebebrand, J. (2006) Prevalence, spectrum, and functional characterization of melanocortin-4 receptor gene mutations in a representative population-based sample and obese adults from Germany. *J Clin Endocrinol Metab* **91**, 1761-1769.

143 Butler, A.A. & Cone, R.D. (2002) The melanocortin receptors: lessons from knockout models. *Neuropeptides* **36**, 77-84.

144 Mencarelli, M., Walker, G.E., Maestrini, S., Alberti, L., Verti, B., Brunani, A., Petroni, M.L., Tagliaferri, M., Liuzzi, A. & Di Blasio, A.M. (2008) Sporadic mutations in melanocortin receptor 3 in morbid obese individuals. *Eur J Hum Genet* **16**, 581-586.

145 Schalin-Jäntti, C., Valli-Jaakola, K., Oksanen, L., Martelin, E., Laitinen, K., Krusius, T., Mustajoki, P., Heikinheimo, M. & Kontula, K. (2003) Melanocortin-3-receptor gene variants in morbid obesity. *Int J Obes Relat Metab Disord* **27**, 70-74.

146 Wong, J., Love, D.R., Kyle, C., Daniels, A., White, M., Stewart, A.W., Schnell, A.H., Elston, R.C., Holdaway, I.M. & Mountjoy, K.G. (2002) Melanocortin-3 receptor gene variants in a Maori kindred with obesity and early onset type 2 diabetes. *Diabetes Res Clin Pract* **58**, 61-71.

147 Feng, N., Young, S.F., Aguilera, G., Puricelli, E., Adler-Wailes, D.C., Sebring, N.G. & Yanovski, J.A. (2005) Co-occurrence of two partially inactivating polymorphisms of MC3R is associated with pediatric-onset obesity. *Diabetes* **54**, 2663-2667.

148 Hani, E.H., Dupont, S., Durand, E., Dina, C., Gallina, S., Gantz, I. & Froguel, P. (2001) Naturally occurring mutations in the melanocortin receptor 3 gene are not associated with type 2 diabetes mellitus in French Caucasians. *J Clin Endocrinol Metab* **86**, 2895-2898.

149 Dina, C., Meyre, D., Gallina, S., Durand, E., Körner, A., Jacobson, P., Carlsson, L.M., Kiess, W., Vatin, V., Lecoeur, C., Delplanque, J., Vaillant, E., Pattou, F., Ruiz, J., Weill, J., Levy-Marchal, C., Horber, F., Potoczna, N., Hercberg, S., Le Stunff, C., Bougnères, P., Kovacs, P., Marre, M., Balkau, B., Cauchi, S., Chèvre, J.C. & Froguel, P. (2007) Variation in FTO contributes to childhood obesity and severe adult obesity. *Nat Genet* **39**, 724-726.

150 Swarbrick, M.M., Waldenmaier, B., Pennacchio, L.A., Lind, D.L., Cavazos, M.M., Geller, F., Merriman, R., Ustaszewska, A., Malloy, M., Scherag, A., Hsueh, W.C., Rief, W., Mauvais-Jarvis, F., Pullinger, C.R., Kane, J.P., Dent, R., McPherson, R., Kwok, P.Y., Hinney, A., Hebebrand, J. & Vaisse, C. (2005) Lack of support for the association between GAD2 polymorphisms and severe human obesity. *PLoS Biol* **3**, e315.

151 Cone, R.D. (2006) Studies on the physiological functions of the melanocortin system. *Endocr Rev* **27**, 736-749.

152 Seeley, R.J., Drazen, D.L. & Clegg, D.J. (2004) The critical role of the melanocortin system in the control of energy balance. *Annu Rev Nutr* **24**, 133-149.

153 Slominski, A., Plonka, P.M., Pisarchik, A., Smart, J.L., Tolle, V., Wortsman, J. & Low, M.J. (2005) Preservation of eumelanin hair pigmentation in proopiomelanocortin-deficient mice on a nonagouti (a/a) genetic background. *Endocrinology* **146**, 1245-1253.

154 Krude, H., Biebermann, H., Luck, W., Horn, R., Brabant, G. & Grüters, A. (1998) Severe early-onset obesity, adrenal insufficiency and red hair pigmentation caused by POMC mutations in humans. *Nat Genet* **19**, 155-157.

155 Farooqi, I.S., Drop, S., Clements, A., Keogh, J.M., Biernacka, J., Lowenbein, S., Challis, B.G. & O'Rahilly, S. (2006) Heterozygosity for a POMC-null mutation and increased obesity risk in humans. *Diabetes* **55**, 2549-2553.

156 Comuzzie, A.G., Hixson, J.E., Almasy, L., Mitchell, B.D., Mahaney, M.C., Dyer, T.D., Stern, M.P., MacCluer, J.W. & Blangero, J. (1997) A major quantitative trait locus determining serum leptin levels and fat mass is located on human chromosome 2. *Nat Genet* **15**, 273-276.

157 Hager, J., Dina, C., Francke, S., Dubois, S., Houari, M., Vatin, V., Vaillant, E., Lorentz, N., Basdevant, A., Clement, K., Guy-Grand, B. & Froguel, P. (1998) A genome-wide scan for human obesity genes reveals a major susceptibility locus on chromosome 10. *Nat Genet* **20**, 304-308.

158 Rotimi, C.N., Comuzzie, A.G., Lowe, W.L., Luke, A., Blangero, J. & Cooper, R.S. (1999) The quantitative trait locus on chromosome 2 for serum leptin levels is confirmed in African-Americans. *Diabetes* **48**, 643-644.

159 Hixson, J.E., Almasy, L., Cole, S., Birnbaum, S., Mitchell, B.D., Mahaney, M.C., Stern, M.P., MacCluer, J.W., Blangero, J. & Comuzzie, A.G. (1999) Normal variation in leptin levels in associated with polymorphisms in the proopiomelanocortin gene, POMC. *J Clin Endocrinol Metab* **84**, 3187-3191.

160 Carroll, L., Voisey, J. & van Daal, A. (2005) Gene polymorphisms and their effects in the melanocortin system. *Peptides* **26**, 1871-1885.

161 Hinney, A., Becker, I., Heibült, O., Nottebom, K., Schmidt, A., Ziegler, A., Mayer, H., Siegfried, W., Blum, W.F., Remschmidt, H. & Hebebrand, J. (1998) Systematic mutation screening of the pro-opiomelanocortin gene: identification of several genetic variants including three different insertions, one nonsense and two missense point mutations in probands of different weight extremes. *J Clin Endocrinol Metab* **83**, 3737-3741.

162 Biebermann, H., Castañeda, T.R., van Landeghem, F., von Deimling, A., Escher, F., Brabant, G., Hebebrand, J., Hinney, A., Tschöp, M.H., Grüters, A. & Krude, H. (2006) A role for beta-melanocyte-stimulating hormone in human body-weight regulation. *Cell Metabolism* **3**, 141-146.

163 Echwald, S.M., Sørensen, T.I., Andersen, T., Tybjaerg-Hansen, A., Clausen, J.O. & Pedersen, O. (1999) Mutational analysis of the proopiomelanocortin gene in Caucasians with early onset obesity. *Int J Obes Relat Metab Disord* **23**, 293-298.

164 Suviolahti, E., Ridderstråle, M., Almgren, P., Klannemark, M., Melander, O., Carlsson, E., Carlsson, M., Hedenbro, J. & Orho-Melander, M. (2003) Pro-opiomelanocortin gene is associated with serum leptin levels in lean but not in obese individuals. *Int J Obes Relat Metab Disord* **27**, 1204-1211.

165 Miraglia Del Giudice, E., Cirillo, G., Santoro, N., D'Urso, L., Carbone, M.T., Di Toro, R. & Perrone, L. (2001) Molecular screening of the proopiomelanocortin (POMC ) gene in Italian obese children: report of three new mutations. *Int J Obes Relat Metab Disord* **25**, 61-67.

166 Buono, P., Pasanisi, F., Nardelli, C., Ieno, L., Capone, S., Liguori, R., Finelli, C., Oriani, G., Contaldo, F. & Sacchetti, L. (2005) Six novel mutations in the proopiomelanocortin and melanocortin receptor 4 genes in severely obese adults living in southern Italy. *Clin Chem* **51**, 1358-1364.

167 Challis, B.G., Pritchard, L.E., Creemers, J.W., Delplanque, J., Keogh, J.M., Luan, J., Wareham, N.J., Yeo, G.S., Bhattacharyya, S., Froguel, P., White, A., Farooqi, I.S. & O'Rahilly, S. (2002) A missense mutation disrupting a dibasic prohormone processing site in pro-opiomelanocortin (POMC) increases

susceptibility to early-onset obesity through a novel molecular mechanism. *Human Molecular Genetics* **11**, 1997-2004.

168 Lee, Y.S., Challis, B.G., Thompson, D.A., Yeo, G.S., Keogh, J.M., Madonna, M.E., Wraight, V., Sims, M., Vatin, V., Meyre, D., Shield, J., Burren, C., Ibrahim, Z., Cheetham, T., Swift, P., Blackwood, A., Hung, C.C., Wareham, N.J., Froguel, P., Millhauser, G.L., O'Rahilly, S. & Farooqi, I.S. (2006) A POMC variant implicates beta-melanocyte-stimulating hormone in the control of human energy balance. *Cell Metabolism* **3**, 135-140.

169 Delplanque, J., Barat-Houari, M., Dina, C., Gallina, P., Clément, K., Guy-Grand, B., Vasseur, F., Boutin, P. & Froguel, P. (2000) Linkage and association studies between the proopiomelanocortin (POMC) gene and obesity in caucasian families. *Diabetologia* **43**, 1554-1557.

170 Clément, K., Vaisse, C., Lahlou, N., Cabrol, S., Pelloux, V., Cassuto, D., Gourmelen, M., Dina, C., Chambaz, J., Lacorte, J.M., Basdevant, A., Bougnères, P., Lebouc, Y., Froguel, P. & Guy-Grand, B. (1998) A mutation in the human leptin receptor gene causes obesity and pituitary dysfunction. *Nature* **392**, 398-401.

171 Bertagna, X., Lenne, F., Comar, D., Massias, J.F., Wajcman, H., Baudin, V., Luton, J.P. & Girard, F. (1986) Human beta-melanocyte-stimulating hormone revisited. *Proc Natl Acad Sci USA* **83**, 9719-9723.

172 Harrold, J.A. & Williams, G. (2006) Melanocortin-4 receptors, beta-MSH and leptin: key elements in the satiety pathway. *Peptides* **27**, 365-371.

173 Rolland-Cachera, M.F., Cole, T.J., Sempé, M., Tichet, J., Rossignol, C. & Charraud, A. (1991) Body Mass Index variations: centiles from birth to 87 years. *European journal of clinical nutrition* **45**, 13-21.

174 Simon, C., Wagner, A., DiVita, C., Rauscher, E., Klein-Platat, C., Arveiler, D., Schweitzer, B. & Triby, E. (2004) Intervention centred on adolescents' physical activity and sedentary behaviour (ICAPS): concept and 6-month results. *Int J Obes Relat Metab Disord* **28 Suppl 3**, S96-S103.

**Publishing Agreement**

*It is the policy of the University to encourage the distribution of all theses, dissertations, and manuscripts. Copies of all UCSF theses, dissertations, and manuscripts will be routed to the library via the Graduate Division. The library will make all theses, dissertations, and manuscripts accessible to the public and will preserve these to the best of their abilities, in perpetuity.*

***Please sign the following statement:***

*I hereby grant permission to the Graduate Division of the University of California, San Francisco to release copies of my thesis, dissertation,or manuscript to the Campus Library to provide access and preservation, in whole or in part, in perpetuity.*

Author Signature

06.09.2009
Date